



ADNEIA DE FÁTIMA ABREU VENCESLAU

**ATEMOIA, MUITO ALÉM DO SABOR DOCE E
AROMA AGRADÁVEL: PRESENÇA DE COMPOSTOS
BIOATIVOS E CAPACIDADE BIOSSORVENTE**

LAVRAS – MG

2021

ADNEIA DE FÁTIMA ABREU VENCESLAU

**ATEMOIA, MUITO ALÉM DO SABOR DOCE E AROMA AGRADÁVEL:
PRESENÇA DE COMPOSTOS BIOATIVOS E CAPACIDADE BIODISSORVENTE**

Tese apresentada à Universidade Federal de Lavras como parte das exigências do Programa de Pós-Graduação em Agroquímica, área de concentração em Bioquímica, para a obtenção do título de Doutora.

Orientadora:

Prof^a. Dr^a. Luciana de Matos Alves Pinto

Coorientadores:

Prof. Dr. Cleiton Antônio Nunes

Prof. Dr. Sergio Scherrer Thomasi

Lavras - MG

2021

Ficha catalográfica elaborada pelo Sistema de Geração de Ficha Catalográfica da Biblioteca
Universitária da UFLA, com dados informados pelo(a) próprio(a) autor(a).

Venceslau, Adneia de Fátima Abreu.

Atemoia, muito além do sabor doce e aroma agradável:
presença de compostos bioativos e capacidade biossorvente. /
Adneia de Fátima Abreu Venceslau. - 2021.
106 p.

Orientador(a): Luciana de Matos Alves Pinto.

Coorientador(a): Cleiton Antônio Nunes, Sergio Scherrer
Thomasi.

Tese (doutorado) - Universidade Federal de Lavras, 2021.

Bibliografia.

1. Adsorvente. 2. Óleo de semente. 3. Annona. I. Pinto, Luciana
de Matos Alves. II. Nunes, Cleiton Antônio. III. Thomasi, Sergio
Scherrer. IV. Título.

ADNEIA DE FÁTIMA ABREU VENCESLAU

**ATEMOIA, MUITO ALÉM DO SABOR DOCE E AROMA
AGRADÁVEL: PRESENÇA DE COMPOSTOS BIOATIVOS E CAPACIDADE
BIOSSORVENTE**

**ATEMOIA, FAR BEYOND THE SWEET FLAVOR AND PLEASANT
AROMA: BIOACTIVE CONTENT AND BIOSORBENT ACTION**

Tese apresentada à Universidade Federal de
Lavras como parte das exigências do Programa de Pós-
Graduação em Agroquímica, área de concentração em
Bioquímica, para a obtenção do título de Doutora.

APROVADA em 25 de março de 2021

Prof ^a . Dr ^a	Elisangela Jaqueline Magalhães/UFLA
Prof ^a . Dr ^a	Iara do Rosário Magalhães Carvalho/UFLA
Prof ^a . Dr ^a	Kalynka Gabriella do Livramento/UFLA
Dr ^a	Juliana Arriel Torres/EMBRAPA

Orientadora:

Prof^a. Dr^a. Luciana de Matos Alves Pinto

Coorientadores:

Prof. Dr. Cleiton Antônio Nunes
Prof. Dr. Sergio Scherrer Thomasi

LAVRAS - MG

2021

Aos meus pais, Margarida e José, por todo amor, exemplo e sabedoria.

Ao Lucas por sua presença, incentivo e amor.

Clarice, minha filha, você é a tradução do amor!

Aos meus irmãos (Adilson, Adriane, Ademir e Adilo), cunhados (Gorety,

Dionaldo, Juliana e Marília) e sobrinhos (Pedro, Rubieny, Diogo e Emanuell).

Clarice, luz em meio ao caos. Lucas, Margarida, José, Angela, Célida e Roberto

por serem presença na minha ausência.

DEDICO.

AGRADECIMENTOS

A Deus por essa vitória.

À minha família por todo o apoio e incentivo! Acreditando e me dando forças, mesmo quando eu mesma não encontrava caminhos!

À minha orientadora Luciana por todos esses anos de orientação, confiança, amizade, paciência, dedicação e ensinamentos que vão muito além da academia!

Aos meus coorientadores Prof Sérgio e Prof Cleiton pela disponibilidade e atenção.

À Andressa, Lílian e Lucas por todo auxílio com a condução do trabalho.

Ao pessoal do laboratório de bioquímica por tudo que me ensinaram, em especial: Mariana, Tamara, Lucimara, Pricila, Lucas, Juliana, Lucilene, Denise e Tatiane. Aos professores: Lu Lopes, Silvana, Juliana e Paulo.

Ao prof. Guilherme Max Dias Ferreira por toda sua tranquilidade, *expertise*, disponibilidade e ensinamentos.

À prof^a. Barbara Sayuri Bellete por sua delicadeza e gentileza em ajudar com a metodologia da extração.

Às professoras e pesquisadoras e aos professores que tanto contribuíram no texto da qualificação, na avaliação de minhas atividades acadêmicas e, agora, nesse texto (tese).

O presente trabalho foi realizado com apoio da Coordenação de Aperfeiçoamento de Pessoal de Nível Superior – Brasil (CAPES) - Código de Financiamento 001.

Ao Programa de Pós-Graduação em Agroquímica pela oportunidade de me desenvolver enquanto realizava esse trabalho.

Ao CAPQ - UFLA pelas análises de infravermelho e DSC.

Ao LME-UFLA pelas análises de microscopia eletrônica de varredura.

A todos que torceram por mim e se fizeram presentes (mesmo que em pensamento!) ao longo desta jornada.

Muito obrigada!

“Você ainda acredita em magia?”

Eu acredito.

...

A magia está em todos os cantos do mundo – na sabedoria, na beleza, no amor e na paz. A magia está em você, nas suas palavras, na sua voz.”

Malala Yousafzai – *in*: Malala e seu lápis mágico, 2017.

RESUMO

A atemoia é um híbrido, gerado do cruzamento artificial na Flórida (EUA) no ano de 1908, entre a ata (*Annona squamosa* L.) e a cherimoia (*Annona cherimola* Mill.). Visando o conceito da economia circular, onde a matéria prima de uma cadeia produtiva é o resíduo de outra, propôs-se a utilização integral do fruto de atemoia *var* Thompson. As suas cascas deram origem à dois biossorventes eficientes na remoção do corante azul de metileno, um submetido a tratamento alcalino e outro *in natura*, com valores de pH_{PZC} próximos a neutralidade e com remoção acima de 80%. Perfil cinético ajustado por modelo de pseudo-segunda ordem e melhor ajuste para isoterma D-R, para ambos os biossorventes. Com capacidade máxima de biossorção de $190,18 \text{ mg g}^{-1}$ (*in natura*) e $264,50 \text{ mg g}^{-1}$ (com tratamento alcalino) na temperatura de $45 \text{ }^{\circ}\text{C}$ e, reutilizável por no mínimo 5 ciclos. De suas sementes o óleo foi extraído de 3 diferentes formas, mecânica, química e particionada sendo identificados os constituintes majoritários de cada extração. Na extração mecânica os principais constituintes foram o ácido elaídico (66,11%) e ácido esteárico (6,67%); na química o (Z)-hexadec-9-enal (49,42%) e trioleína (23,28%), enquanto na particionada, tem-se as frações hidrometanólica: diidroxiacetona (19,16%) e lactona 3-desoxi-d-manóica (16,34%); hexânica: gama-sitosterol (31,73%) e ácido erúcico (14,64%); clorofórmica: gama-sitosterol (22,11%) e ácido vacênico (15,49%); acetato de etila: ácido (Z)-icos-9-enóico (31,28%) e beta-sitosterol (16,29%). Dentre os constituintes, 12 compostos vêm sendo estudados com potencial uso adjuvante no tratamento de SARS-COV 2 e outros componentes com eficácia já comprovada em diversas atividades biológicas.

PALAVRAS-CHAVE: Adsorvente. Águas residuárias. Annona. Atividades biológicas. Óleo de semente.

ABSTRACT

Atemoya is a hybrid from an artificial interbreeding made in Florida (USA) in 1908 between *ata* (*Annona squamosa* L.) and *cherimoya* (*Annona cherimola* Mill.). Based on a concept of circular economy, in which the raw material of a production chain is the waste from another, the full-spectrum utilization of the *atemoya var* Thompson fruit has been proposed. The peel has originated two effective biosorbents for methylene blue, one submitted to alkaline treatment and one *in natura*, with pH_{PZC} values close to neutral, and at least 80% removal. The kinetic profile has been adjusted by pseudo-second order method, and best adjustment for D-R isotherm for both biosorbents, with maximum biosorption capacity of 190.18 mg g^{-1} (*in natura*) and 264.50 mg g^{-1} (with alkaline treatment) at $45 \text{ }^{\circ}\text{C}$, being reusable for at least 5 cycles. From the seeds, the oil has been extracted through three different ways (mechanically, chemically, and by partitioning) and the most abundant constituents have been identified. Mechanical extraction: elaidic acid (66,11%) and stearic acid (6,67%); chemical extraction: (Z)-hexadec-9-enal (49,42%) e triolein (23,28%). By partitioning the following fractions have been obtained, OSA_{HM} : dihydroxyacetone (19,16%) and 3-deoxy-d-mannoic lactone (16,34%); OSA_{HEX} : gamma-sitosterol (31,73%) e erucic acid (14,64%); OSA_{CLO} : gamma-sitosterol (22,11%) and vaccenic acid (15,49%); OSA_{ACE} : (Z)-icos-9-enoic acid (31,28%) and beta-sitosterol (16,29%). Among the constituents identified, 12 have already been identified as potential adjuvant therapy for SARS-COV 2, and others have already been confirmed to have a variety of biological activities.

KEYWORDS: Adsorbent. Annona. Biological activities. Seed oil. Wastewater.

SUMÁRIO

APRESENTAÇÃO	12
PRIMEIRA PARTE	13
1. INTRODUÇÃO	14
2. REFERENCIAL TEÓRICO.....	15
2.1 Família <i>Annonacea</i>	15
2.1.1 Atemoia	15
<u>2.2 Resíduos Agrícolas.....</u>	<u>16</u>
2.3 Adsorção/Biossorção.....	17
2.3.1 Alguns fatores com influência na adsorção.....	19
2.3.2 Cinética de adsorção.....	19
2.3.3 Isotermas de adsorção	21
2.3.4 Azul de metileno como composto modelo	23
2.4 Óleo vegetal.....	24
<u>2.4.1 Métodos mais utilizados para extração de óleo vegetal.....</u>	<u>24</u>
<u>2.4.2 Atividades biológicas da atemoia.....</u>	<u>25</u>
3. CONSIDERAÇÕES FINAIS	26
4. REFERÊNCIAS	27
ARTIGO 1	35
1. INTRODUCTION.....	36
2. MATERIALS AND METHODS	37
2.1 Preparation of the biosorbent.....	37
2.2 Biosorbent characterization	37
2.3 Adsorption and desorption studies	38
3. RESULTS AND DISCUSSION	39

3.1 Biosorbent characterization	39
3.1.1 Infrared spectroscopy	39
3.1.2 Thermogravimetric analyses	40
3.1.3 Scanning electron microscopy	41
3.2 Effect of pH on methylene blue removal capacity	42
3.3 Adsorption kinetics.....	45
3.4 Adsorption isotherms	49
3.5 Desorption analyses.....	53
3.6 Infrared spectra after adsorption of methylene blue.....	54
4. CONCLUSIONS	55
5. ACKNOWLEDGEMENTS	55
6. REFERENCES.....	55
ARTIGO 2.....	68
INTRODUCTION.....	70
EXPERIMENTAL PART	70
Seed preparation and extractions.....	70
RESULTS AND DISCUSSION	71
CONCLUSION	90
ACKNOWLEDGEMENT.....	97
REFERENCES.....	97

APRESENTAÇÃO

Este trabalho de tese está dividido em 2 partes: na primeira, constam a introdução, referencial teórico e considerações finais, e na segunda parte, constam os resultados do trabalho, que estão apresentados sob a forma de artigos. A formatação da primeira parte segue as normas do manual de normalização da UFLA, e a na segunda parte, os artigos seguem as normas das revistas nas quais foram submetidos.

O estudo foi desenvolvido baseando-se no aproveitamento integral do fruto de atemoia *var* Thompson, que vem ganhando mercado mundial, visando agregar valor à essa espécie que já é cultivada localmente. Das cascas foi obtido, caracterizado e avaliado um bioissorvente para remoção de efluentes catiônicos e das sementes foi extraído o óleo de diferentes formas.

O Artigo 1 aborda o preparo, a caracterização e a avaliação do bioissorvente de cascas de atemoia na remoção da molécula modelo azul de metileno. Foram utilizadas cascas de atemoia *in natura* e uma parte foi submetida a tratamento alcalino. Os bioissorventes foram caracterizados por espectroscopia no infravermelho, análise termogravimétrica e microscopia eletrônica de varredura. Foram determinados o ponto de carga zero e o percentual de remoção. Também foram realizados o estudo cinético e isotérmico do perfil de remoção do corante. A capacidade máxima de bioissorção foi determinada, além do teste de dessorção, que mostrou reuso por no mínimo 5 ciclos.

O Artigo 2 aborda diferentes metodologias de extração do óleo de sementes de atemoia, a química, mecânica e fracionada. Cada produto das extrações foi analisado por GC/MS e os constituintes foram relatados quanto a sua ação biológica.

PRIMEIRA PARTE

1. INTRODUÇÃO

O ano de 2020 ficará marcado pela pandemia de COVID-19 e termos como “imunidade”, “saúde” e “ciência” nunca estiveram tão em alta nas conversas virtuais. É notória a crescente demanda no consumo de frutas e vegetais por parte da população mundial visando o ganho de imunidade e a melhoria da saúde em geral.

Referindo-se a frutas, existe uma grande variedade de sabores. Os ditos “exóticos” vêm ganhando força entre os consumidores, seja para vivenciar novas experiências, ou ainda, pelos atributos nutricionais específicos. Assim, a demanda por frutas da família das anonas tem aumentado. Elas que são conhecidas por seu sabor doce, delicado perfume e elevado valor nutricional.

Este trabalho teve como foco principal promover o uso integral do fruto de atemoia *var.* Thompson. De suas cascas um bioissorvente foi produzido e testado com eficiência frente a outros materiais oriundos de resíduos agrícolas. Sabendo que a contaminação de águas residuárias é um agravante para a vida aquática e, por conseguinte, para a população em geral, visto que o equilíbrio entre os reinos é tênue.

De suas sementes, pode ser extraído o óleo, de diferentes formas (mecânica, química e particionada) afim de conhecer suas atividades farmacológicas. Dentre as dezenas de compostos, foi possível identificar constituintes com ação já comprovada em distintas frentes. Propriedades antioxidantes, anti-inflamatórias, antibacterianas, antifúngicas, atividade antitumoral, larvicida e antidiabética. E ainda são potenciais adjuvantes no enfrentamento a SARS-COV 2. Além de alguns serem feromônios, auxiliares em doenças negligenciadas, biomarcadores biológicos, entre outras atividades importantes.

2. REFERENCIAL TEÓRICO

2.1 Família *Annonacea*

Annonaceae é uma importante família de plantas pantropicais (que ocorre em qualquer região dos trópicos) e possui cerca de 2500 espécies, ocorrendo em todas as florestas tropicais principais e secundárias do mundo (COUVREUR; HELMSTETTER; KOENEN; BETHUNE *et al.*, 2019).

Muitas espécies são conhecidas/utilizadas por suas propriedades aromáticas. Acredita-se que o mais agradável e conhecido óleo essencial seja o da espécie asiática ylang-ylang (*Cananga odorata* (Lam.) Hook.f.& Thomson). E, também, por seus frutos carnosos e saborosos, especialmente os frutos do gênero neotropical *Annona* L (CHATROU; ERKENS; RICHARDSON; SAUNDERS *et al.*, 2012).

No Brasil, é considerada nativa, não endêmica, de ocorrência nos domínios fitogeográficos: Amazônia, Caatinga, Cerrado, Mata Atlântica e Pantanal, com 29 gêneros e 373 espécies (MAAS; LUBBERT; WESTRA; VERSPAGEN *et al.*, 2019; MAAS; WESTRA; GUERRERO; LOBÃO *et al.*, 2015). As espécies com maior importância econômica são a graviola (*Annona muricata* L.), a fruta-do-conde (*Annona squamosa* L.), a cherimoia (*Annona cherimola* Mill) e a atemoia (*Annona squamosa* x *Annona cherimola* Mill) (BRAGA SOBRINHO, 2014).

2.1.1. Atemoia

A atemoia (Figura 1) é um híbrido, gerado do cruzamento artificial na Flórida (EUA) no ano de 1908. A fruta-do-conde, pinha ou ata (*Annona squamosa* L.) foi a espécie doadora de pólen, originária da América tropical e a cherimoia (*Annona cherimola* Mill.) a receptora, originária do Equador. Do cruzamento dessas duas espécies surgiu o híbrido atemoia, sendo o prefixo “ata” emprestado do nome comum da *Annona squamosa* e o sufixo “moia” derivado da cherimoia, existindo também híbridos naturais (BARON; AMARO; MACEDO; BOARO *et al.*, 2018).

Figura 1 - Fruto de atemoia



Fonte: DO AUTOR, 2021

O híbrido reúne características interessantes da cherimoia, que produz frutos extremamente saborosos, e da fruta do conde, que se adapta bem nas condições climáticas brasileiras (CRUZ; LIMA; ABREU; CORRÊA *et al.*, 2013; LEMOS, 2014). Por ser um híbrido entre duas espécies, suas características são muito variáveis nas cultivares e dentre as mais cultivadas estão: ‘PR-3’, ‘Gefner’, ‘Thompson’ e ‘African Pride’. A variedade Thompson possui em média 300g, sendo 45% de polpa; 48% de casca e 3% de sementes. Comprimento médio de 10 cm, diâmetro de 8 cm e cerca de 22 sementes por fruto (LEMOS, 2014; MAAS; LUBBERT; WESTRA; VERSPAGEN *et al.*, 2019).

Os frutos, em sua maioria, são consumidos *in natura*, porém devido à considerável perecibilidade, o processamento vem sendo estudado como medida para melhorar sua vida de prateleira, fornecendo diferentes produtos, tais como sucos, geleias, compotas, purês, entre outros, os quais podem ser estocados na forma congelada ou liofilizada (DE SOUZA; DA SILVA FREITAS; BATISTA; DA COSTA *et al.*, 2015). Nas etapas de processamento, que valorizam a polpa do fruto de atemoia, uma grande quantidade de subprodutos é gerada e descartada (SILVA; DA SILVA; BIAZATTI; DOS SANTOS *et al.*, 2016). Esses resíduos constituem uma matéria prima de baixo custo para diversas aplicações, que poderiam agregar valor à cultura da atemoia.

2.2 Resíduos Agrícolas

Todas as substâncias descartadas na produção agropecuária, ganham o nome geral de resíduos agrícolas. Essa categoria inclui, principalmente, resíduos vegetais, esterco de animais e resíduos de processamento (WANG; CHU; FANG; HUANG *et al.*,

2017). É caracterizada por ter ampla e variadas fontes, grande quantidade, ser reprodutível, biodegradável e amiga do meio ambiente (DAI; SUN; WANG; LU *et al.*, 2018).

Os materiais lignocelulósicos são compostos principalmente por componentes não estruturais (como extrativos, cinzas, proteínas e outros componentes menores) e componentes estruturais (celulose, hemicelulose e lignina) (ROMANÍ; ROCHA; MICHELIN; DOMINGUES *et al.*, 2020).

A lignina é um polímero aromático, que consiste em carbonila, hidroxila, metila e outros grupos funcionais. Tanto a hemicelulose quanto a celulose contêm oxigênio funcional e grupos carbonil, hidroxil e éter. Esses grupos funcionais podem ligar tanto íons de elementos traço coordenando-os quanto contaminantes de pequenas moléculas orgânicas fazendo ligações de hidrogênio, normalmente na ocorrência de composto orgânico nitrogenado ou oxigenado, desempenhando um papel importante na preparação de adsorventes (ZHOU; BROWN; BAI, 2015).

O uso dos resíduos agrícolas como adsorvente já está consolidado (FOMINA; GADD, 2014; KUMARA; JOSHIBAA; FEMINAA; VARSHINIA *et al.*, 2019) e pesquisadores vêm demonstrando um aumento na capacidade de adsorção dos resíduos por meio de modificação química e/ou física (DU; CHEN; XU; WANG *et al.*, 2020). Ashrafi e colaboradores (2016) otimizaram as condições de adsorção do azul básico 41 usando casca de arroz modificada com NaOH (ASHRAFI; KAMANI; SOHEIL AREZOMAND; YOUSEFI *et al.*, 2016). Queiroz e colaboradores (2020) produziram um carvão ativado a partir de sementes de açaí com modificações e obtiveram sucesso na remoção de metais (QUEIROZ; DE SOUZA; THOMAZ; LIMA *et al.*, 2020). Em geral, a modificação melhora a capacidade de adsorção dos resíduos agrícolas utilizados como biossorventes.

2.3 Adsorção/Biossorção

Sorção é um termo usado tanto para absorção quanto para adsorção e são, por muitas vezes, confundidos. Absorção é a incorporação de uma substância, em um estado físico, em outro estado diferente ou seja, líquidos sendo absorvidos por um sólido ou gases sendo absorvidos pela água (KATHERESAN; KANSEDO; LAU, 2018; MICHALAK; CHOJNACKA; WITEK-KROWIAK, 2013). A adsorção é um fenômeno de superfície, em que há acumulação de uma substância (adsorvato) em uma interface

(adsorvente). Ocorre com todos os tipos de interface, tais como gás-sólido, solução-sólido, solução-gás, solução α -solução β . Os sólidos, em geral, apresentam capacidade de reter moléculas em sua superfície. Fato este que pode ser bem evidenciado no caso de materiais porosos ou finamente divididos (NGULUBE; GUMBO; MASINDI; MAITY, 2017; SMOCZYŃSKI; PIEROŻYŃSKI; MIKOŁAJCZYK, 2020). As forças envolvidas podem variar desde as de natureza puramente física (adsorção física) até as de natureza química (adsorção química) (FOMINA; GADD, 2014; GADD, 2009; KAUSAR; IQBAL; JAVED; AFTAB *et al.*, 2018). A biossorção é uma subcategoria de adsorção, onde o sorvente é uma matriz biológica (MICHALAK; CHOJNACKA; WITEK-KROWIAK, 2013).

Um processo de adsorção eficiente passa pela escolha de um adsorvente com boa seletividade, com alta capacidade de adsorção, duradouro, com boa disponibilidade e baixo custo (SMOCZYŃSKI; PIEROŻYŃSKI; MIKOŁAJCZYK, 2020).

Trata-se de uma técnica bem vantajosa para o tratamento de águas residuais, por ser de baixo custo, facilidade de design do processo, alta eficiência de remoção e capacidade de tratar poluentes em alta concentração (ASGHER, 2012; KAUSAR; IQBAL; JAVED; AFTAB *et al.*, 2018).

A biossorção é um processo de ligação rápida e reversível de íons de soluções aquosas a grupos funcionais que estão presentes na superfície da biomassa. Este processo é independente do metabolismo celular (NGULUBE; GUMBO; MASINDI; MAITY, 2017). A biossorção é apresentada na literatura como um processo eficiente e seletivo, e geralmente, pode ser realizada em ampla faixa de valores de pH e de temperatura (MICHALAK; CHOJNACKA; WITEK-KROWIAK, 2013).

São inúmeras as fontes de obtenção de biomassas, que podem ser provenientes de resíduos de origem vegetal ou animal, com grande potencial de utilização como um bom biossorvente. Como exemplos têm-se casca de arroz (VITHANAGE; MAYAKADUWA; HERATH; OK *et al.*, 2016), fruta do lobo (ARAÚJO; ALMEIDA; REZENDE; MARCIONILIO *et al.*, 2018), esterco de gado leiteiro (TSAI; HSU; LIN, 2019), algas marinhas (EL-NAGGAR; RABEI, 2020), macrófita invasiva (PÉREZ-MORALES; SÁNCHEZ-GALVÁN; OLGUÍN, 2019), monólitos de geopolímero (NOVAIS; ASCENSAO; TOBALDI; SEABRA *et al.*, 2018), cogumelo Roger (KARIUKI; KIPTOO; ONYANCHA, 2017), dentre outros.

2.3.1 Alguns fatores com influência na adsorção

Um dos fatores mais importantes que afetam a capacidade do adsorvente no tratamento de águas residuais é o pH da solução. A variação no pH leva à variação no grau de ionização da molécula adsortiva e nas propriedades superficiais do adsorvente (CARVALHO; CHAGAS; MARQUES; RAZAFITIANAMAHARAVO *et al.*, 2019; KOSMULSKI, 2018), além de indicar a capacidade de adsorção e o tipo de centros ativos superficiais (BAKATULA; RICHARD; NECULITA; ZAGURY, 2018). O ponto de carga zero (pH_{PCZ}) é o pH no qual a carga superficial é zero e normalmente é usado para identificar as propriedades eletroquímicas de uma superfície. Porém, o valor do pH é usado para descrever pH_{PCZ} apenas para sistemas em que H^+/OH^- são os íons que determinam o potencial (YAGUB; SEN; AFROZE; ANG, 2014). A temperatura também tem uma grande influência nas relações de equilíbrio, pois em nível microscópico a temperatura afeta a dinâmica molecular do sistema, interfere nas forças de atração e repulsão entre as moléculas na fase fluida e entre o adsorvato e o adsorvente (NATARELLI; CLARO; MIRANDA; FERREIRA *et al.*, 2019; RIBEIRINHA; MATEOS-PEDRERO; BOAVENTURA; SOUSA *et al.*, 2018).

2.3.2 Cinética de adsorção

Cinética de adsorção se refere à taxa de remoção do adsorvato na fase fluida em relação ao tempo, envolvendo a transferência de massa de um ou mais componentes presentes da fase líquida para a superfície do adsorvente (TAN; HAMEED, 2017). A cinética de adsorção é importante pois fornece um dado de muito interesse, o tempo de equilíbrio.

Vários modelos cinéticos são utilizados para avaliar/esclarecer o mecanismo do processo de adsorção, tais como adsorção física ou química, controle da difusão e transferência de massa. Os modelos mais utilizados são os de pseudo-primeira ordem, de pseudo-segunda ordem e difusão intrapartícula (WANG; GUO, 2020).

Uma das primeiras equações de taxa estabelecida para adsorção foi a de Lagergren (1898), também conhecida como Equação cinética de pseudo-primeira ordem. Essa Equação (1) é amplamente utilizada em processos de adsorção do soluto de uma solução líquida e está baseada na capacidade de adsorção do sólido (LAGERGREIN, 1898).

$$\frac{q_t}{q_e} = e^{-k_1 t} \quad (1)$$

em que q_t (mg g^{-1}) é a quantidade de adsorção no tempo t (min), q_e (mg g^{-1}) é a quantidade adsorvida no equilíbrio e k_1 (min^{-1}) é a constante de velocidade de pseudo-primeira ordem.

Geralmente, os dados de adsorção de águas residuárias por biossorventes são melhor representados pela cinética de pseudo-segunda ordem (YADAV; ALI; GARG, 2020) que pode ser expresso de acordo com a Equação 2 (HO; MCKAY, 1999):

$$q_t = \frac{q_e^2 k_2 t}{1 + k_2 t q_e} \quad (2)$$

em que q_t (mg g^{-1}) é a quantidade de adsorção no tempo t (min), q_e (mg g^{-1}) é a quantidade adsorvida no equilíbrio e k_2 (min^{-1}) é a constante de taxa de pseudo-segunda ordem. Os parâmetros cinéticos são obtidos plotando $1/q_t$ vs t . A equação de pseudo-segunda ordem tem a vantagem de permitir a avaliação da capacidade de adsorção efetiva, a velocidade inicial de adsorção e a constante de velocidade do modelo cinético de pseudo-segunda ordem (WEN; DU; ZENG; HUANG *et al.*, 2018). Ao contrário do modelo cinético de pseudo-primeira ordem, não há necessidade do conhecimento de algum parâmetro prévio e este modelo prevê o comportamento sobre o período completo da adsorção e está de acordo com um mecanismo de adsorção responsável pela etapa controladora da velocidade (HO; MCKAY, 1999).

O modelo de difusão intrapartícula foi proposto por Weber e Morris em 1963 (WEBER; MORRIS, 1963) e é baseado na hipótese que o processo de adsorção pode ser controlado pelas seguintes etapas, a saber: difusão no filme, difusão na superfície, difusão no poro e a adsorção na superfície do poro do adsorvente. No processo de adsorção, o modelo assume que ocorre a difusão do adsorbato no interior do adsorvente e que o processo é dependente da raiz quadrada do tempo ($t^{1/2}$). O modelo de difusão intrapartícula é expresso pela Equação 3:

$$q_t = k_{int} t^{1/2} + C \quad (3)$$

em que k_{int} é a constante de velocidade de difusão intrapartícula ($\text{mg g}^{-1} \text{min}^{-1/2}$) e C (mg g^{-1}) é a intersecção da reta com o eixo das ordenadas. O valor de C fornece uma

relação quantitativa com a espessura da camada limite de difusão (ou seja, quanto maior o valor de C, maior o efeito da camada limite). Plotando q_t versus $t^{1/2}$ é possível calcular a inclinação da reta, k_{int} . O gráfico do modelo de difusão intrapartícula, em geral, apresenta multilinearidade, indicando que duas ou mais etapas de adsorção podem ocorrer. A primeira representa a adsorção imediata, a segunda é a fase gradual e a terceira é a fase de equilíbrio final onde há redução da velocidade (LIN; JUANG, 2002).

2.3.3 Isotermas de adsorção

O equilíbrio de adsorção fornece informações relevantes sobre um processo de separação por adsorção, como por exemplo de que forma o adsorvato interage com os sítios ativos da superfície dos adsorventes (FERREIRA; FERREIRA; HESPANHOL; DE PAULA REZENDE *et al.*, 2017). Aplicando modelagem matemática e equações isotérmicas, a capacidade máxima de adsorção de um adsorvente pode ser calculada experimentalmente. A fim de criar condições mais favoráveis no processo adsorvativo, faz-se importante estabelecer a melhor correlação entre teoria e curva de equilíbrio. Assim, uma descrição matemática precisa e exata dos estudos isotérmicos torna-se indispensável para a predição dos parâmetros de adsorção e a comparação quantitativa nos mais diferentes sistemas adsorventes (JOSHI; GARG; KATARIA; KADIRVELU, 2019). Existem muitos modelos de isotermas de equilíbrio, destacando-se os modelos de Langmuir, Freundlich, Dubinin-Radushkevich (D-R) e Temkin (AL-GHOUTI; DA'ANA, 2020).

O Modelo de Langmuir assume a superfície do adsorvente como uma monocamada e assim algumas hipóteses são estabelecidas, tais como: os sítios de adsorção são uniformemente energéticos, forma-se uma monocamada do material adsorvido e cada sítio comporta apenas uma molécula adsorvida. A afinidade iônica, independentemente da quantidade de material adsorvido, também considera que não há interação entre moléculas adsorvidas em sítios próximos (KHADIR; NEGARESTANI; GHIASINEJAD, 2020; LANGMUIR, 1916; N'DIAYE, 2018). A expressão matemática da isoterma de Langmuir é dada pela Equação 4:

$$\frac{C_e}{q_e} = \frac{1}{q_m K_L} + \frac{1}{q_m} C_e \quad (4)$$

em que q_e é a quantidade adsorvida no equilíbrio (mg g^{-1}), C_e a concentração de equilíbrio do corante na solução (mg L^{-1}), K_L é a constante de Langmuir e também está relacionada com a afinidade aos locais de fixação e q_m representa a capacidade máxima de adsorção (mg g^{-1}). O parâmetro q_m também está associado à capacidade de adsorção limítrofe da monocamada, sendo assim uma medida eficaz para comparação do desempenho da adsorção (AL-GHOUTI; DA'ANA, 2020).

Em 1907, Freundlich propôs um modelo empírico aplicado à sistemas não ideais que tinha como objetivo estabelecer relação entre a quantidade de material adsorvido e a concentração do material em solução. O modelo de Freundlich descreve a adsorção em multicamadas em sistemas heterogêneos (FREUNDLICH, 1907; N'DIAYE, 2018). A isoterma de Freundlich é uma equação empírica que está apresentada na forma linearizada através da Equação 5:

$$\ln q_e = \ln K_F + \frac{1}{n_F} \ln C_e \quad (5)$$

onde q_e (mg g^{-1}) é a quantidade de soluto adsorvido, C_e (mg L^{-1}) é a concentração de equilíbrio em solução, n é a constante relacionada com a intensidade de adsorção e K_F (mg g^{-1})(mg L^{-1}) $1/n$ é a constante relacionada com a capacidade de adsorção de Freundlich . A partir da inclinação e do intercepto da reta do gráfico de $\log q_e$ em função de $\log C_e$ é possível obter as constantes de Freundlich (K_F e $1/n$). A inclinação da reta corresponde a $1/n$ e o intercepto terá o valor correspondente a $\log K_F$. O valor da constante de Freundlich (n) é usado para avaliar o grau de interação entre adsorvato e adsorvente, quanto menor o valor de n maior será a interação entre o adsorvato e o adsorvente (CORDA; KINI; IGHALO; ADENIYI, 2020).

O modelo de Dubinin-Radushkevich é um modelo de isoterma mais abrangente que o de Langmuir, pois considera a teoria do potencial de adsorção e assume que o processo de adsorção está relacionado ao preenchimento do volume dos microporos ao invés de adsorção camada a camada nas paredes dos poros. Dessa forma, D-R não considera uma superfície como homogênea ou potencial de adsorção constante tornando-se uma equação mais geral (DADA; OLALEKAN; OLATUNYA; DADA, 2012; KAUR; RANI; MAHAJAN; ASIF *et al.*, 2015). A isoterma de Dubinin-Radushkevich (D-R) apresentada na sua forma linearizada é dada pela Equação 6:

$$\ln q_e = \ln q_s - K_{DR} \varepsilon^2 \quad (6)$$

em que q_e é a quantidade de soluto adsorvido e q_s é a capacidade de adsorção, ambos em mg g^{-1} e K_{DR} é a constante associada à energia de adsorção expressa em $\text{mol}^2 \text{kJ}^{-2}$. O parâmetro ε é o potencial de Polanyi dado por $RT \ln[1 + (1/C_e)]$.

A isoterma de Temkin está fundamentada no fato do calor de adsorção ser inversamente proporcional ao aumento do recobrimento da superfície e os efeitos das interações indiretas adsorbato/adsorbato no processo de adsorção. O modelo de Temkin descreve melhor uma faixa intermediária de concentração iônica (AYAWEI; EBELEGI; WANKASI, 2017; RINGOT; LERZY; CHAPLAIN; BONHOURE *et al.*, 2007; VIJAYARAGHAVAN; PADMESH; PALANIVELU; VELAN, 2006). O modelo da isoterma de Temkin é apresentado na sua forma linearizada pela Equação 7:

$$q_e = b_T \ln K_T + b_T \ln C_e \quad (7)$$

Os parâmetros q_e e C_e tem o mesmo significado daqueles parâmetros na isoterma de Langmuir; K_T é a constante de equilíbrio de ligação, em Lg^{-1} e b_T é uma constante associada à variação de entalpia de adsorção. A partir da construção do gráfico de q_e em função de $\ln C_e$ é possível obter pelo método dos mínimos quadrados, os valores “A” e “B”. Onde “A” corresponde a constante de ligação de equilíbrio da isoterma de Temkin K_T (L/g) e “B” é a constante do calor de adsorção (J/mol).

2.3.4 Azul de metileno como composto modelo

O azul de metileno é um corante catiônico que apresenta baixa toxicidade, porém é de difícil degradação (COOKSEY, 2017). Em laboratório, esse corante é bastante utilizado para identificar a capacidade de adsorção dos mais distintos adsorventes (BIEHL; VON DER LÜHE; SCHACHER, 2018). Por apresentar forte absorção na região do visível, alta solubilidade e propriedades semelhantes às dos corantes têxteis, ele vem sendo bastante utilizado como composto modelo de contaminantes orgânicos e também em reações de oxidação (RAFATULLAH; SULAIMAN; HASHIM; AHMAD, 2010).

2.4 Óleo vegetal

Um óleo pode ser definido como insolúvel ou pouco solúvel em água e constituído majoritariamente por glicerídeos, podendo conter, em menor proporção, outros lipídios, como triglicerídeos, fosfolipídios, ceras e álcoois graxos, constituintes saponificáveis e insaponificáveis, esteróis e carotenoides (ANVISA RDC nº 207, 2005).

Nos óleos vegetais, os ácidos graxos desempenham um papel muito especial. Geralmente, são hidrocarbonetos de cadeia longa com carboxila (-COOH) em uma das extremidades. Diferem entre si pelo número de carbonos e a presença ou não de insaturações (PRIMEC; MIČETIĆ-TURK; LANGERHOLC, 2017; SOKOŁA-WYSOCZAŃSKA; WYSOCZAŃSKI; WAGNER; CZYŻ *et al.*, 2018).

2.4.1 Métodos mais utilizados para extração de óleo vegetal

Os métodos que geralmente são utilizados para extração de óleos envolvem técnicas químicas, bioquímicas e mecânicas (NDE; FONCHA, 2020). Dentre essas, estão a prensagem mecânica e extração por solventes.

A extração por prensagem mecânica tem sido muito utilizada por ser considerada uma alternativa limpa, dentro da chamada “química verde”. A matéria-prima, geralmente, passa por um pré-tratamento como despolpamento e redução de granulometria com o intuito de melhorar o rendimento da extração do óleo (HERIAWAN; INDARTONO; KARTIKA, 2018). Também é conhecida como extração a frio e apresenta características interessantes, tais como: reuso da torta, maior segurança, baixa complexidade do processo, qualidade do óleo e, muito importante, uma alternativa eco-friendly. Por outro lado, há uma perda considerável de óleo remanescente na torta (NDE; FONCHA, 2020).

A extração por solvente faz uso de solventes com polaridades semelhantes no intuito de proporcionar maiores interações intermoleculares entre solvente-soluto. Dessa forma, solventes orgânicos (apolares) são empregados na dissolução de óleos vegetais (MAS' UD; MAHENDRADATTA; LAGA; ZAINAL, 2017).




O solvente ideal deve apresentar algumas características básicas: ter alta solubilidade em baixas temperaturas, ter alta seletividade, ser inerte quimicamente, ter baixa viscosidade e tensão superficial, ser facilmente removido do óleo, ser imiscível em água, ter baixa temperatura de ebulição e causar o menor efeito adverso ao meio ambiente. Um solvente que atende à maioria desses pré-requisitos é o hexano, por isso ele vem sendo empregado na indústria. Antes da extração, é importante reduzir a granulometria

da matéria-prima de onde o óleo será obtido (KEMERLI-KALBARAN; OZDEMIR, 2019).

2.4.2 Atividades biológicas da atemoia

Por ser um híbrido relativamente recente, não há relatos de usos tradicionais da atemoia. No entanto, há extensa pesquisa por constituintes fitoquímicos que foram isolados de diferentes partes da planta e avaliados quanto ao seu potencial biológico em estudos *in vivo* e *in vitro* (AL KAZMAN; HARNETT; HANRAHAN, 2020; CHANG; CHEN; LIN; CHIU *et al.*, 1999; DURET; HOCQUEMILLER; CAVÉ, 1997; LIM; KIM; SOHN; YOON *et al.*, 2019; LIU; CHAO; PENG; YANG, 2016; YI; PARK; LEE; HONG *et al.*, 2014). Na Figura 2, os principais fitoquímicos isolados de diversas partes da planta de atemoia são apresentados.

Figura 2 - Principais fitoquímicos presentes nas folhas, frutos/polpa e sementes de atemoia

<i>Annona atemoya</i>		Fitoquímicos	Cultura animal/celular
FOLHAS		Alcaloides Flavonoides	Neuroprotetor Antioxidante Antibacteriano
POLPA		Terpenoides Fenólicos	Hiperlipidêmico Antiobesidade
SEMENTES		Acetogeninas Alcaloides Fenólicos Tryptaminas	Antiangiogênico Antitumoral

Fonte: Adaptada de AL KAZMAN; HARNETT; HANRAHAN, 2020

As acetogeninas de anonáceas são os principais componentes fitoquímicos das sementes, em comparação com os constituintes fenólicos e alcaloides (AL KAZMAN; HARNETT; HANRAHAN, 2020). Chang e colaboradores, por exemplo, identificaram e estabeleceram a estrutura química de 17 acetogeninas de anonáceas nas sementes: 12,15-cis-squamostatin-D, 12,15-cis-squamostatin-A, squamostatin-A, squamostatin-D,

neoannonin, artemoin-A, artemoin-B, artemoin-C, artemoin-D, squamocin, bullatacin, bullatanocin, bullatalicina, 12,15-cis-bullatanocin, 12,15-cis-bullatalicina, desacetilivaricina e isodesacetilivaricina (CHANG; CHEN; LIN; CHIU *et al.*, 1999).

Além das acetogeninas, alcaloides e componentes voláteis também já foram isolados de anonáceas: 12,15-cis-squamostatina-A, bullatacina, anonaína, α -pineno, canfeno, β -pineno, mirceno, espatulenol, germacreno D, esquamostatina D, β -cariofileno, uvariamicina-III, squamocina-G, squamocina-H, squamocina-J, squamocina-K, squamocina-L, squamocina-M; squamostatina-A, squamocina, annotemoyina-1, annotemoyina-2, liriodenine, annonacina, squamocina e molvizarina (AL KAZMAN; HARNETT; HANRAHAN, 2020).

Dentre as ações de extratos etanólicos das sementes de atemoia, temos ação antiangiogênica (YI; PARK; LEE; HONG *et al.*, 2014) e ação nefrotóxica (HÖLLERHAGE; RÖSLER; BERJAS; LUO *et al.*, 2015) e entre os extratos metanólicos, temos: ação larvicida (DE CÁSSIA SEFFRIN; SHIKANO; AKHTAR; ISMAN, 2010) e antioxidante (VAGULA; VISENTAINER; LOPES; MAISTROVICZ *et al.*, 2019).

3. CONSIDERAÇÕES FINAIS

A atemoia é uma fruta que vem ganhando consumidores ao redor do mundo e é um híbrido com pouco mais de cem anos, relativamente recente, e que desperta muito interesse devido às propriedades já conhecidas de sua família.

O uso integral de frutas não só é possível, como mostra-se de suma importância. Além de aumentar a visibilidade da cultura agrícola, valorizando toda a cadeia produtiva e gerando renda para inúmeros agricultores familiares, essa técnica minimiza a produção de rejeitos. Apropriando-se do conceito em um modelo de economia mais saudável ao planeta, em que um processo se inicia onde outro é finalizado, ou seja, a matéria prima de um processo é o resíduo de outro, neste contexto o presente estudo foi conduzido.

Diante disso, dois bioissorventes foram preparados a partir de suas cascas e testados frente à remoção do corante modelo azul de metileno (poluente catiônico). Ambos se mostraram eficientes na remoção desse efluente. Um bioissorvente foi tratado alcalinamente e outro permaneceu *in natura*. Foram obtidos valores de pH_{PCZ} próximos a neutralidade e com no mínimo 80% de remoção. O perfil cinético pôde ser ajustado por modelo de pseudo-segunda ordem e o melhor ajuste foi realizado pela isoterma D-R, para ambos os bioissorventes. A capacidade máxima de bioissorção foi comparável à de

materiais produzidos a partir de biomassa nos últimos cinco anos de pesquisa, com valores de 190,18 mg g⁻¹ (*in natura*) e 264,50 mg g⁻¹ (com tratamento alcalino) na temperatura de 45 °C e reutilizável por no mínimo 5 ciclos.

O óleo foi extraído de suas sementes de 3 diferentes formas: mecânica, química e particionada, e os constituintes majoritários de cada extração foram identificados. OSA_P: ácido elaídico (66,11%) e ácido esteárico (6,67%); OSA_H (Z)-hexadec-9-enal (49,42%) e trioleína (23,28%). Na extração particionada, tem-se as frações OSA_{HM}: diidroxiacetona (19,16%) e lactona 3-desoxi-d-mannóica (16,34%); OSA_{HEX}: gama-sitosterol (31,73%) e ácido erúico (14,64%); OSA_{CLO}: gama-sitosterol (22,11%) e ácido vacênico (15,49%); OSA_{ACE}: ácido (Z)-icos-9-enóico (31,28%) e beta-sitosterol (16,29%). Dentre os constituintes, 12 compostos vêm sendo estudados com potencial uso adjuvante no tratamento da COVID-19 e outros componentes com eficácia já comprovada em diversas atividades biológicas, tais como, antioxidante, anti-inflamatória, larvicida, antibacteriana, antifúngica, antitumoral e antidiabética. Além disso, alguns compostos são feromônios, auxiliares em doenças negligenciadas e biomarcadores biológicos. Com essa triagem de extração realizada, ocasionou um acréscimo de informações acerca da metodologia de extração a ser escolhida, levando-se em conta o constituinte desejado.

4. REFERÊNCIAS

AL KAZMAN, B. S. M.; HARNETT, J. E.; HANRAHAN, J. R. The Phytochemical Constituents and Pharmacological Activities of *Annona atemoya*: A Systematic Review. **Pharmaceuticals**, 13, n. 10, p. 269, 2020.

AL-GHOUTI, M. A.; DA'ANA, D. A. Guidelines for the use and interpretation of adsorption isotherm models: A review. **Journal of Hazardous Materials**, p. 122383, 2020.

ASGHER, M. Biosorption of Reactive Dyes: A Review. **Water, Air, & Soil Pollution**, 223, n. 5, p. 2417-2435, 2012/06/01 2012.

ASHRAFI, S. D.; KAMANI, H.; SOHEIL AREZOMAND, H.; YOUSEFI, N. *et al.* Optimization and modeling of process variables for adsorption of Basic Blue 41 on NaOH-modified rice husk using response surface methodology. **Desalination and Water Treatment**, 57, n. 30, p. 14051-14059, 2016.

AYAWEI, N.; EBELEGI, A. N.; WANKASI, D. Modelling and interpretation of adsorption isotherms. **Journal of Chemistry**, 2017, 2017.

BIEHL, P.; VON DER LÜHE, M.; SCHACHER, F. H. Reversible Adsorption of methylene blue as cationic model cargo onto polyzwitterionic magnetic nanoparticles. **Macromolecular Rapid Communications**, 39, n. 14, p. 1800017, 2018.

CHANG, F.-R.; CHEN, J.-L.; LIN, C.-Y.; CHIU, H.-F. *et al.* Bioactive acetogenins from the seeds of *Annona atemoya*. **Phytochemistry**, 51, n. 7, p. 883-889, 1999/08/01/ 1999.

CHATROU, L. W.; ERKENS, R. H. J.; RICHARDSON, J. E.; SAUNDERS, R. M. K. *et al.* The natural history of Annonaceae. Oxford University Press 2012.

COOKSEY, C. J. Quirks of dye nomenclature. 8. Methylene blue, azure and violet. **Biotechnic & Histochemistry**, 92, n. 5, p. 347-356, 2017.

CORDA, N. C.; KINI, M. S., **A review on adsorption of cationic dyes using activated carbon**. EDP Sciences. 02022.

COUVREUR, T. L. P.; HELMSTETTER, A. J.; KOENEN, E. J. M.; BETHUNE, K. *et al.* Phylogenomics of the major tropical plant family Annonaceae using targeted enrichment of nuclear genes. **Frontiers in plant science**, 9, p. 1941, 2019.

DADA, A. O.; OLALEKAN, A. P.; OLATUNYA, A. M.; DADA, O. Langmuir, Freundlich, Temkin and Dubinin–Radushkevich isotherms studies of equilibrium sorption of Zn²⁺ onto phosphoric acid modified rice husk. **IOSR Journal of Applied Chemistry**, 3, n. 1, p. 38-45, 2012.

DAI, Y.; SUN, Q.; WANG, W.; LU, L. *et al.* Utilizations of agricultural waste as adsorbent for the removal of contaminants: A review. **Chemosphere**, 211, p. 235-253, 2018/11/01/ 2018.

DE CÁSSIA SEFFRIN, R.; SHIKANO, I.; AKHTAR, Y.; ISMAN, M. B. Effects of crude seed extracts of *Annona atemoya* and *Annona squamosa* L. against the cabbage looper, *Trichoplusia ni* in the laboratory and greenhouse. **Crop Protection**, 29, n. 1, p. 20-24, 2010.

DU, Y.; CHEN, H.; XU, X.; WANG, C. *et al.* Surface modification of biomass derived toluene adsorbent: hierarchically porous characterization and heteroatom doped effect. **Microporous and Mesoporous Materials**, 293, p. 109831, 2020.

DURET, P.; HOCQUEMILLER, R.; CAVÉ, A. Annonisin, a bis-tetrahydrofuran acetogenin from *Annona atemoya* seeds. **Phytochemistry**, 45, n. 7, p. 1423-1426, 1997/08/01/ 1997.

FERREIRA, G. M. D.; FERREIRA, G. M. D.; HESPANHOL, M. C.; DE PAULA REZENDE, J. *et al.* Adsorption of red azo dyes on multi-walled carbon nanotubes and activated carbon: A thermodynamic study. **Colloids and Surfaces A: Physicochemical and Engineering Aspects**, 529, p. 531-540, 2017/09/20/ 2017.

FOMINA, M.; GADD, G. M. Biosorption: current perspectives on concept, definition and application. **Bioresource technology**, 160, p. 3-14, 2014.

FREUNDLICH, H. Über die adsorption in lösungen. **Zeitschrift für physikalische Chemie**, 57, n. 1, p. 385-470, 1907.

GADD, G. M. Biosorption: critical review of scientific rationale, environmental importance and significance for pollution treatment. **Journal of Chemical Technology & Biotechnology: International Research in Process, Environmental & Clean Technology**, 84, n. 1, p. 13-28, 2009.

HERIAWAN; INDARTONO, Y. S.; KARTIKA, I. A. Optimization of mechanical oil extraction process of Nyamplung seeds (*Calophyllum inophyllum* L.) by flexible single screw extruder. **AIP Conference Proceedings**, 1984, n. 1, p. 020013, 2018/07/25 2018.

HO, Y.-S.; MCKAY, G. Pseudo-second order model for sorption processes. **Process biochemistry**, 34, n. 5, p. 451-465, 1999.

HÖLLERHAGE, M.; RÖSLER, T. W.; BERJAS, M.; LUO, R. *et al.* Neurotoxicity of dietary supplements from Annonaceae species. **International journal of toxicology**, 34, n. 6, p. 543-550, 2015.

IGHALO, J. O.; ADENIYI, A. G. Adsorption of pollutants by plant bark derived adsorbents: An empirical review. **Journal of Water Process Engineering**, 35, p. 101228, 2020.

JOSHI, S.; GARG, V. K.; KATARIA, N.; KADIRVELU, K. Applications of Fe₃O₄@AC nanoparticles for dye removal from simulated wastewater. **Chemosphere**, 236, p. 124280, 2019.

KATHERESAN, V.; KANSEDO, J.; LAU, S. Y. Efficiency of various recent wastewater dye removal methods: A review. **Journal of Environmental Chemical Engineering**, 6, n. 4, p. 4676-4697, 2018/08/01/ 2018.

KAUR, S.; RANI, S.; MAHAJAN, R. K.; ASIF, M. *et al.* Synthesis and adsorption properties of mesoporous material for the removal of dye safranin: Kinetics, equilibrium, and thermodynamics. **Journal of Industrial and Engineering Chemistry**, 22, p. 19-27, 2015.

KAUSAR, A.; IQBAL, M.; JAVED, A.; AFTAB, K. *et al.* Dyes adsorption using clay and modified clay: A review. **Journal of Molecular Liquids**, 256, p. 395-407, 2018/04/15/ 2018.

KEMERLI-KALBARAN, T.; OZDEMIR, M. Multi-response optimization of oil extraction from pine nut (*Pinus pinea* L.) by response surface methodology: Extraction efficiency, physicochemical properties and antioxidant activity. **LWT**, 103, p. 34-43, 2019/04/01/ 2019.

KHADIR, A.; NEGARESTANI, M.; GHIASINEJAD, H. Low-cost sisal fibers/polypyrrole/polyaniline biosorbent for sequestration of reactive orange 5 from aqueous solutions. **Journal of Environmental Chemical Engineering**, 8, n. 4, p. 103956, 2020/08/01/ 2020.

KUMARA, P. S.; JOSHIBAA, G. J.; FEMINAA, C. C.; VARSHINIA, P. *et al.* A critical review on recent developments in the low-cost adsorption of dyes from wastewater. **Desalin Water Treat**, 172, p. 395-416, 2019.

LAGERGREN, S. K. About the theory of so-called adsorption of soluble substances. **Sven. Vetenskapsakad. Handlingar**, 24, p. 1-39, 1898.

LANGMUIR, I. The constitution and fundamental properties of solids and liquids. Part I. Solids. **Journal of the American chemical society**, 38, n. 11, p. 2221-2295, 1916.

LIM, H.-S.; KIM, Y. J.; SOHN, E.; YOON, J. *et al.* Annona atemoya leaf extract ameliorates cognitive impairment in amyloid- β injected Alzheimer's disease-like mouse model. **Experimental Biology and Medicine**, 244, n. 18, p. 1665-1679, 2019/12/01 2019.

LIN, S.-H.; JUANG, R.-S. Heavy metal removal from water by sorption using surfactant-modified montmorillonite. **Journal of hazardous materials**, 92, n. 3, p. 315-326, 2002.

LIU, T.-T.; CHAO, L. K.-P.; PENG, C.-W.; YANG, T.-S. Effects of processing methods on composition and functionality of volatile components isolated from immature fruits of atemoya. **Food Chemistry**, 202, p. 176-183, 2016/07/01/ 2016.

MAS' UD, F.; MAHENDRADATTA, M.; LAGA, A.; ZAINAL, Z. Optimization of mango seed kernel oil extraction using response surface methodology. **OCL**, 24, n. 5, p. D503, 2017.

MICHALAK, I.; CHOJNACKA, K.; WITEK-KROWIAK, A. State of the Art for the Biosorption Process—a Review. **Applied Biochemistry and Biotechnology**, 170, n. 6, p. 1389-1416, 2013/07/01 2013.

NDE, D. B.; FONCHA, A. C. Optimization methods for the extraction of vegetable oils: A review. **Processes**, 8, n. 2, p. 209, 2020.

NGULUBE, T.; GUMBO, J. R.; MASINDI, V.; MAITY, A. An update on synthetic dyes adsorption onto clay based minerals: A state-of-art review. **Journal of Environmental Management**, 191, p. 35-57, 2017/04/15/ 2017.

N'DIAYE, A. D. Modeling of adsorption isotherms of dyes onto various adsorbents: A Short Review. **Arab. J. Chem. Environ. Res**, 5, p. 42-51, 2018.

PRIMEC, M.; MIČETIĆ-TURK, D.; LANGERHOLC, T. Analysis of short-chain fatty acids in human feces: A scoping review. **Analytical biochemistry**, 526, p. 9-21, 2017.

QUEIROZ, L. S.; DE SOUZA, L. K. C.; THOMAZ, K. T. C.; LIMA, E. T. L. *et al.* Activated carbon obtained from amazonian biomass tailings (acai seed): Modification,

characterization, and use for removal of metal ions from water. **Journal of Environmental Management**, 270, p. 110868, 2020.

RAFATULLAH, M.; SULAIMAN, O.; HASHIM, R.; AHMAD, A. Adsorption of methylene blue on low-cost adsorbents: a review. **Journal of hazardous materials**, 177, n. 1-3, p. 70-80, 2010.

RIBEIRINHA, P.; MATEOS-PEDRERO, C.; BOAVENTURA, M.; SOUSA, J. *et al.* CuO/ZnO/Ga₂O₃ catalyst for low temperature MSR reaction: Synthesis, characterization and kinetic model. **Applied Catalysis B: Environmental**, 221, p. 371-379, 2018.

RINGOT, D.; LERZY, B.; CHAPLAIN, K.; BONHOURE, J.-P. *et al.* In vitro biosorption of ochratoxin A on the yeast industry by-products: Comparison of isotherm models. **Bioresource technology**, 98, n. 9, p. 1812-1821, 2007.

ROMANÍ, A.; ROCHA, C. M. R.; MICHELIN, M.; DOMINGUES, L. *et al.* Chapter 20 - Valorization of lignocellulosic-based wastes. *In: VARJANI, S.; PANDEY, A., et al (Ed.). Current Developments in Biotechnology and Bioengineering*: Elsevier, 2020. p. 383-410.

SMOCZYŃSKI, L.; PIEROŻYŃSKI, B.; MIKOŁAJCZYK, T. The Effect of Temperature on the Biosorption of Dyes from Aqueous Solutions. **Processes**, 8, n. 6, p. 636, 2020.

SOKOŁA-WYSOCZAŃSKA, E.; WYSOCZAŃSKI, T.; WAGNER, J.; CZYŻ, K. *et al.* Polyunsaturated fatty acids and their potential therapeutic role in cardiovascular system disorders—A review. **Nutrients**, 10, n. 10, p. 1561, 2018.

TAN, K. L.; HAMEED, B. H. Insight into the adsorption kinetics models for the removal of contaminants from aqueous solutions. **Journal of the Taiwan Institute of Chemical Engineers**, 74, p. 25-48, 2017.

VAGULA, J. M.; VISENTAINER, J. V.; LOPES, A. P.; MAISTROVICZ, F. C. *et al.* Antioxidant activity of fifteen seeds from fruit processing residues by different methods. **Acta Scientiarum. Technology**, 41, p. e35043, 2019.

VIJAYARAGHAVAN, K.; PADMESH, T. V. N.; PALANIVELU, K.; VELAN, M. Biosorption of nickel (II) ions onto *Sargassum wightii*: application of two-parameter and three-parameter isotherm models. **Journal of hazardous materials**, 133, n. 1-3, p. 304-308, 2006.

WANG, H.; CHU, Y.; FANG, C.; HUANG, F. *et al.* Sorption of tetracycline on biochar derived from rice straw under different temperatures. **PLOS ONE**, 12, n. 8, p. e0182776, 2017.

WANG, J.; GUO, X. Adsorption kinetic models: Physical meanings, applications, and solving methods. **Journal of Hazardous Materials**, 390, p. 122156, 2020.

WEBER, W. J.; MORRIS, J. C. Kinetics of adsorption on carbon from solution. **Journal of the sanitary engineering division**, 89, n. 2, p. 31-60, 1963.

WEN, X.; DU, C.; ZENG, G.; HUANG, D. *et al.* A novel biosorbent prepared by immobilized *Bacillus licheniformis* for lead removal from wastewater. **Chemosphere**, 200, p. 173-179, 2018.

YADAV, V.; ALI, J.; GARG, M. C. Biosorption of Methylene Blue Dye from Textile-Industry Wastewater onto Sugarcane Bagasse: Response Surface Modeling, Isotherms, Kinetic and Thermodynamic Modeling. **Journal of Hazardous, Toxic, and Radioactive Waste**, 25, n. 1, p. 04020067, 2020.

YI, J.-M.; PARK, J.-S.; LEE, J.; HONG, J. T. *et al.* Anti-angiogenic potential of an ethanol extract of *Annona atemoya* seeds in vitro and in vivo. **BMC Complementary and Alternative Medicine**, 14, n. 1, p. 353, 2014/09/23 2014.

SEGUNDA PARTE - ARTIGOS

ARTIGO 1

Normas do Periódico (versão preliminar)

REMOVAL OF METHYLENE BLUE FROM AN AQUEOUS MEDIUM USING ATEMOYA PEEL AS A LOW-COST ADSORBENT

Adneia de Fátima Abreu Venceslau¹, Andressa Campos Mendonça¹, Lucas Bragança Carvalho², Guilherme Max Dias Ferreira¹, Sergio Scherrer Thomasi¹, Luciana Matos Alves Pinto^{1*}

¹ Department of Chemistry, Federal University of Lavras (UFLA), Lavras, Brazil.

² Institute of Science and Technology, São Paulo State University (UNESP), Sorocaba, Brazil.

*Author for correspondence: Department of Chemistry, Federal University of Lavras (UFLA), P.O. Box 3037, 37.200-900, Lavras/MG, Brazil. Tel.: + 55 35 3829-1892, E-mail: luca@ufla.br (L. M. A. Pinto), ORCID # 0000-0001-6013-0163

ABSTRACT: This study prepared a biosorbent from the agricultural waste of atemoya peels, which was then used to remove the model molecule of methylene blue. The atemoya peels were used *in natura*, and some were subjected to an alkaline treatment. The pH values obtained for the points of zero charge were 6.0 and 8.0 for the untreated and alkaline-treated materials, respectively. For neutral and/or alkaline pH values, the untreated and treated materials achieved average removals of approximately 80% and 90%, respectively. A kinetic study of the model dye removal profile showed a higher removal ratio over a shorter period for the alkaline-treated material. This profile is described by the pseudo-second order model, which was the best fit for the D-R isotherm in both biosorbents. The maximum biosorption capacities were 190.18 mg g⁻¹ (untreated) and 264.50 mg g⁻¹ (treated) at 45 °C, and the alkaline-treated materials were shown to be reusable for at least 5 cycles. The findings show that biosorbents made from atemoya peels are low cost, efficient materials for removing methylene blue model molecules.

Keywords: Annona, wastewater treatment, residue, biomass, dye, adsorption, eco-friendly

1. INTRODUCTION

Water contamination by different pollutants causes a series of negative impacts on aquatic ecosystems and poses risks to human health, whether due to water or fish consumption from these sources [1]. This contamination results from high volumes of industrial waste with diverse chemical compositions that is discharged daily into water bodies worldwide [2]. Many studies of contaminants derived from the textile industry and other sectors involving the use of dyes have indicated the potential toxicological risks of these compounds and their degradation products [3, 4]. There are reports of carcinogenic and mutagenic effects that may be cumulative in certain organisms and are capable of causing endocrine disorders [5]. However, the major problem related to the disposal of dye-containing waste concerns the dyes themselves. The presence of these compounds in water prevents the penetration of solar radiation and can interfere with the photosynthetic activity of algae and submerged plants, reducing the amount of oxygen available to other aquatic organisms [4].

In this context, adsorption has emerged as a promising method to efficiently remove dyes from wastewater [6]. However, despite an intense search for new adsorbent materials [7], finding a material that is easily obtained, abundant, has a good adsorption capacity, and is low cost is still a challenge. Therefore, natural compounds such as agricultural waste, which is usually improperly discarded, have emerged as promising candidates for the development of new adsorbents, known as biosorbents [8]. Numerous types of biomass can be used as biosorbents, including rice husks [9], malt bagasse [10], sisal fibers [11], wolf apples [12], dairy cattle manure [13], marine algae [14, 15], invasive macrophytes [16], geopolymer monoliths [17], and Roger mushrooms [18], among others.

Atemoya is a hybrid fruit produced from an artificial cross-breeding between the sweetsop (*Annona squamosa* L.) found in dry climates and a species of cherimoya (*Annona cherimola* Mill.), which grows in high altitude tropical climates [19]. The fruits of the atemoya weigh ~300 g and have a pleasant taste and aroma, with sensory characteristics superior to those of the sweetsop and cherimoya [20]. They are usually consumed *in natura*, but because of their considerable perishability, some forms of processing have been considered, such as juices, jellies, jams and purées, and storage as frozen or freeze-dried products [21]. During processing, which values the pulp of the atemoya fruit, large amounts of byproducts are generated and discarded [22]. These residues include the rough green peel, which accounts for between 28 and 50% of the mass of the fruit [23]. This waste is a low-cost raw material with the potential for several applications that could add value to the atemoya crop.

Methylene blue is a low toxicity cationic dye that is difficult to degrade [24]. This dye is widely used in the laboratory to identify the adsorption capacity of most distinct adsorbents [25]. Owing to its strong absorption in the UV–visible light region of the spectrum, high solubility, and

properties similar to textile dyes, it has been widely used as a model compound for organic contaminants and in oxidation reactions [26]. Based on the above considerations, the objective of this study was to prepare a new biosorbent from agricultural waste consisting of atemoya peels. The removal efficiency of the obtained material was evaluated using an adsorption study of the methylene blue model molecule in aqueous solutions.

2. MATERIALS AND METHODS

2.1 Preparation of the biosorbent

Fresh atemoya fruits of the Thompson variety (Exsicata ESAL 30.249) were purchased from a local rural producer (Lavras/MG) during the 2016–2017 harvest. The biosorbents were prepared from the peels, following the methodology of Carvalho et al. (2018). After removing the pulp, the atemoya peels were oven-dried at 70 °C and crushed in a knife mill with a 150-mesh particle size. After this process, a portion of the material was stored in hermetically sealed flasks ("untreated") The remaining material was mixed with a 1 mol L⁻¹ NaOH solution, stirred for 12 h and vacuum filtered, washed with distilled water to a neutral pH, and dried in an oven at 60 °C for 48 h. This material was then stored in hermetically sealed flasks for further characterization ("treated")

2.2 Biosorbent characterization

The biosorbent materials were characterized using UV spectroscopy, thermogravimetric analyses, and morphological analyses with scanning electron microscopy.

A Digilab Excalibur Fourier transform infrared spectrometer (FTS 3000 series) was used to obtain the absorption spectra in the infrared region using KBr optical windows. In addition to the prepared biosorbents, 10 mg samples of the materials were analyzed after they were exposed to methylene blue (50 mgL⁻¹, pH 7.00) under constant stirring for 12 h at 150 rpm at room temperature (25 ± 2 °C), then filtered and dried in an oven at 40 ± 2 °C for 24 h,. The spectra were obtained in the range of 4000–400 cm⁻¹, with 8 cm⁻¹ resolution and an accumulation number of 32 scans.

Thermogravimetric analyses of the biosorbents were performed in an N₂ atmosphere using a Shimadzu Model 60 AH system with temperatures ranging between 25 and 700 °C, a gas flow of 30 mL min⁻¹, an initial sample mass of ~5 mg, and a 10 °C min⁻¹ heating rate.

Morphological analyses were performed using a LEO EVO 40XVP scanning electron microscope. The samples of the prepared biosorbents were arranged in aluminum stubs and covered with colloidal gold in an argon atmosphere in a vacuum for 180 s in a Balzers Sputter Coater SCD 050. After this procedure, the electron micrographs were obtained.

2.3 Adsorption and desorption studies

Studies of the effect of solution pH on the adsorption process used 20 mg of each biosorbent dispersed in 10 mL of a 20 mgL⁻¹ dye solution. The pH of the initial reaction medium was adjusted using 0.025 mol L⁻¹ HCl and 0.1 mol L⁻¹ NaOH solutions. Analyses at pH values of 1.00, 2.00, 3.00, 4.00, 5.00, 6.00, 7.00, 8.00, 9.00, 10.00, 11.00, and 12.00 were conducted. The systems were agitated at room temperature (25 ± 2 °C) for 12 h at 150 rpm and centrifuged for 5 min at 3500 × g, after which the supernatant was collected for analysis. The amount of adsorbed dye was calculated using Equation 1:

$$q_e = \frac{(C_i - C_e)V}{m} \quad (1)$$

where q_e (mgg⁻¹) is the amount of adsorbed methylene blue, V (L) is the solution volume, C_i and C_e (mgL⁻¹) are the initial and final dye concentrations, respectively, and m (g) is the mass of the adsorbent. The percentage removed was calculated using Equation 2:

$$\%biosorption = \frac{C_i - C_e}{C_i} \times 100 \quad (2)$$

To determine the pH_{ZCP}, 10 mg of each adsorbent was added to 10 mL of a 0.100 mol L⁻¹ aqueous KCl solution, under 12 different initial pH conditions (1.00, 2.00, 3.00, 4.00, 5.00, 6.00, 7.00, 8.00, 9.00, 10.00, 11.00, and 12.00). The pH was adjusted using 0.1 mol L⁻¹ HCl or NaOH solutions. After agitation in a thermostatic bath at 25 ± 2 °C for 24 h, the samples were filtered and the final pH of the solution was measured. The ΔpH_{ZCP} was obtained from the difference between the initial and final pH values.

A 20 mg sample of each biosorbent was transferred to 50 mL flasks for the adsorption kinetics analyses. Then, 20 mL of the 50 mgL⁻¹ dye solution was added. At predetermined intervals (0, 2, 5, 10, 15, 20, 25, 30, 40, 50, 60, 90, 120, 150, 180, and 210 min), 200 μL aliquots of the solution were collected and diluted in 5000 μL of deionized water, after which the dye concentration was measured. The experiments were conducted under continuous stirring at 150 rpm at four different temperatures (25, 35, 45, and 55 °C) and at a pH of 7.00.

Adsorption equilibrium analyses were conducted by dispersing 10 mg of each atemoya biosorbent into 10 mL of dye solutions with different initial concentrations (10, 25, 50, 75, 100, 150, and 200 mgL⁻¹) at a pH of 7.00. The samples remained under continuous stirring (150 rpm) for 12 h at 25, 35, 45, and 55 °C. Afterwards, they were centrifuged for 5 min at 3500 × g and the supernatant was collected to determine the equilibrium concentration of the dye.

For desorption analyses, samples of each biosorbent were loaded with methylene blue as in the adsorption experiments (10 mg biosorbent, 10 mL of a 50 mgL⁻¹ methylene blue solution, stirred at 150 rpm for 1 h, at pH 7.00 and 25 ± 2 °C). The mixture of the biosorbent and the loaded dye was centrifuged for 5 min at 3500 × g, the supernatant was removed, and the amount of adsorbed dye was determined using Equation 1. Then, 10 mL of 0.200 mol L⁻¹ HCl solution was added to the dye-loaded material and agitated for 1 h at 150 rpm. Finally, a 200 µL aliquot of the supernatant was removed and diluted in 5000 µL of deionized water to determine the desorbed dye concentration. The remaining material was vacuum filtered and washed with deionized water up to pH 7.00. and reused in batches for 5 successive adsorption/desorption cycles.

All adsorption tests were performed in triplicate and the quantification of the methylene blue in the solutions was performed using UV-vis molecular absorption spectrophotometry at a 665 nm wavelength.

3. RESULTS AND DISCUSSION

3.1 Biosorbent characterization

3.1.1 Infrared spectroscopy

The surface of a chemically modified biosorbent can modulate the specific number of active bonding sites in the material, improving its ion exchange properties and its adsorption capacity [27]. Infrared spectroscopy can provide important information on the chemical modifications due to the alkaline treatment of the biosorbents obtained from the atemoya peels. Figure 1 shows the infrared spectra of the prepared biosorbents. The main functional groups on the surfaces of these materials that influence adsorption behavior can be identified.

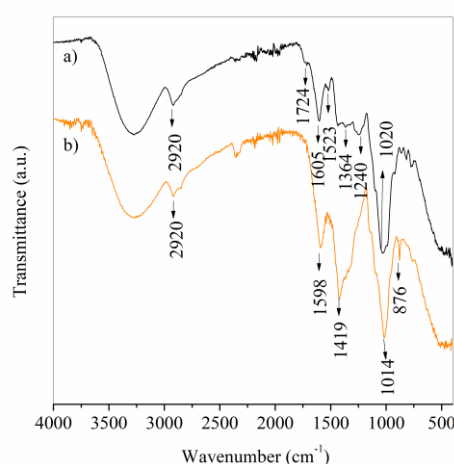


Figure 1 - Infrared spectra of the atemoya biosorbent samples that were a) untreated and b) alkaline-treated.

The wide bands between 3000 and 3600 cm^{-1} observed in the infrared spectra of the alkaline-treated and untreated atemoya peel materials are related to the vibrational elongation of the O–H bond of the hydroxyls in lignin, cellulose, and water [28, 29]. The band at 2920 cm^{-1} in both spectra corresponds to the strain vibrations of C–H bonds in alkanes, aliphatic acids, and aldehydes, which are bonds of cellulose, hemicellulose, and lignin structures [30, 31]. The band at 1724 cm^{-1} is related to the symmetrical stretching of the keto tautomer of carbonyl C=O in cellulose, hemicellulose, and lignin [32] and is present only in the spectrum of the untreated biosorbent. This band disappears after alkaline treatment, suggesting that this process partially removes the non-cellulosic compounds from the atemoya peel. Accordingly, the band related to the elongation vibration of the C=C bonds in the aromatic rings of the lignin structure, observed at 1605 cm^{-1} in the untreated material, shifted to 1598 cm^{-1} after alkaline treatment. This confirms that a compositional modification is caused by the alkaline treatment applied to the atemoya peel and is related to the partial solubilization of lignin [33].

This hypothesis is also corroborated by observed changes in the biosorbent spectra at 876 and 1014 cm^{-1} . The band at 1014 cm^{-1} is associated with cellulose and hemicellulose C–O vibrations [34], as well as aromatic and vinyl ethers present in the flavonoids characteristic of the *Annona* species, and appeared after the alkaline treatment. In the material *in natura*, this band is superimposed on the 1020 cm^{-1} band and is associated with the angular deformation vibrations of C–H bonds in the planes of lignin aromatic rings. In addition, the bands at 1423 and 1364 cm^{-1} in both spectra, with differing intensities, correspond to the angular deformations of $-\text{CH}_3$ and $-\text{CH}_2$ adjacent to carbonyl, respectively.

3.1.2 Thermogravimetric analyses

Thermogravimetric analyses (TGA) were performed to assess the thermal stability of the untreated (Figure 2-a) and alkaline-treated (Figure 2-b) biosorbents.

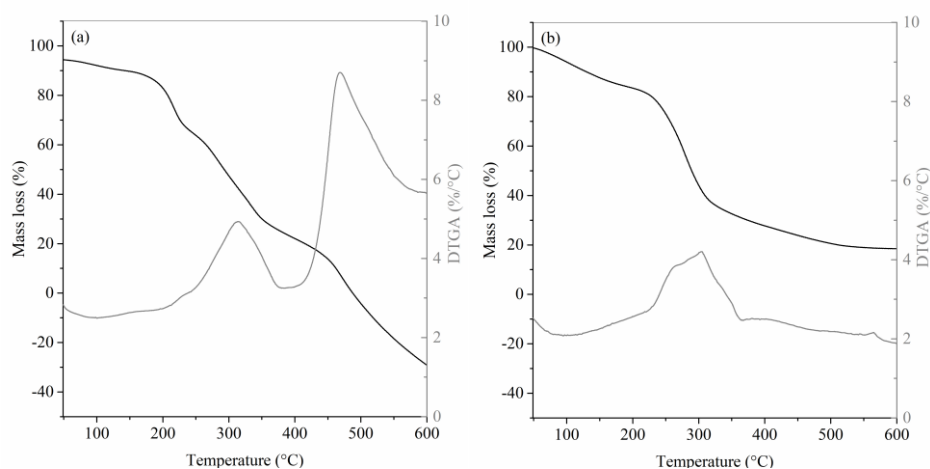


Figure 2 - Thermogravimetric analyses of the a) untreated and b) alkaline-treated atemoya biosorbent.

The TGA thermogram profiles of the materials were very different, confirming that the alkaline treatment modified the composition of the biosorbent. The elimination of low molar mass volatile compounds and surface-adsorbed water from the biosorbent occurred between 50 and 183 °C in the untreated material (Figure 2-a) and between 50 and 229 °C in the alkaline-treated material (Figure 2-b), with 14 and 20% losses in mass, respectively.

The thermal decomposition stages of the materials were observed at temperatures above those at which volatilization compounds were eliminated. For biomass *in natura*, the stages at which the largest mass losses occurred started at 270 °C and were associated with the decomposition of the extractives composed of hemicellulose (271°C, 58%) and cellulose (315 °C, 42%). The decomposition of lignin and other compounds occurred above 466 °C (8%) [35], and at 488 °C the material was completely degraded.

The thermal stability of the material increased after the alkaline treatment, starting at 314 °C (38%). This was probably due to the loss of part of the hemicellulose content, which has a lower thermal stability than cellulose [36] possibly due to a lower crystallinity. The complete decomposition of the organic material in the alkaline treated biosorbent occurred at 600 °C. Above this temperature (data not shown), the mass remained constant, leaving ~20% of the mass as ash. The production of ash in the decomposition process indicates that the protonated acid groups of the material *in natura* were ionized during the alkaline treatment, leading to the formation of complexes with sodium ions.

3.1.3 Scanning electron microscopy

The microstructures of the untreated (Figure 3-a) and alkaline-treated atemoya biosorbents (Figure 3-b) were observed using scanning electron microscopy at 300x magnification.

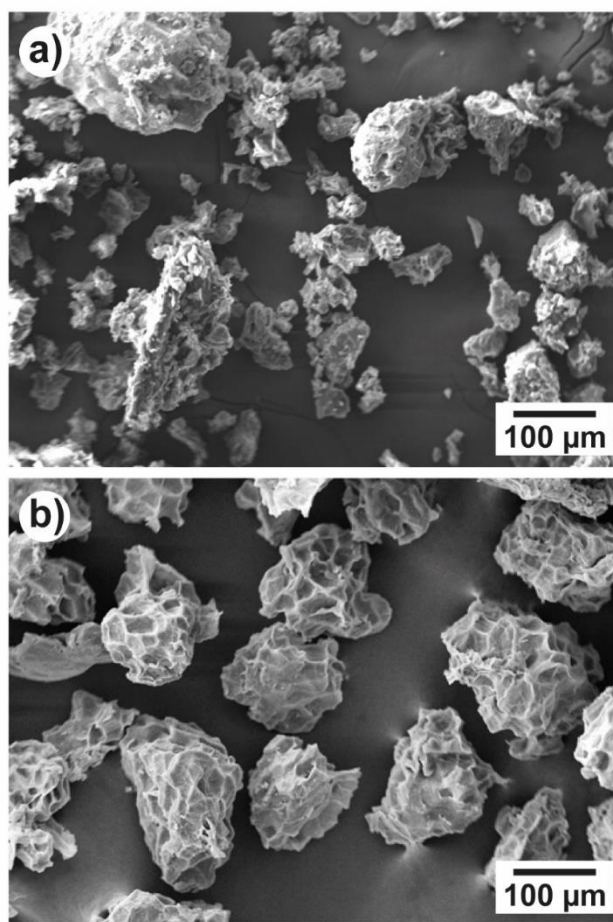


Figure 3 - Scanning electron microscope images of the (a) untreated and (b) alkaline-treated atemoya peels.

The material *in natura* (Figure 3-a) exhibited an irregular surface, with cracks and pores of varying diameters and depths, many of which were obstructed, characterizing a heterogeneous surface. After the alkaline treatment, the material exhibited a rougher surface (Figure 3-b). Moreover, the treatment seems to have promoted the opening of the pores, leading to a larger specific surface area that was configured as a favorable modification for the adsorption of larger molecules in solution. This process must have been associated with the dissolution of lignocellulosic and hemicellulose components by the NaOH solution, which can cause swelling of the fibers and results in an increase in the internal surface area [37]. These observations suggest that treating atemoya peels with 1 mol L^{-1} NaOH modified the biomass properties that favor their use in adsorption processes, as previously reported in studies of other adsorbents [38].

3.2 Effect of pH on methylene blue removal capacity

pH is an important parameter regarding the removal capacity of an adsorbent, as it affects both the adsorbate charge distribution in the solution and the adsorbent surface charge distribution,

especially because of the protonation/deprotonation processes of the acid and basic surface functional groups [39]. Thus, the pH of the zero-charge point (pH_{ZCP}) is an important parameter for obtaining qualitative information about the liquid charge of an adsorbent as a function of pH, enabling the understanding of adsorption behavior at different pH values. The pH_{ZCP} of the untreated (*in natura*) and alkaline-treated materials were determined using the solid addition method, as shown in Figure 4.

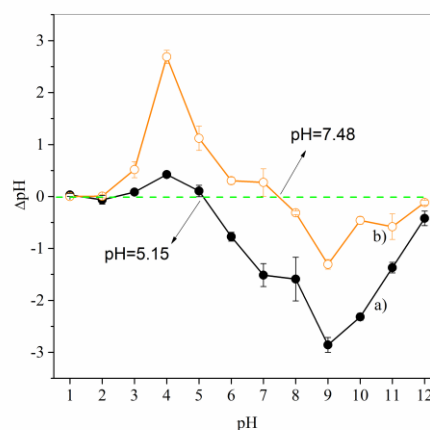


Figure 4 - pH of zero-charge points (pH_{ZCP}) of the a) untreated and b) alkaline-treated atemoya biosorbents.

The untreated and alkaline-treated materials had pH_{ZCP} values of 5.15 and 7.48, respectively. At pH values below the pH_{ZCP} , the adsorbent surface has a positive liquid charge, with a greater capacity for adsorbing anionic species, while above the pH_{ZCP} the liquid charge is negative, favoring the adsorption of cationic species such as methylene blue [40].

The increase in the pH_{ZCP} of the modified material is in accordance with the loss of organic matter content (hemicelluloses and lignin), which resulted in the loss of acid groups with low pK_a values in hemicelluloses and a consequent increase in the specific number of basic sites of the material. Although the working pH range suitable for cation adsorption decreased in the modified biosorbent (*i.e.*, a $\text{pH} > 7.48$ compared to a $\text{pH} > 5.15$ of the untreated material), it is expected that neutral to slightly basic media will result in a good removal capacity for the alkaline-treated material. The reason for this is that the microstructural modification of the biosorbent promoted by the alkaline treatment can compensate for the loss of the acid groups. Analyses of the effect of pH on the adsorption of methylene blue by the biosorbents were conducted to confirm this hypothesis and are presented in Figure 5.

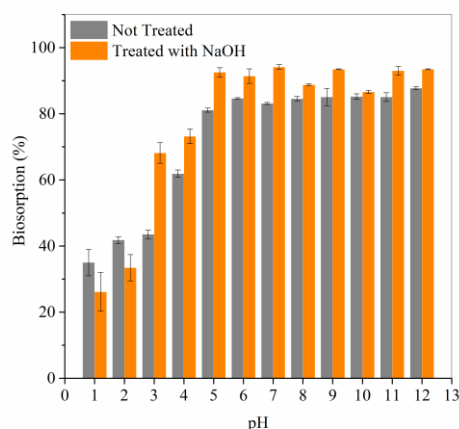


Figure 5 - Effect of pH on the removal of methylene blue (20 mg L^{-1}) by biosorbents obtained from atemoya peels. The mixtures were stirred at room temperature ($25 \pm 2 \text{ }^\circ\text{C}$) for 12 h at 150 rpm.

For both adsorbents, the percentage of biosorption increased with an increase in pH, remaining constant for pH values above 5.00. The material *in natura* yielded dye removal capacities of 81–88% in a pH range of 5.00–12.00, while the alkaline-treated material yielded removal capacities of 86–94% in the same pH range. Although the removal of methylene blue using the modified biosorbent at higher pH values was more efficient, the material *in natura* adsorbed the methylene blue better at pH values below 3.00. This suggests that a change in the surface charge density of the materials occurred that was mediated by the pH.

According to Yanishpolskii et al. (2000), the pK_a value of the methylene blue molecule cannot be experimentally determined since it is above a pH of 13.00. Its high alkalinity forces its ions to behave in a similar manner as alkaline metal ions, holding a positive charge in all investigated pH ranges. Thus, the lower removal percentages of the methylene blue model dye for pH values below 5.00 result from electrostatic repulsion between the adsorbate and the surface of the adsorbents (also positively charged), since in this range the pH is lower than the pH_{ZCP} values of the two biosorbents.

At pH values of 1.00 and 2.00, the removal of part of the hemicellulose and lignin fractions from the treated material increased the specific fraction of protonable sites on its surface. This promoted a greater competition of H^+ ions at high concentrations at the adsorption sites on the material, increasing the positive surface charge and leading to lower removal percentages than those of the untreated material. When the pH was increased to 3.00, the positive surface charge was reduced, decreasing the electrostatic repulsion between the dye and the surface while reducing the competition of H^+ ions at the adsorption sites. Under these conditions, the alkaline-treated material had the highest methylene blue dye removal rates, reinforcing the concept that the alkaline treatment modified the microstructure of the material.

A pH of 7.00 was chosen for the other analyses because it yielded high removal percentages and does not require a pH adjustment for disposal after biosorbent use in potential textile effluent dye removal applications.

3.3 Adsorption kinetics

Evaluating the kinetic parameters is an important factor for describing the effectiveness of an adsorption process. The kinetic model cannot only estimate the adsorption rate, but can also provide evidence of the possible mechanisms involved [41, 42]. The kinetic adsorption behaviors of the methylene blue model molecule in untreated (Figure 6-a) and alkaline-treated biosorbents (Figure 6-b) were monitored for 210 min at a pH of 7.00 and at temperatures of 25, 35, 45, and 55 °C.

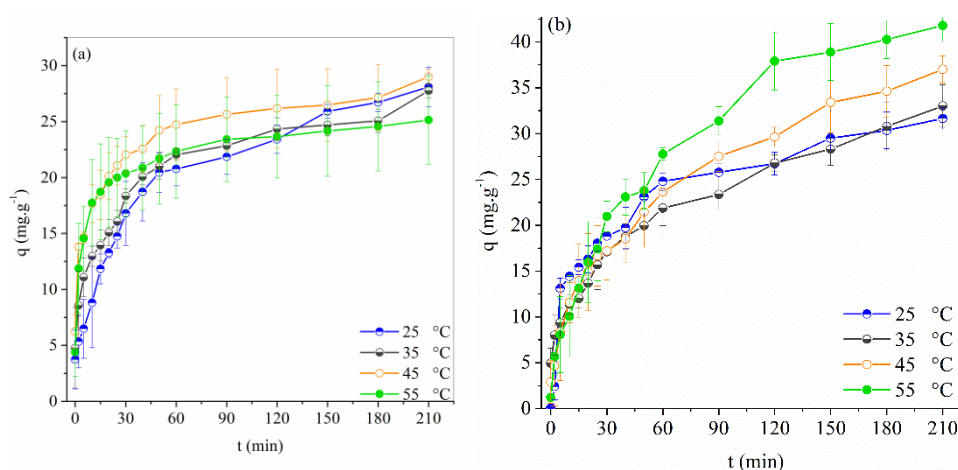


Figure 6 - Effect of contact time on methylene blue removal at different temperatures for the a) untreated and b) alkaline-treated atemoya biosorbents. The mixtures were stirred for 210 min at 150 rpm, an initial pH of 7.00, and an initial 50 mg L^{-1} dye concentration.

The results of the methylene blue adsorption kinetics analyses for both biosorbents indicated a rapid adsorption process in which the highest adsorption rates occurred in the first 60 min of contact between the adsorbent and the adsorbate. Equilibrium was reached at 150 min for both untreated and alkaline-treated materials at 25 °C. This decreased to 90 min for the untreated material and 120 min for the alkaline-treated material when the temperature reached 55 °C. Franco et al. (2020) also identified this biosorption profile when working with *Annona crassiflora* seeds, which has a kinetic profile that shows initial rapid dye removal from the solution, followed by a slower removal process. This can be explained by the fact that more adsorption sites are available on the biosorbent surface [43].

Several kinetic models were used to determine the adsorption mechanism. This study evaluated the pseudo-first order [44, 45], pseudo-second order [45, 46], and intraparticle diffusion

[47] models. The pseudo-first order model assumes non-dissociated molecular adsorption on the surface of the material [44, 45] and is expressed linearly using Equation 3;

$$\frac{q_t}{q_e} = e^{-k_1 t} \quad (3)$$

where q_t (mg g^{-1}) is the adsorption amount at time t (min), q_e (mg g^{-1}) is the amount adsorbed at equilibrium, and k_1 (min^{-1}) is the pseudo-first order speed constant. The kinetic parameters for this model were obtained by plotting $\ln(q_e - q_t)$ vs. t .

The pseudo-second order model assumes an adsorption process by chemisorption [45, 46] and is expressed in its non-linear form as:

$$q_t = \frac{q_e^2 k_2 t}{1 + k_2 t q_e} \quad (4)$$

where q_t (mg g^{-1}) is the adsorption amount at time t (min), q_e (mg g^{-1}) is the amount adsorbed at equilibrium, and k_2 (min^{-1}) is the pseudo-second order constant rate. The kinetic parameters were obtained by plotting $1/q_t$ vs. t .

The intraparticle diffusion model assumes that adsorption depends on the transfer rate of the adsorbate from the solution phase to the surface of the adsorbent particles, and is controlled by one or more steps (e.g., film or external diffusion, pore diffusion, and surface diffusion) [47]. The model is expressed by:

$$q_t = k_{int} t^{1/2} + C \quad (5)$$

where k_{int} is the intraparticle diffusion speed constant ($\text{mg g}^{-1} \text{min}^{-1/2}$) and C (mg g^{-1}) is the intersection of the straight line with the ordinate axis. The value of C provides a quantitative relationship with the thickness of the diffusion limit layer (i.e., the higher the value of C , the greater the effect of the limit layer). By plotting q_t versus $t^{1/2}$, it is possible to calculate the slope of the line, k_{int} . A plot of the intraparticle diffusion model generally exhibits multi-linearity, indicating that two or more adsorption steps can occur. The first step represents immediate adsorption, the second step is a gradual phase, and the third is the final equilibrium phase where speed reduction occurs [48].

The validity of each model was evaluated using the obtained linear regression data, including the correlation coefficient (R^2) and the root mean square (RMS) function, defined by:

$$RMS = \frac{\sqrt{\sum_{i=1}^n (y_i - \hat{y}_i)^2}}{n} \quad (6)$$

where y^{\wedge} are the experimentally determined values, y are the values predicted by the model, and n is the number of analyzed data points. Table 1 shows the evaluated kinetic model parameters and Figures S1, S2, S3, and S4 (Supplementary material) present the graphs with the appropriate adjustments.

Table 1 - Kinetic adsorption parameters of the biosorbents for the methylene blue model molecule

Untreated biosorbent					
Pseudo-first order					
T (K)	q_e exp (mg g⁻¹)	q_e calc (mg g⁻¹)	k_1 (min⁻¹)	R²	RMS
298.15	29.33	21.45	1.26×10^{-02}	0.9678	0.130
308.15	28.02	18.09	1.49×10^{-02}	0.8570	0.143
318.15	32.02	15.13	7.66×10^{-03}	0.8499	0.187
328.15	27.22	10.85	8.79×10^{-03}	0.8208	0.194
Pseudo-second order					
T (K)	q_e exp (mg g⁻¹)	q_e calc (mg g⁻¹)	k_2 (g mg⁻¹ min⁻¹)	R²	RMS
298.15	29.33	30.86	1.29×10^{-03}	0.9911	0.018
308.15	28.02	28.60	2.23×10^{-03}	0.9928	0.029
318.15	32.02	30.51	2.90×10^{-03}	0.9890	0.030
328.15	27.22	26.41	4.65×10^{-03}	0.9953	0.026
Intraparticle diffusion Line 1					
T (K)	C_2 (mg g⁻¹)	k_{int} (mg g⁻¹ min^{-1/2})	R²		
298.15	1.99	2.57	0.9728		
308.15	5.45	2.22	0.9895		
318.15	9.40	2.19	0.9276		
328.15	7.08	3.36	0.9999		
Intraparticle diffusion Line 2					
T (K)	C_2 (mg g⁻¹)	k_{int} (mg g⁻¹ min^{-1/2})	R²		
298.15	11.47	1.14×10^0	0.9719		
308.15	14.49	8.65×10^{-1}	0.8844		
318.15	15.70	9.50×10^{-1}	0.7887		
328.15	17.23	5.90×10^{-1}	0.9550		
Treated biosorbent					
Pseudo-first order					
T (K)	q_e exp (mg g⁻¹)	q_e calc (mg g⁻¹)	k_1 (min⁻¹)	R²	RMS

298.15	37.50	25.75	7.62×10^{-3}	0.9064	0.155
308.15	36.96	28.05	8.74×10^{-3}	0.9823	0.137
318.15	39.75	32.75	1.10×10^{-2}	0.9871	0.113
328.15	43.31	38.40	1.48×10^{-2}	0.9917	0.084
Pseudo-second order					
T (K)	$q_{e \text{ exp}} \text{ (mg g}^{-1}\text{)}$	$q_{e \text{ calc}} \text{ (mg g}^{-1}\text{)}$	$k_2 \text{ (g mg}^{-1} \text{ min}^{-1}\text{)}$	R^2	RMS
298.15	37.50	36.53	1.03×10^{-3}	0.9759	0.046
308.15	36.96	37.40	8.11×10^{-3}	0.9662	0.041
318.15	39.75	42.61	6.27×10^{-4}	0.9760	0.038
328.15	43.31	49.11	5.20×10^{-4}	0.9861	0.026
Intraparticle diffusion Line 1					
T (K)	$C^1 \text{ (mg g}^{-1}\text{)}$	$k_{\text{int}} \text{ (mg g}^{-1} \text{ min}^{-1/2}\text{)}$	R^2		
298.15	2.11	3.06	0.9038		
308.15	4.54	2.20	0.9907		
318.15	1.97	2.94	0.9752		
328.15	0.62	3.41	0.9843		
Intraparticle diffusion Line 2					
T (K)	$C^2 \text{ (mg g}^{-1}\text{)}$	$k_{\text{int}} \text{ (mg g}^{-1} \text{ min}^{-1/2}\text{)}$	R^2		
298.15	8.14	1.74	0.8362		
308.15	3.02	2.12	0.9669		
318.15	5.64	2.20	0.9911		
328.15	13.45	1.99	0.9289		

Based on the correlation coefficient ($R^2 > 0.9662$) and RMS ($\text{RMS} < 0.046$) values, the kinetic studies indicate that the pseudo-second order model provided the best adjustments for the experimental data of both treated and untreated materials independent of the adsorption temperature. This indicates that the reaction mechanism was kinetically controlled by chemical adsorption. The occurrence of chemisorption suggests an exchange or sharing of electrons between the functional groups on the surface of the biosorbent and the methylene blue [49]. The second-order speed constants increased with increasing system temperatures, indicating that an activation energy needs to be supplied for this specific interaction between the adsorbate and adsorbent sites to occur. Removal of methylene blue using *Agrobacterium fabrum* biomass [50] and using apple peels [51], as well as the removal of copper ions using *Annona squamosa* L. seeds [52] exhibit kinetic behaviors similar to those observed in this study.

The intraparticle diffusion graphs (q_t vs. $t^{1/2}$ curves) for the dye adsorption by the adsorbents exhibited two stages (Figures S5 a, b, c, and d and S6 a, b, c, and d). The lines representing the first

stage of adsorption did not cross the origin ($C_l \neq 0$), indicating that the adsorption was affected by the diffusion of the dye through the solvent layer around the surface of the biosorbents. The obtained k_{int} values increased with temperature in the case of the treated material; however, the untreated material exhibited the opposite behavior. This suggests that the solvent layer around the surface of the material has distinct water molecule solvation structures, probably due to differences in hydrophobicity promoted by the removal of more hydrophilic compounds during the heat treatment. In the final equilibrium stage (second linear region in the q_t vs. $t^{1/2}$ graph), diffusion through the film decreased because of the low dye concentration in the solution and a low number of available adsorption sites on the surface of the biosorbents.

3.4 Adsorption isotherms

Adsorption isotherms provide important information for describing how the adsorbate interacts with active sites on the surface of the adsorbents. The adsorption isotherms of the investigated biosorbents for methylene blue dye are presented in Figure 7.

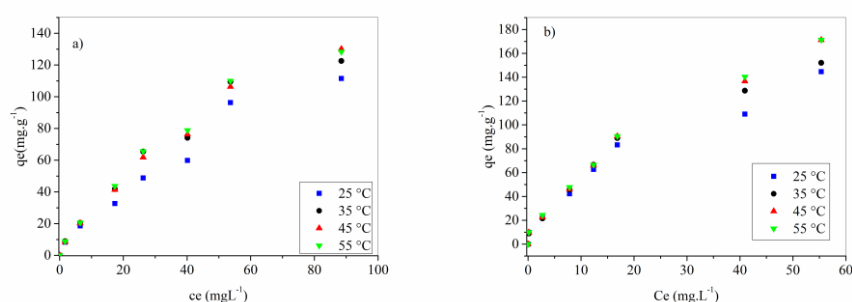


Figure 7 - Isothermal equilibria of the removal of methylene blue at different temperatures for the a) untreated and b) alkaline-treated atemoya biosorbent. The mixtures were stirred for 12 h at 150 rpm, with an initial pH of 7.00 and different initial concentrations (10, 25, 50, 75, 100, 150 and 200 mgL^{-1})

The isotherms obtained for the untreated and alkaline-treated biosorbents have ascending profiles with a decrease in the adsorption rate with C_e , which can be explained by a decrease in the availability of adsorption sites as the equilibrium concentration increases. In the case of the untreated biosorbent (Figure 7-a), at lower equilibrium concentrations the temperature did not affect the amount adsorbed. As the equilibrium concentration increased, the temperature increase slightly increased the amount adsorbed. In the case of the alkaline-treated biosorbent isotherms (Figure 7-b), the adsorption was constant at all temperatures and an equilibrium concentration of 75 mgL^{-1} .

The experimental methylene blue adsorption data were adjusted using the linear forms of the Langmuir, Freundlich, Dubinin-Radushkevich, and Temkin models. The Langmuir model is valid for monolayer adsorption on a homogeneous surface [53] and is represented by Eq. 7.

$$\frac{C_e}{q_e} = \frac{1}{q_m K_L} + \frac{1}{q_m} C_e \quad (7)$$

where q_e is the amount adsorbed at equilibrium (mg g^{-1}), C_e is the dye equilibrium concentration of the solution (mgL^{-1}), K_L is the Langmuir constant, and q_m represents the maximum adsorption capacity (mg g^{-1}).

The Freundlich model adequately describes the adsorption on energetically heterogeneous surfaces with the linear form of the Freundlich isotherm [54] as shown in Equation 8:

$$\ln q_e = \ln K_F + \frac{1}{n_F} \ln C_e \quad (8)$$

where q_e and C_e have the same meaning as those parameters in the Langmuir isotherm and K_F and n_F are the constants related to the Freundlich adsorption capacity and intensity, respectively.

The Dubinin-Radushkevich (D-R) isotherm is similar to the Langmuir isotherm with respect to adsorption occurring in a single layer. However, it is more general because it does not assume a homogeneous surface or a constant adsorption potential [55-57]. Equation 9 is the linear expression of the D-R isotherm:

$$\ln q_e = \ln q_s - K_{DR} \varepsilon^2 \quad (9)$$

where q_e is the amount of adsorbed solute and q_s is the adsorption capacity, both in mgg^{-1} , and K_{DR} is the constant associated with the adsorption energy ($\text{mol}^2 \text{kJ}^{-2}$). The parameter ε is the Polanyi potential and is given by $RT \ln[1 + (1/C_e)]$.

Finally, the Temkin model considers the effects of indirect interactions between the adsorbate molecules on the surface of the adsorbent, assuming that the variation in adsorption enthalpy decreases linearly as the dye adsorbs [55, 56, 58]. The Temkin isotherm in its linear form is given by Equation 10:

$$q_e = b_T \ln K_T + b_T \ln C_e \quad (10)$$

where parameters q_e and C_e have the same meanings as in the Langmuir isotherm, K_T is the bonding equilibrium constant (L g^{-1}) and b_T is a constant associated with the variation in adsorption enthalpy. Table 2 shows the adjusted isotherm parameters for all of the evaluated models in the studied mixtures. Figures S7, S8, S9, S10, S11, S12, S13, and S14 (Supplementary material) display the adjustments made for each model.

Table 2 - Adsorption isotherms of the biosorbents for the methylene blue model molecule. Methylene blue concentrations (10; 25; 50 ;75; 100; 150 and 200 mgL⁻¹), initial pH = 7.00, 12 h stirring at 150 rpm.

Untreated					
Langmuir					
T (K)	q _m (mg g ⁻¹)	K _L (L mg ⁻¹)	R ²	RMS	
298.15	177.89	1.69 x 10 ⁻²	0.7244	0.076	
308.15	157.08	4.62 x 10 ⁻²	0.9420	0.070	
318.15	190.18	3.03 x 10 ⁻²	0.9688	0.035	
328.15	168.00	4.59 x 10 ⁻²	0.9501	0.067	
Freundlich					
T (K)	n _F	K _F [mg g ⁻¹ (L mg ⁻¹) ^{1/n}]	R ²	RMS	
298.15	1.48	5.39	0.9873	0.036	
308.15	1.59	9.97	0.9359	0.078	
318.15	1.40	7.48	0.9702	0.057	
328.15	1.51	9.87	0.9235	0.091	
D-R					
T (K)	q _s (mol kg ⁻¹)	K _{DR} (kJ ² mol ⁻²)	R ²	RMS	E (kJ mol ⁻¹)
298.15	2.961	5.37 x 10 ⁻³	0.9776	0.048	1.04 x 10 ⁻¹
308.15	3.665	4.62 x 10 ⁻³	0.9503	0.070	9.61 x 10 ⁻²
318.15	5.429	4.97 x 10 ⁻³	0.9825	0.044	9.97 x 10 ⁻²
328.15	4.695	4.31 x 10 ⁻³	0.9440	0.078	9.28 x 10 ⁻²
Temkin					
T (K)	b _T (mol kg ⁻¹)	K _T (L mol ⁻¹)	R ²	RMS	
298.15	0.08058	1.34 x 10 ⁵	0.8207	0.312	
308.15	0.08800	2.59 x 10 ⁵	0.9149	0.254	
318.15	0.10110	1.78 x 10 ⁵	0.9432	0.277	
328.15	0.09640	2.42 x 10 ⁵	0.9511	0.236	
Treated					
Langmuir					
T (K)	q _m (mg g ⁻¹)	K _L (L mg ⁻¹)	R ²	RMS	
298.15	168.83	6.15 x 10 ⁻²	0.8546	0.132	
308.15	239.61	4.17 x 10 ⁻²	0.8455	0.074	
318.15	264.50	5.73 x 10 ⁻²	0.5084	0.140	
328.15	189.94	1.59 x 10 ⁻¹	0.7343	0.174	

Freundlich					
T (K)	n_F	K_F [mg g⁻¹ (L mg⁻¹)^{1/n}]	R²	RMS	
298.15	2.17	19.49	0.9584	0.073	
308.15	1.27	10.49	0.9257	0.102	
318.15	1.76	22.78	0.9207	0.115	
328.15	2.53	38.74	0.9344	0.090	
D-R					
T (K)	q_s (mol kg⁻¹)	K_{DR} (kJ² mol⁻²)	R²	RMS	E (kJ mol⁻¹)
298.15	1.504	3.16 x 10 ⁻³	0.9278	0.099	7.95 x 10 ⁻²
308.15	11.491	5.66 x 10 ⁻³	0.9469	0.085	1.06 x 10 ⁻¹
318.15	3.172	3.30 x 10 ⁻³	0.8915	0.139	8.12 x 10 ⁻²
328.15	1.469	2.00 x 10 ⁻³	0.9044	0.112	6.32 x 10 ⁻²
Temkin					
T (K)	b_T (mol kg⁻¹)	K_T (L mol⁻¹)	R²	RMS	
298.15	0.0655	1.06 x 10 ⁶	0.7580	0.400	
308.15	0.1306	2.42 x 10 ⁵	0.9487	0.294	
318.15	0.0901	1.02 x 10 ⁶	0.6919	0.523	
328.15	0.0623	6.61 x 10 ⁶	0.6721	0.439	

In general, the D-R model presented the best adjustments (high R² values with lower RMS values) for both biosorbents at temperatures of 308.15 and 318.15 K. At 298.15 K, the Freundlich model provided the best adjustments for both materials, while at 328.15 K the isotherm obtained for the material *in natura* fit the Langmuir model better, and the isotherm obtained for the modified material fit the Freundlich model better. Nevertheless, at these temperature extremes, the D-R model also yielded good adjustments and could be used to explain the dye adsorption process on the biosorbents at the evaluated conditions, suggesting an adsorption process involving heterogeneous sites. It is interesting to note that the K_{DR} value tends to be lower at the highest temperatures, indicating larger variations in adsorption free energy under this thermodynamic condition.

The q_m parameter in the Langmuir equation allows the estimation of the maximum adsorption capacities of the biosorbents, which were 190.18 mgg⁻¹ and 264.50 mgg⁻¹ for the untreated and alkaline-treated biosorbents, respectively. A comparison between these capacities and those of other biosorbents studied recently is presented in Table 3, showing that the biosorbents made from the atemoya peel, both alkaline-treated and untreated, can be considered good alternatives for remediating water contaminated with cationic dyes.

Table 3 - Adsorption capacities of the different biosorbents for the methylene blue model molecule

Adsorbent material	pH	T (K)	q_{\max} (mg g ⁻¹)	References
Seed pods from <i>Capparis flexuosa</i>	10.0	298	280.78	[59]
<i>Araticum</i> seed powder	7.5	328	300.90	[60]
Pará chestnut husks	6.5	298	83.8	[61]
Dragon fruit peels	5.6	303	192.31	[62]
Sugarcane bagasse	10.0	298	17.43	[63]
Soursop residue	10.0	298	55.30	[63]
Functionalized peanut husks	8.0	313	43.5	[64]
Brazilian berry seeds	8.0	328	189.60	[65]
Untreated atemoya peels	7.0	318	190.18	This work
Treated atemoya peels	7.0	318	264.50	This work

3.5 Desorption analyses

The reuse of adsorbents is of great importance, as it enables economically viable pollutant removal in water treatment processes. The desorption analyses consisted of removing the methylene blue molecules previously adsorbed, allowing the biosorbent to be reused for the next cycle. Figure 8 shows the dye removal profile for five cycles of adsorption and desorption.

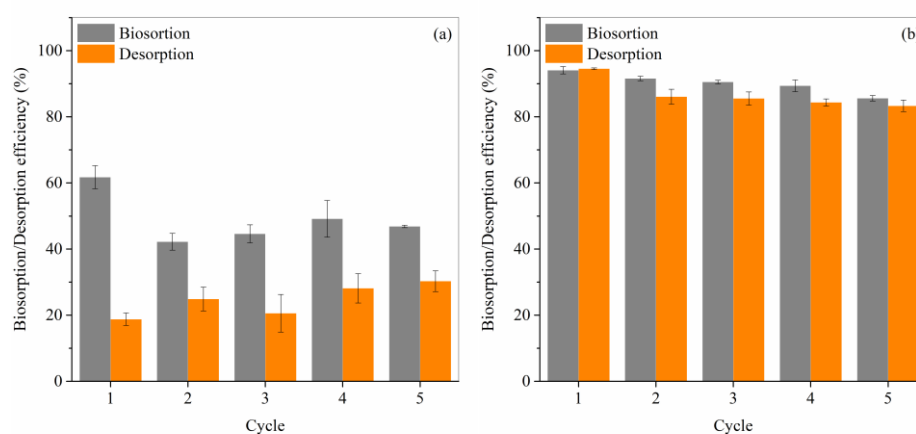


Figure 8 - Efficiency of biosorption/desorption for the a) untreated and b) treated atemoya biosorbents. Methylene blue concentration = 50 mgL⁻¹, initial pH = 7.00, stirred for 1 h at 150 rpm.

The adsorption efficiency for the untreated material was reduced from 61.06% to 41.14% from the first to the second adsorption cycle, remaining practically constant for additional cycles. This may be related to the strong chemical interactions between some functional groups on the untreated material surface and the methylene blue cations. Functional groups are likely capable of developing specific interactions, such as carboxylic groups negatively charged to hemicelluloses. The remaining dye in the untreated material was experimentally visible, since the material had a very dark color (close to black) at the end of the fifth cycle after 1 h of desorption.

The adsorption and desorption efficiencies of the alkaline-treated material remained high for all 5 cycles, presenting only small decreases in removal efficiency from 93.82 to 84.96% and from 92.28% to 82.65% in desorption percentages. In general, the reuse of the modified material proved feasible, since the average efficiencies of the adsorption and desorption processes of the alkaline-treated material were above 80%, indicating the material's potential for low-cost application use.

3.6 Infrared spectra after adsorption of methylene blue

The infrared spectra for the untreated and alkaline-treated materials filled with the adsorbed dye are shown in Figure 9.

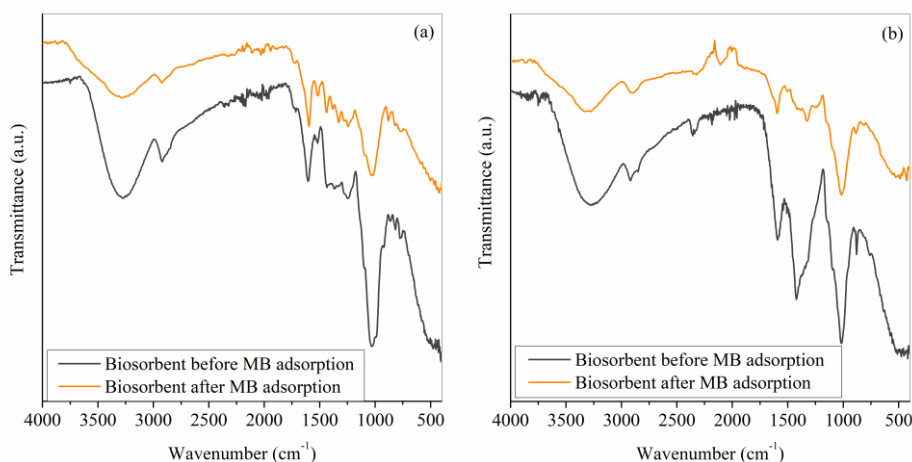


Figure 9 - Infrared spectra of the a) untreated and b) alkaline-treated atemoya biosorbents after adsorption of methylene blue (50 mgL^{-1} , initial pH = 7.00, 12 h constant stirring at 150 rpm, and room temperature ($25 \pm 2 \text{ }^\circ\text{C}$), then filtered and dried in oven at $40 \pm 2 \text{ }^\circ\text{C}$ for 24 h).

Figure 9 shows a significant decrease in the $3100\text{--}3400 \text{ cm}^{-1}$ peak for both biosorbents related to OH vibrational stretching, leading to the belief that this functional group participated in the methylene blue adsorption process. Furthermore, band shifts were observed (Table 4), indicating interactions between methylene blue and both the alkaline-treated and untreated biosorbents. These results provide evidence that the adsorption of methylene blue occurred in materials with and without

alkaline treatment. Xia et al. (2015), working with magnetically modified yeasts and methylene blue adsorption, obtained a similar profile.

Table 4 - Main band shifts observed in the infrared spectra after methylene blue adsorption

Untreated		Alkaline-treated	
Wavelength (cm ⁻¹)		Wavelength (cm ⁻¹)	
Before	After	Before	After
1605	1593	1598	1588
1423/1364	Separation and decrease	1419	1330

4. CONCLUSIONS

The biosorbents prepared from the atemoya peel agricultural waste were characterized using infrared spectra, thermogravimetry, and scanning electronic microscopy, demonstrating that the alkaline-treated biosorbent was more efficient in removing the methylene blue model molecule. Positive changes in the morphology, porosity, thermal stability, and adsorption efficiency of the material were observed. Experimental adsorption data were adjusted using the D–R model and pseudo-second order kinetics over a wide pH range, indicating that the adsorption mechanism is chemisorption. Moreover, the alkaline-treated biosorbent proved to be reusable for at least 5 cycles, with a removal efficiency in the range of 80%, indicating that it is a good low-cost alternative for removing cationic effluents.

5. ACKNOWLEDGEMENTS

The authors would like to thank the Laboratory of Electronic Microscopy and Ultrastructural Analysis of the Federal University of Lavras and Finep, Fapemig, CNPq, and Capes for supplying the equipment and technical support for the experiments involving electron microscopy, as well as the Chemical Analysis and Prospection Center (CAPQ/UFLA). This study was supported in part by the Coordination for the Improvement of Higher Education Personnel - Brazil (CAPES) - Finance Code 001 and Institutional Scientific Initiation Scholarship Program – PIBIC/UFLA.

6. REFERENCES

- [1] S. D. Richardson and T. A. Ternes, "Water Analysis: Emerging Contaminants and Current Issues," *Analytical Chemistry*, vol. 90, no. 1, pp. 398-428, 2018/01/02 2018, doi: 10.1021/acs.analchem.7b04577.
- [2] J. Mateo-Sagasta, S. M. Zadeh, H. Turrall, and J. Burke, *Water pollution from agriculture: a global review. Executive summary*. Rome, Italy: FAO Colombo, Sri Lanka: International Water Management ..., 2017.

- [3] P. A. Carneiro, G. A. Umbuzeiro, D. P. Oliveira, and M. V. B. Zanoni, "Assessment of water contamination caused by a mutagenic textile effluent/dyehouse effluent bearing disperse dyes," *Journal of hazardous materials*, vol. 174, no. 1-3, pp. 694-699, 2010.
- [4] A. Tkaczyk, K. Mitrowska, and A. Posyniak, "Synthetic organic dyes as contaminants of the aquatic environment and their implications for ecosystems: A review," *Science of The Total Environment*, vol. 717, p. 137222, 2020.
- [5] A. Bafana, S. S. Devi, and T. Chakrabarti, "Azo dyes: past, present and the future," *Environmental Reviews*, vol. 19, no. NA, pp. 350-371, 2011.
- [6] L. Smoczyński, B. Pierożyński, and T. Mikołajczyk, "The Effect of Temperature on the Biosorption of Dyes from Aqueous Solutions," *Processes*, vol. 8, no. 6, p. 636, 2020.
- [7] P. S. Kumara *et al.*, "A critical review on recent developments in the low-cost adsorption of dyes from wastewater," *Desalin Water Treat*, vol. 172, pp. 395-416, 2019.
- [8] M. Fomina and G. M. Gadd, "Biosorption: current perspectives on concept, definition and application," *Bioresource technology*, vol. 160, pp. 3-14, 2014.
- [9] M. Vithanage, S. S. Mayakaduwa, I. Herath, Y. S. Ok, and D. Mohan, "Kinetics, thermodynamics and mechanistic studies of carbofuran removal using biochars from tea waste and rice husks," *Chemosphere*, vol. 150, pp. 781-789, 2016.
- [10] P. T. Juchen, H. H. Piffer, M. T. Veit, G. da Cunha Gonçalves, S. M. Palácio, and J. C. Zanette, "Biosorption of reactive blue BF-5G dye by malt bagasse: kinetic and equilibrium studies," *Journal of Environmental Chemical Engineering*, vol. 6, no. 6, pp. 7111-7118, 2018/12/01/ 2018, doi: <https://doi.org/10.1016/j.jece.2018.11.009>.
- [11] A. Khadir, M. Negarestani, and H. Ghiasinejad, "Low-cost sisal fibers/polypyrrole/polyaniline biosorbent for sequestration of reactive orange 5 from aqueous solutions," *Journal of Environmental Chemical Engineering*, vol. 8, no. 4, p. 103956, 2020/08/01/ 2020, doi: <https://doi.org/10.1016/j.jece.2020.103956>.
- [12] C. S. T. Araújo, I. L. S. Almeida, H. C. Rezende, S. M. L. O. Marcionilio, J. J. L. León, and T. N. de Matos, "Elucidation of mechanism involved in adsorption of Pb (II) onto lobeira fruit (*Solanum lycocarpum*) using Langmuir, Freundlich and Temkin isotherms," *Microchemical Journal*, vol. 137, pp. 348-354, 2018.
- [13] W.-T. Tsai, C.-H. Hsu, and Y.-Q. Lin, "Highly porous and nutrients-rich biochar derived from dairy cattle manure and its potential for removal of cationic compound from water," *Agriculture*, vol. 9, no. 6, p. 114, 2019.
- [14] N. E.-A. El-Naggar and N. H. Rabei, "Bioprocessing optimization for efficient simultaneous removal of methylene blue and nickel by *Gracilaria* seaweed biomass," *Scientific Reports*, vol. 10, no. 1, pp. 1-21, 2020.

- [15] N. Mokhtar, E. A. Aziz, A. Aris, W. F. W. Ishak, and N. S. Mohd Ali, "Biosorption of azo-dye using marine macro-alga of *Euchema Spinosum*," *Journal of Environmental Chemical Engineering*, vol. 5, no. 6, pp. 5721-5731, 2017/12/01/ 2017, doi: <https://doi.org/10.1016/j.jece.2017.10.043>.
- [16] J. M. Pérez-Morales, G. Sánchez-Galván, and E. J. Olguín, "Continuous dye adsorption and desorption on an invasive macrophyte (*Salvinia minima*)," *Environmental Science and Pollution Research*, vol. 26, no. 6, pp. 5955-5970, 2019.
- [17] R. M. Novais, G. Ascensao, D. M. Tobaldi, M. P. Seabra, and J. A. Labrincha, "Biomass fly ash geopolymer monoliths for effective methylene blue removal from wastewaters," *Journal of Cleaner Production*, vol. 171, pp. 783-794, 2018.
- [18] Z. Kariuki, J. Kiptoo, and D. Onyancha, "Biosorption studies of lead and copper using rogers mushroom biomass '*Lepiota hystrix*'," *South African Journal of Chemical Engineering*, vol. 23, pp. 62-70, 2017.
- [19] J. F. Morton, *Fruits of warm climates*. JF Morton, 1987.
- [20] D. Baron, A. C. E. Amaro, A. C. Macedo, C. S. F. Boaro, and G. Ferreira, "Physiological changes modulated by rootstocks in atemoya (*Annona x atemoya* Mabb.): gas exchange, growth and ion concentration," *Brazilian Journal of Botany*, vol. 41, no. 1, pp. 219-225, 2018.
- [21] P. A. de Souza, R. V. da Silva Freitas, E. M. Batista, F. B. da Costa, and P. B. Maracajá, "Armazenamento de atemoias, *Annona squamosa* x *Annona cherimola*, recobertas com filme PVC," *Revista Verde de Agroecologia e Desenvolvimento Sustentável*, vol. 10, no. 5, p. 39, 2015.
- [22] G. M. C. Silva, M. P. S. da Silva, M. A. Biazatti, P. C. dos Santos, N. M. da Silva, and G. P. Mizobutsi, "Uso do 1-MCP e atmosfera modificada na pós-colheita de atemoia '*Gefner*'," *Revista Brasileira de Ciências Agrárias*, vol. 11, no. 2, pp. 67-72, 2016.
- [23] L. S. d. Cruz, R. Z. Lima, C. M. P. d. Abreu, A. D. Corrêa, and L. d. M. A. Pinto, "Physical and chemical characterization of fractions of fruit atemoya Gefner," *Ciência Rural*, vol. 43, no. 12, pp. 2280-2284, 2013.
- [24] C. J. Cooksey, "Quirks of dye nomenclature. 8. Methylene blue, azure and violet," *Biotechnic & Histochemistry*, vol. 92, no. 5, pp. 347-356, 2017.
- [25] P. Biehl, M. von der Lühe, and F. H. Schacher, "Reversible Adsorption of methylene blue as cationic model cargo onto polyzwitterionic magnetic nanoparticles," *Macromolecular Rapid Communications*, vol. 39, no. 14, p. 1800017, 2018.
- [26] M. Rafatullah, O. Sulaiman, R. Hashim, and A. Ahmad, "Adsorption of methylene blue on low-cost adsorbents: a review," *Journal of hazardous materials*, vol. 177, no. 1-3, pp. 70-80, 2010.
- [27] L. Ramrakhiani, S. Ghosh, and S. Majumdar, "Surface modification of naturally available biomass for enhancement of heavy metal removal efficiency, upscaling prospects, and management aspects of spent biosorbents: a review," *Applied biochemistry and biotechnology*, vol. 180, no. 1, pp. 41-78, 2016.

- [28] M. A. Mohamed *et al.*, "Physicochemical characterization of cellulose nanocrystal and nanoporous self-assembled CNC membrane derived from Ceiba pentandra," *Carbohydrate polymers*, vol. 157, pp. 1892-1902, 2017.
- [29] H. N. Tran, S.-J. You, A. Hosseini-Bandegharaei, and H.-P. Chao, "Mistakes and inconsistencies regarding adsorption of contaminants from aqueous solutions: a critical review," *Water research*, vol. 120, pp. 88-116, 2017.
- [30] G. P. Gerola, N. V. Boas, J. Caetano, C. R. T. Tarley, A. C. Gonçalves, and D. C. Dragunski, "Utilization of passion fruit skin by-product as lead (II) ion biosorbent," *Water, Air, & Soil Pollution*, vol. 224, no. 2, p. 1446, 2013.
- [31] S. Sadaf and H. N. Bhatti, "Batch and fixed bed column studies for the removal of Indosol Yellow BG dye by peanut husk," *Journal of the Taiwan Institute of Chemical Engineers*, vol. 45, no. 2, pp. 541-553, 2014.
- [32] M. Schwanninger, J. C. Rodrigues, and K. Fackler, "A review of band assignments in near infrared spectra of wood and wood components," *Journal of Near Infrared Spectroscopy*, vol. 19, no. 5, pp. 287-308, 2011.
- [33] E. V. Costa *et al.*, "A Pyrimidine- β -carboline and Other Alkaloids from *Annona foetida* with Antileishmanial Activity," *Journal of natural products*, vol. 69, no. 2, pp. 292-294, 2006.
- [34] S. S. Mohtar *et al.*, "Extraction and characterization of lignin from oil palm biomass via ionic liquid dissolution and non-toxic aluminium potassium sulfate dodecahydrate precipitation processes," *Bioresource technology*, vol. 192, pp. 212-218, 2015.
- [35] B. Shanmugarajah, I. M. Chew, N. M. Mubarak, T. S. Choong, C. Yoo, and K. Tan, "Valorization of palm oil agro-waste into cellulose biosorbents for highly effective textile effluent remediation," *Journal of cleaner production*, vol. 210, pp. 697-709, 2019.
- [36] R. L. Singh, P. K. Singh, and R. P. Singh, "Enzymatic decolorization and degradation of azo dyes—A review," *International Biodeterioration & Biodegradation*, vol. 104, pp. 21-31, 2015.
- [37] E. Rojo, M. V. Alonso, J. C. Domínguez, B. D. Saz-Orozco, M. Oliet, and F. Rodriguez, "Alkali treatment of viscose cellulosic fibers from eucalyptus wood: structural, morphological, and thermal analysis," *Journal of Applied Polymer Science*, vol. 130, no. 3, pp. 2198-2204, 2013.
- [38] H. I. Chieng, L. B. L. Lim, and N. Priyantha, "Enhancement of crystal violet dye adsorption on *Artocarpus camansi* peel through sodium hydroxide treatment," *Desalin. Water Treat.*, vol. 58, pp. 320-331, 2017.
- [39] L. B. Carvalho *et al.*, "Removal of the synthetic hormone methyltestosterone from aqueous solution using a β -cyclodextrin/silica composite," *Journal of Environmental Chemical Engineering*, vol. 7, no. 6, p. 103492, 2019/12/01/ 2019, doi: <https://doi.org/10.1016/j.jece.2019.103492>.
- [40] J. R. Regalbuto and J. Robles, "The engineering of Pt/carbon catalyst preparation," *University of Illinois, Chicago*, vol. 1, pp. 1-14, 2004.

- [41] K. Y. Foo and B. H. Hameed, "An overview of landfill leachate treatment via activated carbon adsorption process," *Journal of hazardous materials*, vol. 171, no. 1-3, pp. 54-60, 2009.
- [42] J.-H. Kwak *et al.*, "Biochar properties and lead (II) adsorption capacity depend on feedstock type, pyrolysis temperature, and steam activation," *Chemosphere*, vol. 231, pp. 393-404, 2019.
- [43] M. Kilic, E. Apaydin-Varol, and A. E. Pütün, "Adsorptive removal of phenol from aqueous solutions on activated carbon prepared from tobacco residues: equilibrium, kinetics and thermodynamics," *Journal of Hazardous Materials*, vol. 189, no. 1-2, pp. 397-403, 2011.
- [44] S. K. Lagergren, "About the theory of so-called adsorption of soluble substances," *Sven. Vetenskapsakad. Handlingar*, vol. 24, pp. 1-39, 1898.
- [45] W. Rudzinski and W. Plazinski, "Studies of the kinetics of solute adsorption at solid/solution interfaces: on the possibility of distinguishing between the diffusional and the surface reaction kinetic models by studying the pseudo-first-order kinetics," *The Journal of Physical Chemistry C*, vol. 111, no. 41, pp. 15100-15110, 2007.
- [46] Y.-S. Ho and G. McKay, "Pseudo-second order model for sorption processes," *Process biochemistry*, vol. 34, no. 5, pp. 451-465, 1999.
- [47] W. J. Weber and J. C. Morris, "Kinetics of adsorption on carbon from solution," *Journal of the sanitary engineering division*, vol. 89, no. 2, pp. 31-60, 1963.
- [48] S.-H. Lin and R.-S. Juang, "Heavy metal removal from water by sorption using surfactant-modified montmorillonite," *Journal of hazardous materials*, vol. 92, no. 3, pp. 315-326, 2002.
- [49] S. Rangabhashiyam, S. Lata, and P. Balasubramanian, "Biosorption characteristics of methylene blue and malachite green from simulated wastewater onto *Carica papaya* wood biosorbent," *Surfaces and Interfaces*, vol. 10, pp. 197-215, 2018.
- [50] S. Sharma, A. Hasan, N. Kumar, and L. M. Pandey, "Removal of methylene blue dye from aqueous solution using immobilized *Agrobacterium fabrum* biomass along with iron oxide nanoparticles as biosorbent," *Environmental Science and Pollution Research*, vol. 25, no. 22, pp. 21605-21615, 2018.
- [51] I. Enniya and A. Jourani, "Study of Methylene Blue Removal by a biosorbent prepared with Apple peels," *J. Mater. Environ. Sci.*, vol. 8, no. 12, pp. 4573-4581, 2017.
- [52] R. Sivakumar, P. S. Renganathan, H. M. Helan, and T. Rajachandrasekar, "Removal of copper ion from aqueous solution using seeds of sugar apple (*Annona Squamosa* L.)," 2019.
- [53] I. Langmuir, "The constitution and fundamental properties of solids and liquids. Part I. Solids," *Journal of the American chemical society*, vol. 38, no. 11, pp. 2221-2295, 1916.
- [54] H. Freundlich, "Über die adsorption in lösungen," *Zeitschrift für physikalische Chemie*, vol. 57, no. 1, pp. 385-470, 1907.

- [55] A. O. Dada, A. P. Olalekan, A. M. Olatunya, and O. Dada, "Langmuir, Freundlich, Temkin and Dubinin–Radushkevich isotherms studies of equilibrium sorption of Zn²⁺ unto phosphoric acid modified rice husk," *IOSR Journal of Applied Chemistry*, vol. 3, no. 1, pp. 38-45, 2012.
- [56] D. Balarak, F. K. Mostafapour, H. Azarpira, and A. Joghataei, "Langmuir, Freundlich, Temkin and Dubinin–radushkevich isotherms studies of equilibrium sorption of ampicilin unto montmorillonite nanoparticles," *Journal of Pharmaceutical Research International*, pp. 1-9, 2017.
- [57] S. G. Chen and R. T. Yang, "Theoretical basis for the potential theory adsorption isotherms. The Dubinin-Radushkevich and Dubinin-Astakhov equations," *Langmuir*, vol. 10, no. 11, pp. 4244-4249, 1994.
- [58] M. Temkin and V. Pyzhev, "Kinetics of the synthesis of ammonia on promoted iron catalysts," *Jour Phys Chem (USSR)*, vol. 13, pp. 851-867, 1940.
- [59] L. d. O. Yamil *et al.*, "Transforming pods of the species *Capparis flexuosa* into effective biosorbent to remove blue methylene and bright blue in discontinuous and continuous systems," *Environmental Science and Pollution Research*, pp. 1-14, 2020.
- [60] D. S. P. Franco *et al.*, "Araticum (*Annona crassiflora*) seed powder (ASP) for the treatment of colored effluents by biosorption," *Environmental Science and Pollution Research*, vol. 27, no. 10, pp. 11184-11194, 2020.
- [61] J. Georgin, B. S. Marques, E. C. Peres, D. Allasia, and G. L. Dotto, "Biosorption of cationic dyes by Pará chestnut husk (*Bertholletia excelsa*)," *Water Science and Technology*, vol. 77, no. 6, pp. 1612-1621, 2018.
- [62] A. H. Jawad, A. M. Kadhum, and Y. S. Ngoh, "Applicability of dragon fruit (*Hylocereus polyrhizus*) peels as low-cost biosorbent for adsorption of methylene blue from aqueous solution: kinetics, equilibrium and thermodynamics studies," *Desalin Water Treat*, vol. 109, pp. 231-240, 2018.
- [63] L. Meili *et al.*, "Adsorption of methylene blue on agroindustrial wastes: experimental investigation and phenomenological modelling," *Progress in biophysics and molecular biology*, vol. 141, pp. 60-71, 2019.
- [64] A. A. Aryee *et al.*, "Iminodiacetic acid functionalized magnetic peanut husk for the removal of methylene blue from solution: characterization and equilibrium studies," *Environmental Science and Pollution Research*, pp. 1-15, 2020.
- [65] [65] J. Georgin, D. S. P. Franco, M. S. Netto, D. Allasia, M. L. S. Oliveira, and G. L. Dotto, "Treatment of water containing methylene by biosorption using Brazilian berry seeds (*Eugenia uniflora*)," *Environmental Science and Pollution Research*, pp. 1-13, 2020.
- [66] S. Xia, L. Zhang, G. Pan, P. Qian, and Z. Ni, "Photocatalytic degradation of methylene blue with a nanocomposite system: synthesis, photocatalysis and degradation pathways," *Physical Chemistry Chemical Physics*, vol. 17, no. 7, pp. 5345-5351, 2015.

SUPPLEMENTARY MATERIAL

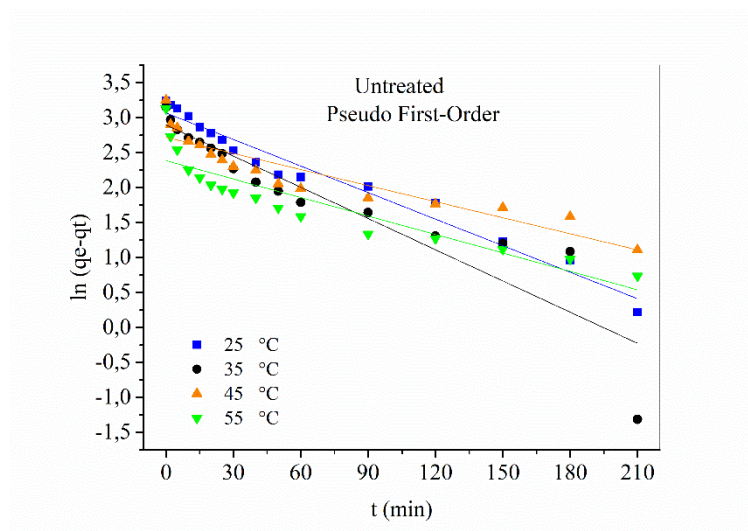


Figure S1 - Effect of contact time on methylene blue removal at different temperatures for the untreated atemoya biosorbents. The mixtures were stirred for 210 min at 150 rpm, an initial pH of 7.00, and an initial 50 mg L^{-1} dye concentration. Model pseudo-first order.

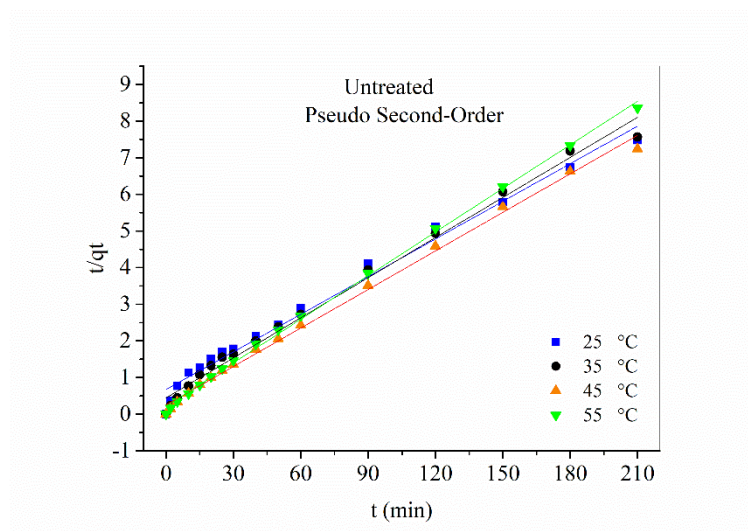


Figure S2 - Effect of contact time on methylene blue removal at different temperatures for the untreated atemoya biosorbents. The mixtures were stirred for 210 min at 150 rpm, an initial pH of 7.00, and an initial 50 mg L^{-1} dye concentration. Model pseudo-second order.

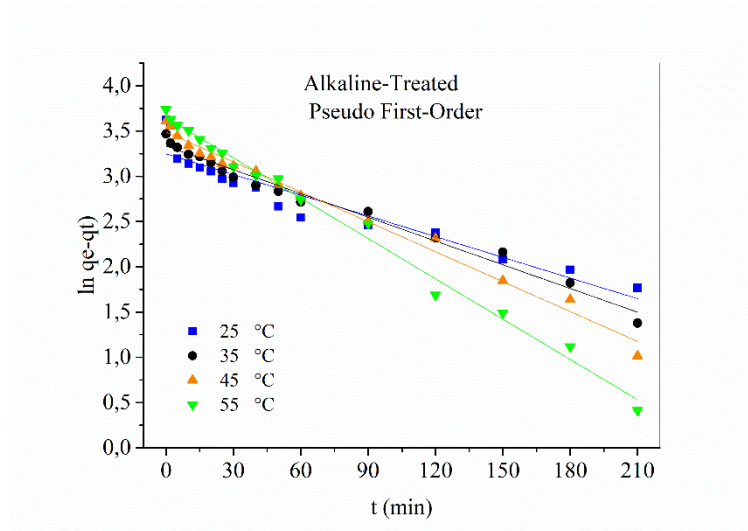


Figure S3 - Effect of contact time on methylene blue removal at different temperatures for the alkaline-treated atemoya biosorbents. The mixtures were stirred for 210 min at 150 rpm, an initial pH of 7.00, and an initial 50 mg L^{-1} dye concentration. Model pseudo-first order.

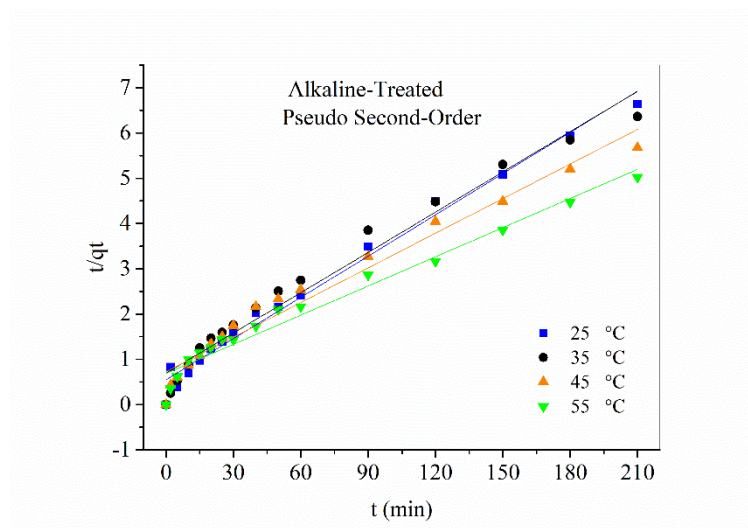
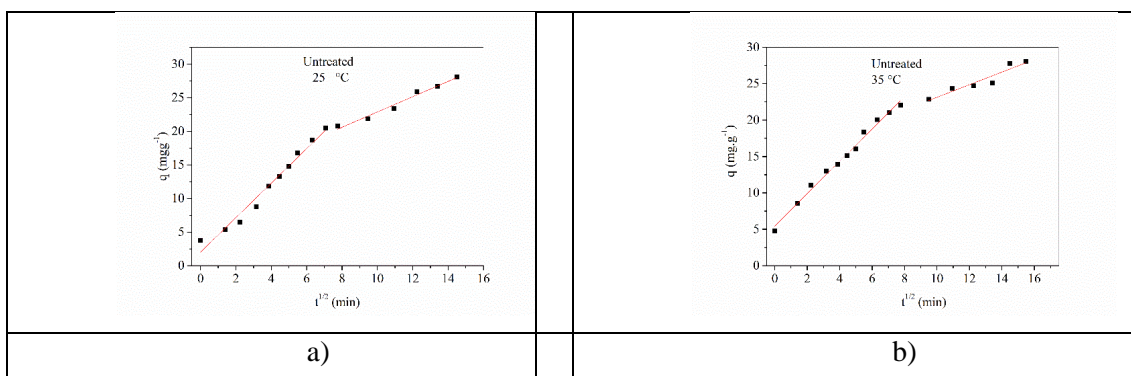


Figure S4 - Effect of contact time on methylene blue removal at different temperatures for the alkaline-treated atemoya biosorbents. The mixtures were stirred for 210 min at 150 rpm, an initial pH of 7.00, and an initial 50 mg L^{-1} dye concentration. Model pseudo-second order.



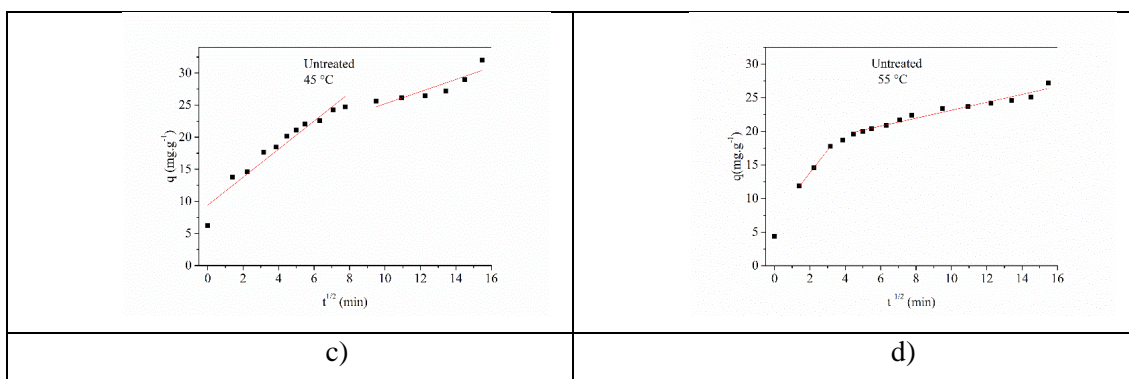


Figure S5 – Intraparticle diffusion untreated atemoya biosorbents a) 25 °C; b) 35 °C; c) 45 °C and d) 55 °C.

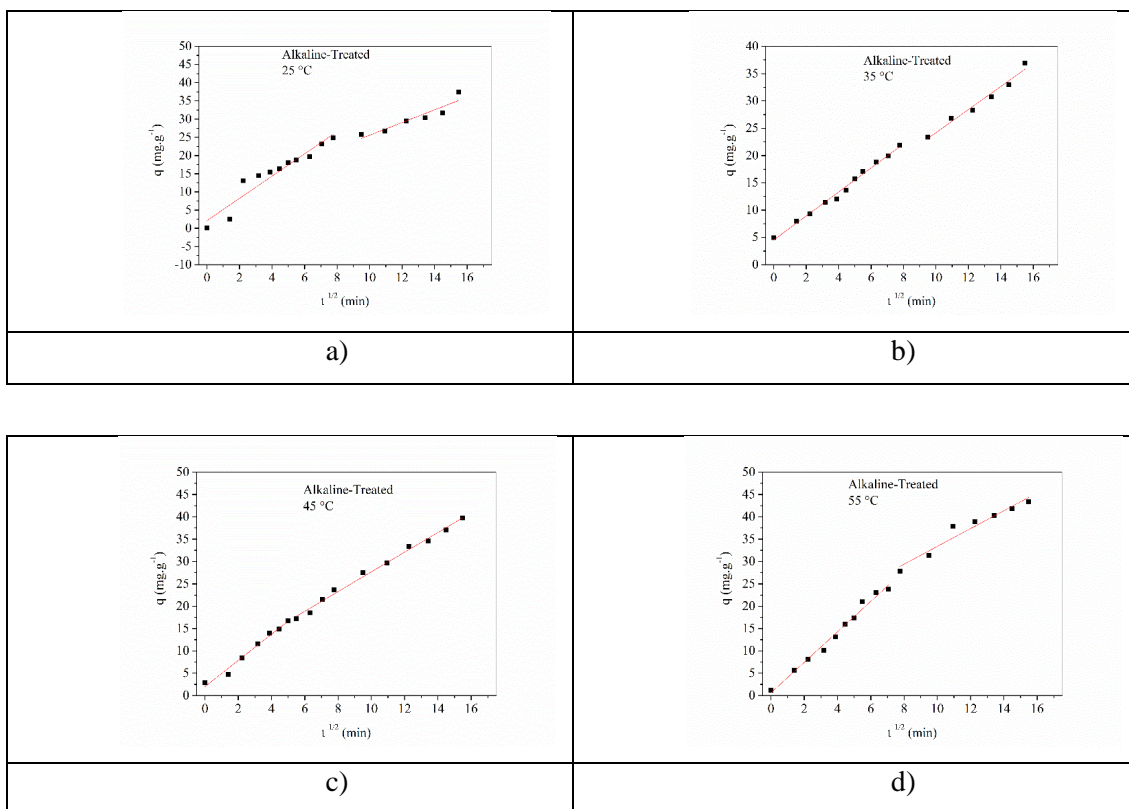


Figure S6 - Intraparticle diffusion alkaline-treated atemoya biosorbents a) 25 °C; b) 35 °C; c) 45 °C and d) 55 °C.

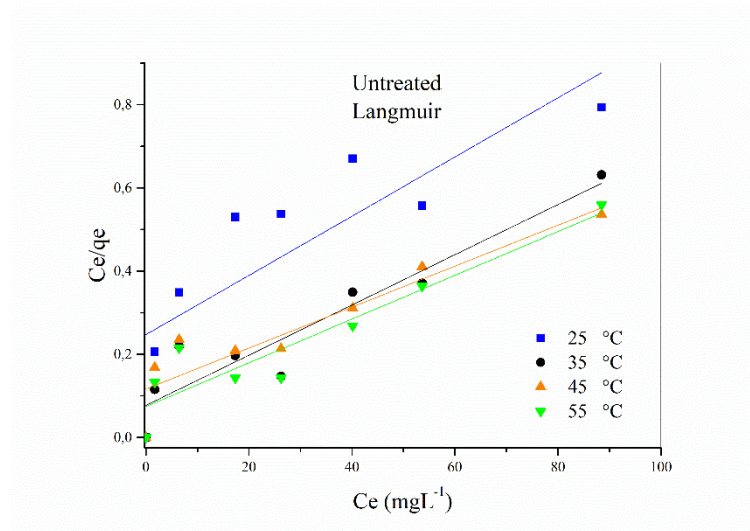


Figure S7 – Isothermal equilibria of the removal of methylene blue at different temperatures for the untreated atemoya biosorbent. The mixtures were stirred for 12 h at 150 rpm, with an initial pH of 7.00 and different initial concentrations (10, 25, 50, 75, 100, 150 and 200 mg L⁻¹). Model Langmuir.

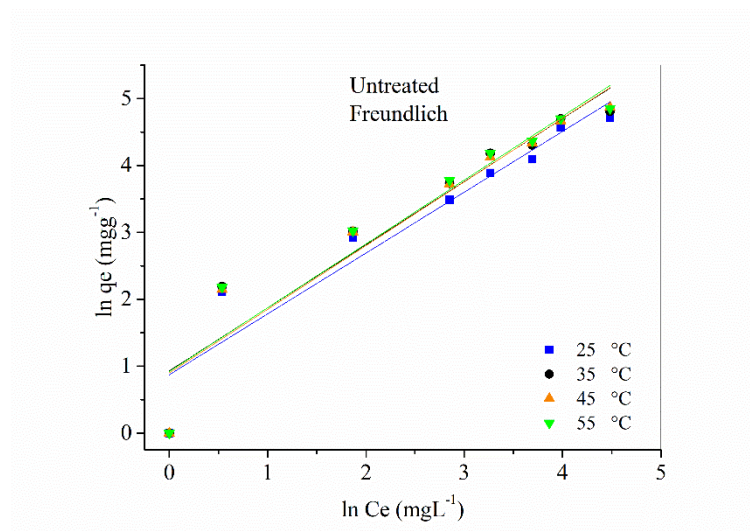


Figure S8 – Isothermal equilibria of the removal of methylene blue at different temperatures for the untreated atemoya biosorbent. The mixtures were stirred for 12 h at 150 rpm, with an initial pH of 7.00 and different initial concentrations (10, 25, 50, 75, 100, 150 and 200 mg L⁻¹). Model Freundlich.

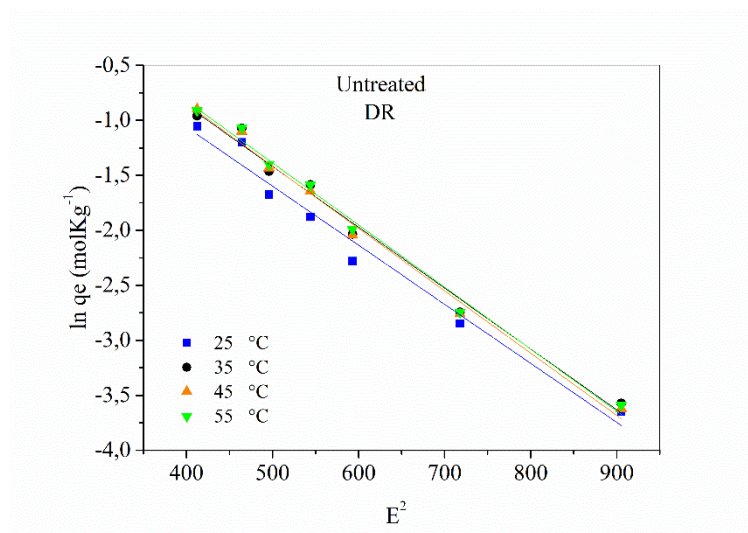


Figure S9 – Isothermal equilibria of the removal of methylene blue at different temperatures for the untreated atemoya biosorbent. The mixtures were stirred for 12 h at 150 rpm, with an initial pH of 7.00 and different initial concentrations (10, 25, 50, 75, 100, 150 and 200 mg L⁻¹). Model DR.

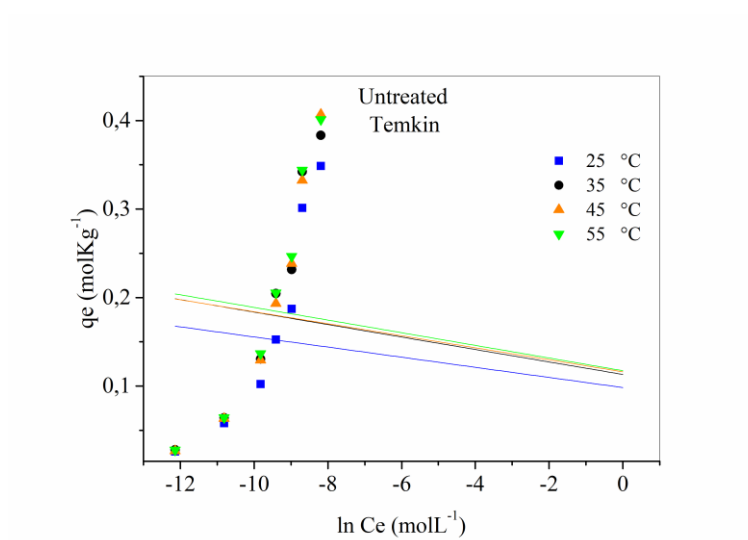


Figure S10 – Isothermal equilibria of the removal of methylene blue at different temperatures for the untreated atemoya biosorbent. The mixtures were stirred for 12 h at 150 rpm, with an initial pH of 7.00 and different initial concentrations (10, 25, 50, 75, 100, 150 and 200 mg L⁻¹). Model Temkin.

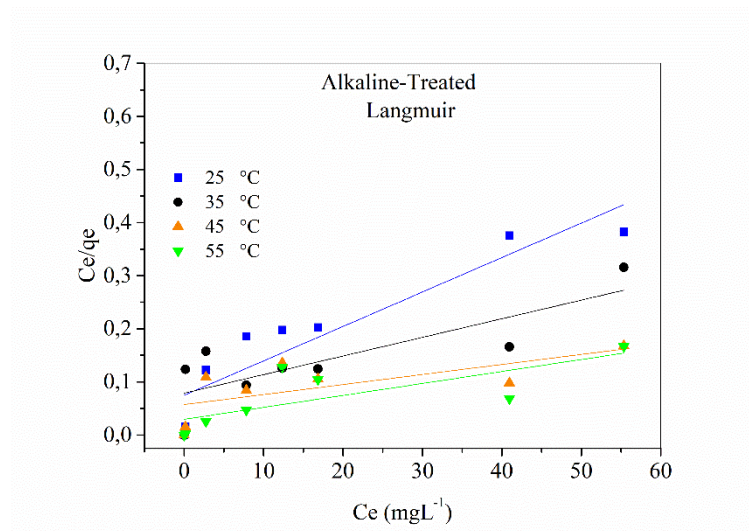


Figure S11 – Isothermal equilibria of the removal of methylene blue at different temperatures for the alkaline - treated atemoya biosorbent. The mixtures were stirred for 12 h at 150 rpm, with an initial pH of 7.00 and different initial concentrations (10, 25, 50, 75, 100, 150 and 200 mg L^{-1}). Model Langmuir.

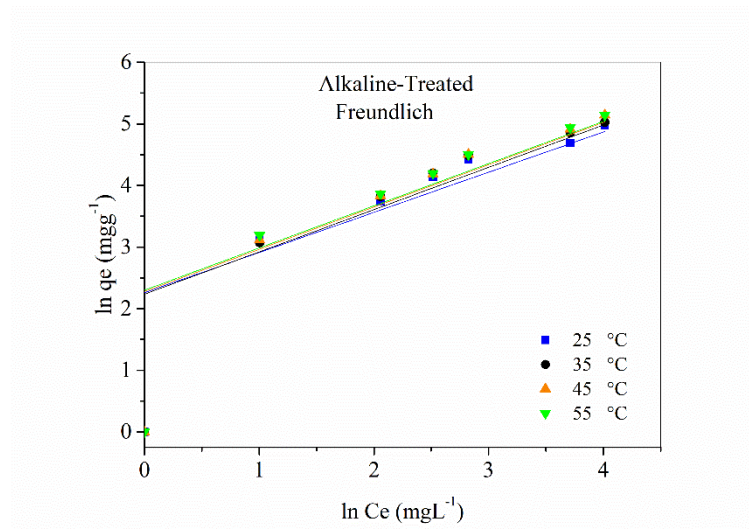


Figure S12 – Isothermal equilibria of the removal of methylene blue at different temperatures for the alkaline - treated atemoya biosorbent. The mixtures were stirred for 12 h at 150 rpm, with an initial pH of 7.00 and different initial concentrations (10, 25, 50, 75, 100, 150 and 200 mg L^{-1}). Model Freundlich.

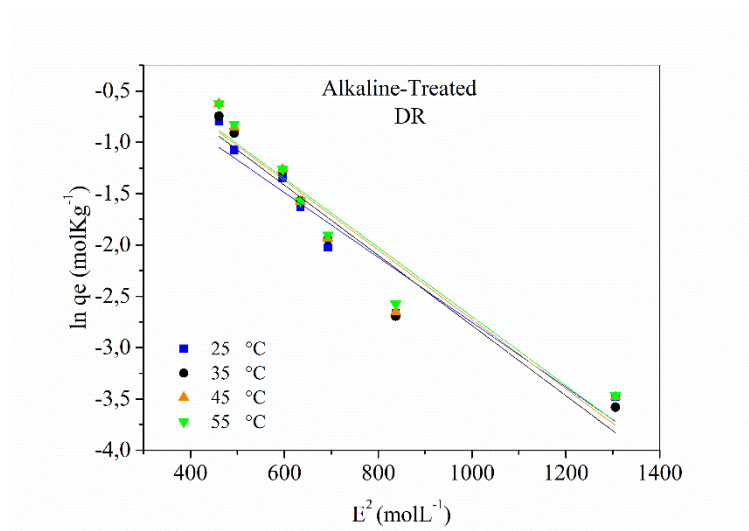


Figure S13 – Isothermal equilibria of the removal of methylene blue at different temperatures for the alkaline - treated atemoya biosorbent. The mixtures were stirred for 12 h at 150 rpm, with an initial pH of 7.00 and different initial concentrations (10, 25, 50, 75, 100, 150 and 200 mg L⁻¹). Model DR.

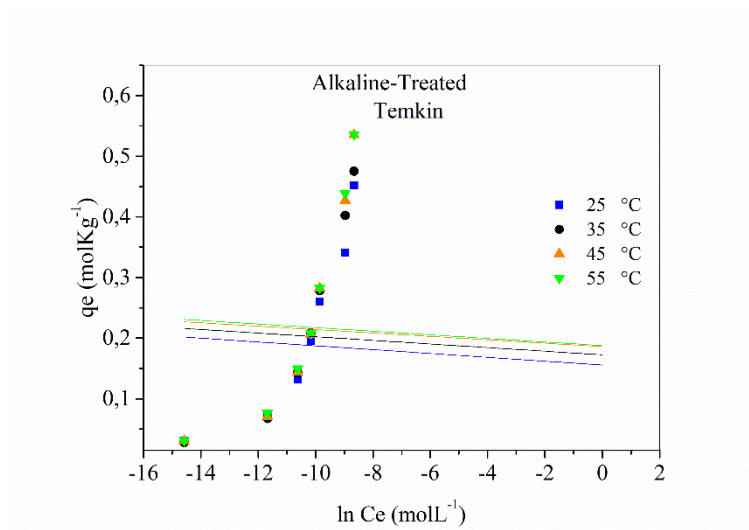


Figure S14 Isothermal equilibria of the removal of methylene blue at different temperatures for the alkaline - treated atemoya biosorbent. The mixtures were stirred for 12 h at 150 rpm, with an initial pH of 7.00 and different initial concentrations (10, 25, 50, 75, 100, 150 and 200 mg L⁻¹). Model Temkin.

ARTIGO 2

Normas do Periódico (versão preliminar)

ANALYSIS OF THE CHEMICAL CONSTITUENTS OF *THOMPSON***ATEMOYA SEED OIL**

Adneia F. A. Venceslau^a, Andressa C. Mendonça^a, Lilian A. Z. Benedick^a, Sergio S.

Thomasi^a, Cleiton A. Nunes^a, Luciana M. A. Pinto^{a*}

^a Department of Chemistry, Universidade Federal de Lavras (UFLA), P.O. Box 3037,

Lavras/MG, 37.200-900, Brazil.

*e-mail: luca@ufla.br

ANALYSIS OF THE CHEMICAL CONSTITUENTS OF *THOMPSON*

ATEMOYA SEED OIL

ABSTRACT: The objective of this study was to characterize extracts of atemoya (*var.* Thompson) seed oil obtained via different extraction methods. The following extraction methods were performed: chemical extraction using hexane, mechanical extraction using a press, and partitioned extraction. The composition of each of the extracts was analysed by gas chromatography-mass spectrometry (GC-MS), and more than 100 compounds were identified. The major constituents of the hexane extraction were (*Z*)-hexadec-9-enal (49.42%) and triolein (23.28%), and the mechanically obtained extract contained elaidic acid (66.11%) and stearic acid (6.67%). In the partitioned extraction, the hydromethanolic fraction contained dihydroxyacetone (19.16%), 3-deoxy-d-mannonic lactone (16.34%), 5-hydroxymethylfurfural (10.77%), and 3-propanediol, 2-(hydroxymethyl)-2-nitro (9.89%); the hexane fraction contained gamma-sitosterol (31.73%), erucic acid (14.64%), stigmaterol (13.30%) and triolein (10.90%); the chloroform fraction contained gamma-sitosterol (22.11%), vaccenic acid (15.49%), triolein (14.65%) and stigmaterol (10.65%); and the ethyl acetate fraction contained (*Z*)-icos-9-enoic acid (31.28%), beta-sitosterol (16.29%), pentadecanoic acid (11.53%) and eicosanoic acid (8.01%).

Keywords: *Annona atemoya*; characterization; extraction; GC-MS

INTRODUCTION

The family Annonaceae comprises a large number of genera and species, with approximately 2500 species, and occurs in all primary and secondary tropical forests worldwide (Couvreur, Helmstetter et al. 2019). Atemoya is an interspecific hybrid fruit resulting from artificial crossing between cherimoya (*Annona cherimola* Mill.) and sugar apple (*Annona squamosa* L.). The first recorded crosses occurred in 1908, and there are also natural hybrids (Morton 1987). The fruits are known to have a pleasant aroma and flavour (Baron, Amaro et al. 2018) and have been gaining market share. The fame of *Annona* goes far beyond flavour. Since the 1980s, the acetogenins of Annonaceae have been extensively studied due to their highly valuable pharmacological properties, such as antitumour activity (Rupprecht, Chang et al. 1986, Hoye and Zhuang 1988, Cavé, Figadère et al. 1997, Zafra-Polo, Figadère et al. 1998, Neske, Ruiz Hidalgo et al. 2020).

Extracts from various parts of Annonaceae plants have been shown to have significant antibacterial, antifungal, anti-inflammatory, antioxidant, and cytotoxic properties (Taechowisan, Singtotong et al. 2016, Costa, Santana et al. 2017, Ma, Wang et al. 2017, Tamfu, Tagatsing Fotsing et al. 2019). Regardless of the proportions and identity of the constituents in the total extract, they have the potential for biological activity (Krimat, Metidji et al. 2017). The seeds are considered the plant component with the greatest diversity and richness of phytochemicals, including acetogenins, alkaloids and phenolic compounds (Al Kazman, Harnett et al. 2020).

Different extraction methods give rise to different constituents. Hexane extracts constituents with low polarity, while mechanical extraction is considered an ecofriendly alternative with good yield (Petropoulos, Fernandes et al. 2018). Methanol allows the extraction of a greater number of compounds via the liquid-liquid partitioning process with solvents of increasing polarity (Krim, Rihani et al. 2020). The objective of this study was to determine the constituents of atemoya (*var* Thompson) seed oil obtained from different extraction methods by gas chromatography-mass spectrometry (GC-MS) analysis.

EXPERIMENTAL PART

Seed preparation and extractions

Fresh fruits of atemoya variety Thompson (ESAL Exsiccate 30,249) were purchased from a farmer in the city of Lavras/MG (21° 14' South, 44° 59' West) during the 2016/2017 harvest. The seeds were removed, washed in deionized water, dried in a forced-air oven at a temperature of 60-65 °C for 7 days and placed in hermetically sealed pots for subsequent extraction.

Part of the atemoya seeds (150 g) was crushed, sieved (150 mesh) and placed in hexane reflux (500 mL) for 24 hours at 100 °C. The solvent was removed by rotary evaporation, and the

yield was calculated. The material obtained in this procedure was called ASO_H (atemoya seed oil, ASO).

A second portion of the seeds (150 g) was also ground and evaluated for grain size (150 mesh). Mechanical extraction with a bench screw press (Yoda - MQO001) was used to obtain the resulting material, which was called ASO_P. At the end of the process, the yield was calculated.

The third portion of the seeds was subjected to partitioned extraction. A total of 180 g of dried, ground, and sieved seeds (150 mesh) was placed in 500 mL of methanol. The seeds were left in contact with the methanol for 3 days at a temperature of 25 ± 2 °C. After filtration, the residue was extracted two more times, as previously described. The solvent was removed by rotary evaporation at 50 °C and lyophilized, leaving 6.714 g of crude extract.

The crude extract was resuspended in methanol (20 mL) + ultrapure water (20 mL) and vigorously stirred at room temperature (25 ± 2 °C), and after 45 minutes of decantation, it was centrifuged for 10 minutes at 3500 xg. The supernatant was collected and called the hydromethanolic fraction (ASO_{HM}). The precipitate was subjected to extraction with hexane (20 mL) with vigorous stirring at room temperature (25 ± 2 °C) and 15 minutes of decantation. This process was repeated 4 times, and centrifugation was performed for 10 minutes at 3500 xg. The supernatant was collected and called the hexane fraction (ASO_{HEX}). A total of 20 mL of chloroform was added to the precipitate, followed by vigorous stirring at room temperature (25 ± 2 °C) and 15 minutes of decantation. This process was repeated 4 times, and then centrifugation was performed for 10 minutes at 3500 xg. The supernatant was collected and called the chloroform fraction (ASO_{CHLO}). A total of 20 mL of ethyl acetate was added to the precipitate, followed by vigorous stirring at room temperature (25 ± 2 °C) and 15 minutes of decantation. This process was repeated 4 times, and at the end, there was no phase separation. The entire extract was collected and called the ethyl acetate fraction (ASO_{ACE}).

The elimination of all solvents was performed in an open amber flask protected from light in a desiccator until reaching constant weight. Finally, the samples were sent to the Analytical Centre of the Chemistry Institute of the University of Sao Paulo (USP) for analysis by GC-MS (QP2020 - Shimadzu). The analyses were performed using a capillary column (30 m x 0.25 mm x 0.25 µm, ZB-5HT, CarbolWAX). The injection conditions were 250 °C and 2.50 mL min⁻¹ for ASO_H and ASO_P and 320 °C and 3.00 mL min⁻¹ for ASO_{HM}, ASO_{HEX}, ASO_{CHLO} and ASO_{ACE}. The components of the ASO samples were identified through standard spectrum libraries for organic compounds, such as NIST107 and Wiley 229.

RESULTS AND DISCUSSION

The yield of each extraction is shown in Table 1, and the constituents identified in each extract by GC-MS and their biological activities are shown in Tables 2, 3, 4, 5, 6 and 7.

Table 1 – ASO yield in each extraction

Extraction	Mass obtained (g)	Yield (%)
1 st extraction ASO _H	23.881	15.92
2 nd extraction ASO _P	22.562	14.97
3 rd partitioned extraction	6.714	3.73
ASO _{HM}	2.173	32.37
ASO _{HEX}	0.466	6.94
ASO _{CHLO}	1.107	16.49
ASO _{ACE}	0.255	3.80

Table 2 - Bioactive components of ASO_H analysed by GC-MS.

Compound	Area (%)	Molecular Formula	Bioactivity
(Z)-Hexadec-9-enal	49.42	C ₁₆ H ₃₀ O	Pheromone (Teal, Heath et al. 1981)
2,3-bis[[<i>(Z)</i> -Octadec-9-enoyl]oxy]propyl (<i>Z</i>)-octadec-9-enoate	23.28	C ₅₇ H ₁₀₄ O ₆	Adjuvant treatment for brain tumours (Kim, Kim et al. 2016)
(3E,12Z)-Nonadeca-1,3,12-triene-5,14-diol	3.90	C ₁₉ H ₃₄ O ₂	Antidiabetic and antilipidaemic (Ahmadi, Khalili et al. 2017)
(3S,8S,9S,10R,13R,14S,17R)-17-[(2R,5S)-5-Ethyl-6-methylheptan-2-yl]-10,13-dimethyl-2,3,4,7,8,9,11,12,14,15,16,17-dodecahydro-1H-cyclopenta[a]phenanthren-3-ol	3.36	C ₂₉ H ₅₀ O	Phytosterol (Liu, Chen et al. 2012) Potentially useful candidate for COVID-19 (Chowdhury 2020, Luo, Jiang et al. 2020, Maurya, Kumar et al. 2020, Narkhede, Pise et al. 2020, Wang, Zhang et al. 2020)
Decane	2.09	C ₁₀ H ₂₂	Marker/mechanism in erythema and sleep apnoea, obstructive (Mallampati, Patlolla et al. 2010, Aoki, Nagaoka et al. 2017)
1-Methyl-3-methylidene-8-propan-2-yltricyclo decane	1.82	C ₁₅ H ₂₄	Antibacterial (Ajiboye, Mohammed et al. 2016) Sesquiterpene contributing to the flavour and aroma of wine (Dueholm, Drew et al. 2019)
(3S,8S,9S,10R,13R,14S,17R)-17-[(E,2R,5S)-5-Ethyl-6-methylhept-3-en-2-yl]-10,13-dimethyl-2,3,4,7,8,9,11,12,14,15,16,17-dodecahydro-1H-cyclopenta[a]phenanthren-3-ol	1.65	C ₂₉ H ₄₈ O	Phytosterol (Ulbricht 2016) and anti-nociceptive (Walker, Oliveira et al. 2017)

			Potentially useful candidates for COVID-19 (Huang, Zheng et al. 2020, Kar, Sharma et al. 2020, Luo, Jiang et al. 2020, Zhenjie, Xiaoying et al. 2020)
ethyl-octadec-9-enoate	1.58	C ₂₀ H ₃₈ O ₂	Antitumoural, pheromone and biomarker of excessive alcohol chronic use (González-Illán, Ojeda-Torres et al. 2011, Politi, Mari et al. 2011, Castillo, Chen et al. 2012, Manosroi, Jantrawut et al. 2012)
[(E)-10,13,13-trimethyltetradec-11-enyl] acetate	1.47	C ₁₉ H ₃₆ O ₂	No activities listed.
(5-formyl-5,9-dimethyl-14-tetracyclo [11.2.1.01,10.04,9]hexadecanyl) methyl acetate	1.31	C ₂₂ H ₃₄ O ₃	No activities listed.
Undecane	1.22	C ₁₁ H ₂₄	Pheromone (Yamagata, Fujiwara-Tsujii et al. 2005, Lenz, Krasnec et al. 2013)
(3E,12Z)-nonadeca-1,3,12-triene-5,14-diol	1.15	C ₁₉ H ₃₄ O ₂	No activities listed.
3-O-(2,2-dimethylpropyl) 1-O-tridecyl propanedioate	0.90	C ₂₁ H ₄₀ O ₄	No activities listed.
[(3S,8S,9S,10R,13R,14S,17R)-17-[(2R,5R)-5-ethyl-6-methylheptan-2-yl]-10,13-dimethyl-2,3,4,7,8,9,11,12,14,15,16,17-dodecahydro-1H-cyclopenta[a]phenanthren-3-yl] acetate	0.90	C ₃₁ H ₅₂ O ₂	Antioxidant, antitumoural, anti-diarrhoeal, analgesic, anti-diabetic, antiproliferative, antibacterial and anti-inflammatory (El-Shazly, El-Sayed et al. 2012, Stefani, Garza-González et al. 2019, Islam 2020, Ogunlakin, Sonibare et al. 2020)

2-butyloctan-1-ol	0.85	C ₁₂ H ₂₆ O	Antioxidant, anti-inflammatory and pheromone (Tang, Zhang et al. 2016, Ahmed, Akbar et al. 2017)
(3S)-17-(5,6-dimethylheptan-2-yl)-10,13-dimethyl-2,3,4,7,8,9,11,12,14,15,16,17-dodecahydro-1H-cyclopenta[a]phenanthren-3-ol	0.83	C ₂₈ H ₄₈ O	Adjuvant in determination of sitosterolemia, synthesis of vitamins D (Komba, Kotake-Nara et al. 2019, Lee, Song et al. 2020)
(1S,6S,7S,8S)-1-methyl-3-methylidene-8-propan-2-yltricyclo[4.4.0.0 ^{2,7}]decane (1S,6S,7S,8S)-1-methyl-3-methylidene-8-propan-2-yltricyclo[4.4.0.0 ^{2,7}]decane	0.80	C ₁₅ H ₂₄	Pheromone and antimicrobial (Flath, Cunningham et al. 1994, Jeliazkova, V et al. 2018)
(1Z,6Z,8S)-1-methyl-5-methylidene-8-propan-2-ylcyclodeca-1,6-diene	0.80	C ₁₅ H ₂₄	Anti-inflammatory, anti-oedematogenic, antiproliferative, antileishmanial, antibacterial, antifungal and antioxidant (Siqueira, Serain et al. 2015, Oliveira-Tintino, Pessoa et al. 2018)
(2Z)-2,6-dimethylocta-2,7-diene-1,6-diol	0.80	C ₁₀ H ₁₈ O ₂	No activities listed.

Table 3 - Bioactive components of ASO_P analysed by GC-MS.

Compound	Area (%)	Molecular Formula	Bioactivity
(E)-octadec-9-enoic acid	66.11	C ₁₈ H ₃₄ O ₂	Potential biomarker in biological age (Zhao, Wang et al. 2020)
Octadecanoic acid	8.81	C ₁₈ H ₃₆ O ₂	Immunoregulatory and anti-inflammatory (Calder 1998)

(Z)-icos-9-en-1-ol	6.67	C ₂₀ H ₄₀ O	No activities listed.
Hexadecanoic acid	3.76	C ₁₆ H ₃₂ O ₂	Antitumoural, anti-inflammatory (Harada, Yamashita et al. 2002, Joshi-Barve, Barve et al. 2007) Can be successful as anti-COVID-19 agent (Elfiky 2020)
(1S,6S,7S,8S)-1-methyl-3-methylidene-8-propan-2-yltricyclo[4.4.0.0 ^{2,7}]decane (1S,6S,7S,8S)-1-methyl-3-methylidene-8-propan-2-yltricyclo[4.4.0.0 ^{2,7}]decane	2.85	C ₁₅ H ₂₄	Antibacterial (Ajiboye, Mohammed et al. 2016) Sesquiterpenes contribute to the flavour and aroma of wine (Dueholm, Drew et al. 2019)
(E)-octadec-9-en-1-ol	2.24	C ₁₈ H ₃₆ O	No activities listed.
(1S,6S,7S,8S)-1-methyl-3-methylidene-8-propan-2-yltricyclo[4.4.0.0 ^{2,7}]decane (1S,6S,7S,8S)-1-methyl-3-methylidene-8-propan-2-yltricyclo[4.4.0.0 ^{2,7}]decane	1.31	C ₁₅ H ₂₄	Pheromone and antimicrobial (Flath, Cunningham et al. 1994, Jeliaskova, V et al. 2018)
(1R,4aR,4bS,7S,10aR)-7-ethenyl-1,4a,7-trimethyl-3,4,4b,5,6,8,10,10a-octahydro-2H-phenanthrene-1-carbaldehyde	1.24	C ₂₀ H ₃₀ O	No activities listed.
(3E,12Z)-Nonadeca-1,3,12-triene-5,14-diol	1.02	C ₁₉ H ₃₄ O ₂	No activities listed.
2-[(9Z,12Z)-Octadeca-9,12-dienoxy]ethanol	0.97	C ₂₀ H ₃₈ O ₂	No activities listed.
Heptacos-1-ene	0.92	C ₂₇ H ₅₄	Pheromone (Evison, Ferreira et al. 2012)

(1Z,6Z,8S)-1-Methyl-5-methylidene-8-propan-2-ylcyclodeca-1,6-diene	0.83	C ₁₅ H ₂₄	Anti-inflammatory, anti-oedematogenic, antiproliferative, antileishmanial, antibacterial, antifungal and antioxidant (Siqueira, Serain et al. 2015, Oliveira-Tintino, Pessoa et al. 2018)
5,5,9-Trimethyl-14-methylidenetetracyclo[11.2.1.01,10.04,9]hexadecane	0.75	C ₂₀ H ₃₂	Human metabolite and anti-allergic (Cheenpracha, Yodsaoue et al. 2006, Lingwood and Simons 2010)
(S,1Z,6Z)-8-Isopropyl-1-methyl-5-methylenecyclodeca-1,6-diene	0.61	C ₁₅ H ₂₄	Anti-inflammatory, anti-oedematogenic, antiproliferative, antileishmanial, antibacterial, antifungal and antioxidant (Siqueira, Serain et al. 2015, Oliveira-Tintino, Pessoa et al. 2018)
(S,1Z,6Z)-8-Isopropyl-1-methyl-5-methylenecyclodeca-1,6-diene	0.48	C ₁₅ H ₂₄	Anti-inflammatory, anti-oedematogenic, antiproliferative, antileishmanial, antibacterial, antifungal and antioxidant (Siqueira, Serain et al. 2015, Oliveira-Tintino, Pessoa et al. 2018)
(S,1Z,6Z)-8-Isopropyl-1-methyl-5-methylenecyclodeca-1,6-diene	0.38	C ₁₅ H ₂₄	Anti-inflammatory, anti-oedematogenic, antiproliferative, antileishmanial, antibacterial, antifungal and antioxidant (Siqueira, Serain et al. 2015, Oliveira-Tintino, Pessoa et al. 2018)
(2E,4E)-Deca-2,4-dienal	0.35	C ₁₀ H ₁₆ O	No activities listed.
(1R,2S,6S,7S,8S)-1,3-Dimethyl-8-propan-2-yltricyclo[4.4.0.02,7]dec-3-ene	0.29	C ₁₅ H ₂₄	Antioxidant, anti-inflammatory, and anticancer (Ketha, Vedula et al. 2020)

(S,1Z,6Z)-8-Isopropyl-1-methyl-5-methylenecy	0.20	C ₁₅ H ₂₄	Anti-inflammatory, anti-oedematogenic, antiproliferative, antileishmanial, antibacterial, antifungal and antioxidant (Siqueira, Serain et al. 2015, Oliveira-Tintino, Pessoa et al. 2018)
--	------	---------------------------------	---

Table 4 - Bioactive components of ASO_{HM} analysed by GC-MS.

Compound	Area (%)	Molecular Formula	Bioactivity
Dihydroxyacetone	19.16	C ₃ H ₆ O ₃	Treatment of vitiligo, antifungal, photoprotector (Fesq, Brockow et al. 2001, Fusaro and Rice 2005, Stopiglia, Vieira et al. 2011)
3,5-Dihydroxy-6-(hydroxymethyl)oxan-2-one	16.34	C ₆ H ₁₀ O ₅	Antimicrobial activity (Shobana, Vidhya et al. 2009)
5-Hydroxymethylfurfural	10.77	C ₆ H ₆ O ₃	Antioxidant, antiproliferative (Zhao, Chen et al. 2013) Potentially used to improve hypoxemia in COVID-19 patients (Woyke, Rauch et al.)
2-(Hydroxymethyl)-2-nitropropane-1,3-diol	9.89	C ₄ H ₉ NO ₅	Antimicrobial (Beier, Duke et al. 2008, Amponin, Przybek-Skrzypecka et al. 2020)
4-Hydroxy-3-methylbutan-2-one	6.68	C ₅ H ₁₀ O ₂	Hypoglycaemic, antiviral, anti-inflammatory, antioxidant, and anti-apoptotic (Avetisyan, Dzhandzhapanyan et al. 1982, Hafez, Elblehi et al. 2020)
6-Oxoheptanoic acid	5.37	C ₇ H ₁₂ O ₃	No activities listed.
4-Hydroxyoxolan-2-one	4.19	C ₄ H ₆ O ₃	C4 chiral synthon for the synthesis of chiral pharmaceuticals and nutraceuticals such as HIV

			inhibitors, synthetic statins, and L-carnitine (Lee and Park 2009)
3-Hydroxyoxolan-2-one	3.37	C ₄ H ₆ O ₃	Antibacterial (Murugan, Sekar et al. 2013)
1-(2-Hydroxypropoxy)propan-2-ol	3.25	C ₆ H ₁₄ O ₃	Larvicidal (Sheng, Jian et al. 2020)
1-(2-Methyltetrazol-5-yl)ethenyl acetate	3.20	C ₆ H ₈ N ₄ O ₂	No activities listed.
5,5-Dimethyl-1,3-oxazolidine-2,4-dione	2.98	C ₅ H ₇ NO ₃	Pancreatic stone dissolution and anticonvulsant (Okamoto, Rosenberg et al. 1977, Noda, Shibata et al. 1984)
2,3-Dihydroxypropyl acetate	2.97	C ₅ H ₁₀ O ₄	Potential mosquito repellent (Gaddaguti, Rao et al. 2016)
3-Methylideneoxolane-2,5-dione	2.65	C ₅ H ₄ O ₃	<i>In vitro</i> cytotoxic activity against human breast tumours (Poudel, Satyal et al. 2015)
3,5-Dihydroxy-6-methyl-2,3-dihydropyran-4-one	1.70	C ₆ H ₈ O ₄	Antioxidant (Mozafari, Vafae et al. 2018)
Pent-4-enoic acid	1.62	C ₅ H ₈ O ₂	Marker/mechanism in fatty liver and Reye syndrome (Tang, Borel et al. 1995, Ghonghadze, Antelava et al. 2017)
Furan-2-ylmethanol	1.60	C ₅ H ₆ O ₂	Marker/mechanism in adenoma, dermatitis, allergic contact, dermatitis, irritant, kidney neoplasms and respiratory hypersensitivity (Spalding, French et al. 2000, Franko, Jackson et al. 2012)
Furan-2-carbaldehyde	1.32	C ₅ H ₄ O ₂	Agrochemical (Badawy 2008)

5-Oxo-2-propylhexanal	1.11	C ₉ H ₁₆ O ₂	No activities listed.
2,5-Dimethyloxolane-3,4-dione	0.97	C ₆ H ₈ O ₃	No activities listed.

Table 5 - Bioactive components of ASO_{HEX} analysed by GC-MS.

Compound	Area (%)	Molecular Formula	Bioactivity
(3S,8S,9S,10R,13R,14S,17R)-17-[(2R,5S)-5-Ethyl-6-methylheptan-2-yl]-10,13-dimethyl-2,3,4,7,8,9,11,12,14,15,16,17-dodecahydro-1H-cyclopenta[a]phenanthren-3-ol	31.73	C ₂₉ H ₅₀ O	Phytosterol (Liu, Chen et al. 2012) Potentially useful candidate for COVID-19 (Chowdhury 2020, Luo, Jiang et al. 2020, Maurya, Kumar et al. 2020, Narkhede, Pise et al. 2020, Wang, Zhang et al. 2020)
(Z)-Docos-13-enoic acid	14.64	C ₂₂ H ₄₂ O ₂	Antimicrobial, antitumour and cardiac (Suresh, Praveenkumar et al. 2014, Altinoz, Bilir et al. 2018)
(3S,8S,9S,10R,13R,14S,17R)-17-[(E,2R,5S)-5-Ethyl-6-methylhept-3-en-2-yl]-10,13-dimethyl-2,3,4,7,8,9,11,12,14,15,16,17-dodecahydro-1H-cyclopenta[a]phenanthren-3-ol	13.30	C ₂₉ H ₄₈ O	Phytosterol (Ulbricht 2016) and anti-nociceptive (Walker, Oliveira et al. 2017) Potentially useful candidate for COVID-19 (Huang, Zheng et al. 2020, Kar, Sharma et al. 2020, Luo, Jiang et al. 2020, Zhenjie, Xiaoying et al. 2020)
2,3-bis[[[(Z)-Octadec-9-enoyl]oxy]propyl (Z)-octadec-9-enoate	10.90	C ₅₇ H ₁₀₄ O ₆	Adjuvant treatment for brain tumours (Kim, Kim et al. 2016)
(3S)-17-(5,6-Dimethylheptan-2-yl)-10,13-dimethyl-2,3,4,7,8,9,11,12,14,15,16,17-dodecahydro-1H-cyclopenta[a]phenanthren-3-ol	6.01	C ₂₈ H ₄₈ O	Adjuvant in determination of sitosterolemia, synthesis of vitamin D (Komba, Kotake-Nara et al. 2019, Lee, Song et al. 2020)
Hexadecanoic acid	5.12	C ₁₆ H ₃₂ O ₂	Antitumour, anti-inflammatory (Harada, Yamashita et al. 2002, Joshi-Barve, Barve et al. 2007)

			Can be successful as an anti-COVID-19 agent (Elfiky 2020)
(11E,13Z)-Octadeca-1,11,13-triene	3.35	C ₁₈ H ₃₂	Antitumour (Swantara, Rita et al. 2019)
2-[12-(Oxiran-2-yl)dodecyl]oxirane	2.70	C ₁₆ H ₃₀ O ₂	No activities listed.
Eicosanoic acid	2.33	C ₂₀ H ₄₀ O ₂	Antioxidant and antiproliferative (Haruenkit, Poovarodom et al. 2010)
1,3-Dihydroxypropan-2-yl hexadecanoate	2.03	C ₁₉ H ₃₈ O ₄	Marker/mechanism in diabetes mellitus type 2 (Piccolo, Graham et al. 2016)
Methyl 8-(2-hexylcyclopropyl)octanoate	1.08	C ₁₈ H ₃₄ O ₂	No activities listed.
5-(6-Bromo-2-hydroxy-2,5,5,8a-tetramethyl-3,4,4a,6,7,8-hexahydro-1H-naphthalen-1-yl)-3-methylidenepentane-1,2-diol	0.98	C ₂₀ H ₃₅ BrO ₃	No activities listed.
(1S,4R,5R)-4-Methyl-1-propan-2-ylbicyclo[3.1.0]hexan-3-one	0.96	C ₁₀ H ₁₆ O	Antifungal (Bai, Wang et al. 2020)
N-(2-Hydroxyethyl)octanamide	0.83	C ₁₀ H ₂₁ NO ₂	Larvicidal (Chandrasekaran, Seetharaman et al. 2018)
2-(Dimethylamino)ethyl 2-methylprop-2-enoate	0.79	C ₈ H ₁₅ NO ₂	Used for drug delivery (Xu, Yuan et al. 2006)
Pentadecanal	0.76	C ₁₅ H ₃₀ O	Antioxidant and cytotoxicity (Sharopov, Satyal et al. 2020)
1,3-Dihydroxypropan-2-yl hexadecanoate	0,71	C ₁₉ H ₃₈ O ₄	Marker/mechanism in diabetes mellitus type 2 (Piccolo, Graham et al. 2016)

1-Hexadecyl-2,3-dihydro-1H-indene	0.68	C ₂₅ H ₄₂	Biomarker in exhaled air for the diagnosis, classification and monitoring of lung cancer (National Center for Biotechnology Information. "PubChem Compound Summary for CID 266426, 1-n-Hexadecylindan" PubChem , https://pubchem.ncbi.nlm.nih.gov/compound/1-n-Hexadecylindan . Accessed 14 November, 2020.) ^[94] ("National Center for Biotechnology Information. "PubChem Compound Summary for CID 266426, 1-n-Hexadecylindan" PubChem, https://pubchem.ncbi.nlm.nih.gov/compound/1-n-Hexadecylindan . Accessed 14 November, 2020.") ⁽⁹⁴⁾ ^[94] ⁹⁴
6-Ethyldecane-3-yloxy(trimethyl)silane	0.62	C ₁₅ H ₃₄ OSi	No activities listed.

Table 6 - Bioactive components of ASO_{CHLO} analysed by GC-MS.

Compound	Area (%)	Molecular Formula	Bioactivity
(3S,8S,9S,10R,13R,14S,17R)-17-[(2R,5S)-5-Ethyl-6-methylheptan-2-yl]-10,13-dimethyl-	22.11	C ₂₉ H ₅₀ O	Phytosterol (Liu, Chen et al. 2012) Potentially useful candidate for COVID-19 (Chowdhury 2020, Luo, Jiang et al. 2020, Maurya,

2,3,4,7,8,9,11,12,14,15,16,17-dodecahydro-1H-cyclopenta[a]phenanthren-3-ol			Kumar et al. 2020, Narkhede, Pise et al. 2020, Wang, Zhang et al. 2020)
(Z)-Octadec-11-enoic acid	15.49	C ₁₈ H ₃₄ O ₂	Anti-inflammatory (Sales-Campos, Souza et al. 2013)
2,3-bis[[[(Z)-Octadec-9-enoyl]oxy]propyl (Z)-octadec-9-enoate	14.65	C ₅₇ H ₁₀₄ O ₆	Adjuvant treatment for brain tumours (Kim, Kim et al. 2016)
(3S,8S,9S,10R,13R,14S,17R)-17-[(E,2R,5S)-5-Ethyl-6-methylhept-3-en-2-yl]-10,13-dimethyl-2,3,4,7,8,9,11,12,14,15,16,17-dodecahydro-1H-cyclopenta[a]phenanthren-3-ol	10.65	C ₂₉ H ₄₈ O	Phytosterol (Ulbricht 2016) and anti-nociceptive(Walker, Oliveira et al. 2017) Potentially useful candidate for COVID-19 (Huang, Zheng et al. 2020, Kar, Sharma et al. 2020, Luo, Jiang et al. 2020, Zhenjie, Xiaoying et al. 2020)
(3S)-17-(5,6-Dimethylheptan-2-yl)-10,13-dimethyl-2,3,4,7,8,9,11,12,14,15,16,17-dodecahydro-1H-cyclopenta[a]phenanthren-3-ol	5.57	C ₂₈ H ₄₈ O	Adjuvant in determination of sitosterolemia, synthesis of vitamin D (Komba, Kotake-Nara et al. 2019, Lee, Song et al. 2020)
Dodecyl 3-(3-dodecoxy-3-oxopropyl) sulfanylpropanoate	4.56	C ₃₀ H ₅₈ O ₄ S	Antioxidant
Hexadecanoic acid	4.23	C ₁₆ H ₃₂ O ₂	Antitumour, anti-inflammatory (Harada, Yamashita et al. 2002, Joshi-Barve, Barve et al. 2007) Can be successful as an anti-COVID-19 agent (Elfiky 2020)
1,3-Dihydroxypropan-2-yl hexadecanoate	3.48	C ₁₉ H ₃₈ O ₄	Marker/mechanism in diabetes mellitus type 2 (Piccolo, Graham et al. 2016)

(9Z,12Z)-Octadeca-9,12-dienoic acid	3.34	C ₁₈ H ₃₂ O ₂	Therapeutic use: Barth syndrome, dermatitis, fatty liver, hepatitis C, hypercholesterolemia, hyperlipidaemia, hypertriglyceridemia, lung neoplasms, neoplasm invasiveness and metastasis and anti-inflammatory (Toriyama-Baba, Iigo et al. 2001, Sheu, Fowler et al. 2002, Yano, Ikeda et al. 2007, Jang, Srinivasan et al. 2008, Chen, Chao et al. 2013, Malhotra, Kahlon et al. 2014, Kothapalli, Park et al. 2020) Binding pocket in the locked structure of SARS-CoV-2 spike protein (Toelzer, Gupta et al. 2020)
Octadecanoic acid	3.14	C ₁₈ H ₃₆ O ₂	Immunoregulatory and anti-inflammatory (Calder 1998)
(9Z,12Z)-Octadeca-9,12-dienoyl chloride	3.02	C ₁₈ H ₃₁ ClO	No activities listed.
6-Ethyldecane-3-yloxy(trimethyl)silane	1.62	C ₁₅ H ₃₄ OSi	No activities listed.
1,3-Dihydroxypropan-2-yl pentadecanoate	1.57	C ₁₈ H ₃₆ O ₄	Potentially used in the detection of colorectal cancer (Monleón, Morales et al. 2009, Ritchie, Ahiahonu et al. 2010, Weir, Manter et al. 2013, Goedert, Sampson et al. 2014, Phua, Chue et al. 2014, Sinha, Ahn et al. 2016)
Octadecanamide	1.21	C ₁₈ H ₃₇ NO	Potentially used in the detection of colorectal cancer (Monleón, Morales et al. 2009, Ritchie,

			Ahiahonu et al. 2010, Weir, Manter et al. 2013, Goedert, Sampson et al. 2014, Phua, Chue et al. 2014, Sinha, Ahn et al. 2016)
N-(2-Hydroxyethyl)octanamide	1.20	C ₁₀ H ₂₁ NO ₂	Larvicidal (Chandrasekaran, Seetharaman et al. 2018)
5,5-bis(Heptylsulfanyl)pentane-1,2,3-triol	1.03	C ₁₉ H ₄₀ O ₃ S ₂	No activities listed.
(3-Hexadecanoyloxy-2-trimethylsilyloxypropyl) hexadecanoate	0.86	C ₃₈ H ₇₆ O ₅ Si	No activities listed.
3,5- <i>ditert</i> -Butylphenol	0.82	C ₁₄ H ₂₂ O	No activities listed.
(<i>Z</i>)-Docos-13-enamide	0.77	C ₂₂ H ₄₃ NO	Antidepressant and anxiolytic-like behavioural effect (Li, Jiang et al. 2017)

Table 7 - Bioactive components of ASO_{ACE} analysed by GC-MS.

Compound	Area (%)	Molecular Formula	Bioactivity
(Z)-Icos-9-enoic acid	31.28	C ₂₀ H ₃₈ O ₂	Antioxidant and cardiovascular disease protection (Bailão, Devilla et al. 2015)
(3S,8S,9S,10R,13R,14S,17R)-17-[(2R,5R)-5-Ethyl-6-methylheptan-2-yl]-10,13-dimethyl-2,3,4,7,8,9,11,12,14,15,16,17-dodecahydro-1H-cyclopenta[a]phenanthren-3-ol	16.29	C ₂₉ H ₅₀ O	Antioxidant, antimicrobial and induces apoptosis in MCF-7 cells (Chai, Kuppusamy et al. 2008, Hidayathulla, Shahat et al. 2018) Potentially useful candidate for COVID-19 (Chowdhury 2020, Luo, Jiang et al. 2020, Maurya, Kumar et al. 2020, Wang, Zhang et al. 2020, Zhenjie, Xiaoying et al. 2020)
Pentadecanoic acid	11.53	C ₁₅ H ₃₀ O ₂	Potential natural agrochemical and antifungal (Manilal, Sujith et al. 2010, Ding, Guo et al. 2019)
Eicosanoic acid	8.01	C ₂₀ H ₄₀ O ₂	Antioxidant and antiproliferative (Haruenkit, Poovarodom et al. 2010)
(3S,8S,9S,10R,13R,14S,17R)-17-[(E,2R,5S)-5-Ethyl-6-methylhept-3-en-2-yl]-10,13-dimethyl-2,3,4,7,8,9,11,12,14,15,16,17-dodecahydro-1H-cyclopenta[a]phenanthren-3-ol	6.41	C ₂₉ H ₄₈ O	Phytosterol (Ulbricht 2016) and anti-nociceptive (Walker, Oliveira et al. 2017) Potentially useful candidate for COVID-19 (Huang, Zheng et al. 2020, Kar, Sharma et al. 2020, Luo, Jiang et al. 2020, Zhenjie, Xiaoying et al. 2020)

(3S)-17-(5,6-Dimethylheptan-2-yl)-10,13-dimethyl-2,3,4,7,8,9,11,12,14,15,16,17-dodecahydro-1H-cyclopenta[a]phenanthren-3-ol	3.13	C ₂₈ H ₄₈ O	Adjuvant in determination of sitosterolemia, synthesis of vitamin D (Komba, Kotake-Nara et al. 2019, Lee, Song et al. 2020)
(1E,4E)-1,5-Diphenylpenta-1,4-dien-3-one	2.86	C ₁₇ H ₁₄ O	Antioxidant (Naseer, Lone et al. 2015)
(9Z)-Octadeca-9,17-dienal	2.63	C ₁₈ H ₃₂ O	Potential selective MAO-A inhibitor (depression, anxiety, and cognitive impairments in Alzheimer's and Parkinson's diseases) (Margret, Begum et al. 2015)
(Z)-Hexadec-7-enal	2.35	C ₁₆ H ₃₀ O	Pheromone (Teal, Heath et al. 1981)
Diocetyl benzene-1,2-dicarboxylate	1.97	C ₂₄ H ₃₈ O ₄	Antitumour (Maruyama, Amanuma et al. 1994, Angelini, Centurione et al. 2011, Habib and Karim 2012)
[2-[2-[(E)-3-Phenylprop-2-enoyl]oxyphenyl]phenyl] (E)-3-phenylprop-2-enoate	1.88	C ₃₀ H ₂₂ O ₄	No activities listed.
[(3S,8S,9S,10R,13R,14S,17R)-10,13-Dimethyl-17-[(2R)-6-methylheptan-2-yl]-2,3,4,7,8,9,11,12,14,15,16,17-dodecahydro-1H-cyclopenta[a]phenanthren-3-yl] carbonochloridate	1.78	C ₂₈ H ₄₅ ClO ₂	Used in long circulating liposomes (Deodhar, Dash et al. 2020)
(9Z,12Z)-Octadeca-9,12-dienoyl chloride	1.49	C ₁₈ H ₃₁ ClO	No activities listed.
(1E,4E)-1,5-Diphenylpenta-1,4-dien-3-one	1.45	C ₁₇ H ₁₄ O	Antioxidant (Naseer, Lone et al. 2015)

(Z)-Octadec-9-enamide	1.43	C ₁₈ H ₃₅ NO	Therapeutic use: amnesia and seizures (Heo, Park et al. 2003, Wu, Li et al. 2003)
4-[[<i>(E)</i> -2-Methoxyhexadec-4-enoxy]methyl]-2,2-dimethyl-1,3-dioxolane	1.27	C ₂₃ H ₄₄ O ₄	No activities listed.
1-Acetyloxyethyl acetate	1.25	C ₆ H ₁₀ O ₄	No activities listed.
2-Hydroxyethyl acetate	1.15	C ₄ H ₈ O ₃	No activities listed.
Bicyclo[3.3.1]nonan-2-ol	0.99	C ₉ H ₁₆ O	No activities listed.

Table 1 shows the yield data for each extraction. As predicted, each extraction resulted in distinct constituents with diverse biological activities. These data are presented in detail for each constituent in Tables 2, 3, 4, 5, 6 and 7.

Among the one hundred and fourteen compounds identified, 20 had antioxidant activity, 17 had anti-inflammatory activity, 10 had antibacterial activity, 9 had antifungal activity, 7 had antitumour activity, 4 had auxiliary activity in the treatment of cancer, 3 had larvicidal activity and 2 showed antidiabetic activity. Furthermore, 12 are potential adjuvants in coping with COVID-19. In addition, some compounds are pheromones, have auxiliary effects in neglected diseases, and act as biological biomarkers, among other important activities.

CONCLUSION

Extractions of *atemoya* (*var* Thompson) seed oil were conducted, and the obtained extracts evaluated for constituents by GC-MS. The results demonstrated that each extraction has a specific biological potential. Among the constituents, 12 compounds were shown in 2020 to have potential adjuvant use in the treatment of SARS-COV-2, and other components have proven efficacy in the form of several biological activities. These results provide important information to assist in the selection of extraction methods when considering the desired constituents.

ACKNOWLEDGMENT

This study was funded in part by the Brazilian Federal Agency for the Support and Evaluation of Graduate Education (CAPES) - Finance Code 001.

REFERENCES

- "National Center for Biotechnology Information. "PubChem Compound Summary for CID 266426, 1-n-Hexadecylindan" *PubChem*, <https://pubchem.ncbi.nlm.nih.gov/compound/1-n-Hexadecylindan> . Accessed 14 November, 2020."
- Ahmadi, A., M. Khalili, F. Mashae and B. Nahri-Niknafs (2017). "The Effects of Solvent Polarity on Hypoglycemic and Hypolipidemic Activities of *Vaccinium Arctostaphylos* L. Unripe Fruits." *Pharmaceutical Chemistry Journal* **50**(11): 746-752.
- Ahmed, A., S. Akbar and W. A. Shah (2017). "Chemical composition and pharmacological potential of aromatic water from *Salix caprea* inflorescence." *Chinese Journal of Integrative Medicine*.
- Ajiboye, T. O., A. O. Mohammed, S. A. Bello, I. I. Yusuf, O. B. Ibitoye, H. F. Muritala and I. B. Onajobi (2016). "Antibacterial activity of *Syzygium aromaticum* seed: Studies on oxidative stress biomarkers and membrane permeability." *Microbial Pathogenesis* **95**: 208-215.
- Al Kazman, B. S. M., J. E. Harnett and J. R. Hanrahan (2020). "The Phytochemical Constituents and Pharmacological Activities of *Annona atemoya*: A Systematic Review." *Pharmaceuticals* **13**(10): 269.
- Altinoz, M. A., A. Bilir and İ. Elmaci (2018). "Erucic acid, a component of Lorenzo's oil and PPAR- δ ligand modifies C6 glioma growth and toxicity of doxorubicin. Experimental data and a comprehensive literature analysis." *Chem Biol Interact* **294**: 107-117.
- Amponin, D. E., J. Przybek-Skrzypecka, M. Zyablitskaya, A. Takaoka, L. H. Suh, T. Nagasaki, S. L. Trokel and D. C. Paik (2020). "Ex vivo anti-microbial efficacy of various formaldehyde releasers against antibiotic resistant and antibiotic sensitive microorganisms involved in infectious keratitis." *BMC Ophthalmology* **20**(1): 28.
- Angelini, A., L. Centurione, S. Sancilio, M. L. Castellani, P. Conti, C. Di Ilio, E. Porreca, F. Cuccurullo and R. Di Pietro (2011). "The effect of the plasticizer diethylhexyl phthalate on transport activity

and expression of P-glycoprotein in parental and doxo-resistant human sarcoma cell lines." J Biol Regul Homeost Agents **25**(2): 203-211.

Aoki, T., T. Nagaoka, N. Kobayashi, M. Kurahashi, C. Tsuji, H. Takiguchi, K. Tomomatsu, T. Oguma, K. Magatani, S. Takeda, K. Asano and T. Abe (2017). "Editor's Highlight: Prospective Analyses of Volatile Organic Compounds in Obstructive Sleep Apnea Patients." Toxicol Sci **156**(2): 362-374.

Avetisyan, A. A., A. N. Dzhandzhapanyan, A. V. Galstyan, S. K. Karagez, V. I. Votyakov, S. V. Khlyustov, G. V. Vladyko, V. Y. Klimovich, L. V. Korobchenko, M. N. Shashikhina and S. V. Zhavrid (1982). "Research on unsaturated lactones. 75. Antiviral activity of some lactones." Pharmaceutical Chemistry Journal **16**(8): 580-582.

Badawy, M. E. I. (2008). "Chemical modification of chitosan: synthesis and biological activity of new heterocyclic chitosan derivatives." Polymer International **57**(2): 254-261.

Bai, L., W. Wang, J. Hua, Z. Guo and S. Luo (2020). "Defensive functions of volatile organic compounds and essential oils from northern white-cedar in China." BMC Plant Biology **20**(1): 500.

Bailão, E. F. L. C., I. A. Devilla, E. C. Da Conceição and L. L. Borges (2015). "Bioactive compounds found in Brazilian Cerrado fruits." International journal of molecular sciences **16**(10): 23760-23783.

Baron, D., A. C. E. Amaro, A. C. Macedo, C. S. F. Boaro and G. Ferreira (2018). "Physiological changes modulated by rootstocks in atemoya (*Annona x atemoya* Mabb.): gas exchange, growth and ion concentration." Brazilian Journal of Botany **41**(1): 219-225.

Beier, R. C., S. E. Duke, R. L. Ziprin, R. B. Harvey, M. E. Hume, T. L. Poole, H. M. Scott, L. D. Highfield, W. Q. Alali, K. Andrews, R. C. Anderson and D. J. Nisbet (2008). "Antibiotic and Disinfectant Susceptibility Profiles of Vancomycin-Resistant *Enterococcus faecium* (VRE) Isolated from Community Wastewater in Texas." Bulletin of Environmental Contamination and Toxicology **80**(3): 188-194.

Calder, P. C. (1998). "Immunoregulatory and anti-inflammatory effects of n-3 polyunsaturated fatty acids." Brazilian Journal of Medical and Biological Research **31**: 467-490.

Castillo, C., H. Chen, C. Graves, A. Maisonnasse, Y. Le Conte and E. Plettner (2012). "Biosynthesis of ethyl oleate, a primer pheromone, in the honey bee (*Apis mellifera* L.)." Insect Biochem Mol Biol **42**(6): 404-416.

Cavé, A., B. Figadère, A. Laurens and D. Cortes (1997). Acetogenins from annonaceae. Fortschritte der Chemie organischer Naturstoffe Progress in the Chemistry of Organic Natural Products, Springer: 81-288.

Chai, J. W., U. R. Kuppusamy and M. S. Kanthimathi (2008). "Beta-sitosterol induces apoptosis in MCF-7 cells." Malaysian Journal of Biochemistry and Molecular Biology **16**(2): 28-30.

Chandrasekaran, R., P. Seetharaman, M. Krishnan, S. Gnanasekar and S. Sivaperumal (2018). "Carica papaya (Papaya) latex: a new paradigm to combat against dengue and filariasis vectors *Aedes aegypti* and *Culex quinquefasciatus* (Diptera: Culicidae)." 3 Biotech **8**(2): 83.

Cheenpracha, S., O. Yodsaoue, C. Karalai, C. Ponglimanont, S. Subhadhirasakul, S. Tewtrakul and A. Kanjana-opas (2006). "Potential anti-allergic ent-kaurene diterpenes from the bark of *Suregada multiflora*." Phytochemistry **67**(24): 2630-2634.

Chen, H. W., C. Y. Chao, L. L. Lin, C. Y. Lu, K. L. Liu, C. K. Lii and C. C. Li (2013). "Inhibition of matrix metalloproteinase-9 expression by docosahexaenoic acid mediated by heme oxygenase 1 in 12-O-tetradecanoylphorbol-13-acetate-induced MCF-7 human breast cancer cells." Arch Toxicol **87**(5): 857-869.

Chowdhury, P. (2020). "In silico investigation of phytoconstituents from Indian medicinal herb 'Tinospora cordifolia (giloy)' against SARS-CoV-2 (COVID-19) by molecular dynamics approach." Journal of Biomolecular Structure and Dynamics: 1-18.

Costa, M. S., A. E. G. Santana, L. L. Oliveira, J. C. Zanuncio and J. E. Serrão (2017). "Toxicity of squamocin on *Aedes aegypti* larvae, its predators and human cells." Pest management science **73**(3): 636-640.

Couvreur, T. L. P., A. J. Helmstetter, E. J. M. Koenen, K. Bethune, R. D. Brandão, S. A. Little, H. Sauquet and R. H. J. Erkens (2019). "Phylogenomics of the Major Tropical Plant Family Annonaceae Using Targeted Enrichment of Nuclear Genes." Frontiers in Plant Science **9**: 1941.

Deodhar, S., A. K. Dash, E. J. North and M. Hulce (2020). "Development and In Vitro Evaluation of Long Circulating Liposomes for Targeted Delivery of Gemcitabine and Irinotecan in Pancreatic Ductal Adenocarcinoma." AAPS PharmSciTech **21**(6): 231.

Ding, L., W. Guo and X. Chen (2019). "Exogenous addition of alkanolic acids enhanced production of antifungal lipopeptides in *Bacillus amyloliquefaciens* Pc3." Applied Microbiology and Biotechnology **103**(13): 5367-5377.

Dueholm, B., D. P. Drew, C. Sweetman and H. T. Simonsen (2019). "In planta and in silico characterization of five sesquiterpene synthases from *Vitis vinifera* (cv. Shiraz) berries." Planta **249**(1): 59-70.

El-Shazly, A., A. El-Sayed and E. Fikrey (2012). "Bioactive secondary metabolites from *Salix tetrasperma* Roxb." Z Naturforsch C J Biosci **67**(7-8): 353-359.

Elfiky, A. A. (2020). "Natural products may interfere with SARS-CoV-2 attachment to the host cell." Journal of Biomolecular Structure and Dynamics: 1-10.

Evison, S. E. F., R. S. Ferreira, P. D'Ettore, D. Fresneau and C. Poteaux (2012). "Chemical Signature and Reproductive Status in the Facultatively Polygynous ant *Pachycondyla Verena*." Journal of Chemical Ecology **38**(11): 1441-1449.

Fesq, H., K. Brockow, K. Strom, M. Mempel, J. Ring and D. Abeck (2001). "Dihydroxyacetone in a new formulation--a powerful therapeutic option in vitiligo." Dermatology **203**(3): 241-243.

Flath, R. A., R. T. Cunningham, T. R. Mon and J. O. John (1994). "Additional male mediterranean fruitfly (*Ceratitis capitata* wied.) Attractants from Angelica seed oil (*Angelica archangelica* L.)." J Chem Ecol **20**(8): 1969-1984.

Franko, J., L. G. Jackson, A. Hubbs, M. Kashon, B. J. Meade and S. E. Anderson (2012). "Evaluation of furfuryl alcohol sensitization potential following dermal and pulmonary exposure: enhancement of airway responsiveness." Toxicol Sci **125**(1): 105-115.

Fusaro, R. M. and E. G. Rice (2005). "The maillard reaction for sunlight protection." Ann N Y Acad Sci **1043**: 174-183.

Gaddaguti, V., T. V. Rao and A. P. Rao (2016). "Potential mosquito repellent compounds of *Ocimum* species against 3N7H and 3Q8I of *Anophelesgambiae*." 3 Biotech **6**(1): 26.

Ghonghadze, M., N. Antelava, K. Liluashvili, M. Okujava and K. Pachkoria (2017). "Action of L-carnitine, corvutin and their combination on functional state of liver in experimental model of Reye syndrome in rats." Georgian Med News(263): 105-111.

Goedert, J. J., J. N. Sampson, S. C. Moore, Q. Xiao, X. Xiong, R. B. Hayes, J. Ahn, J. Shi and R. Sinha (2014). "Fecal metabolomics: assay performance and association with colorectal cancer." Carcinogenesis **35**(9): 2089-2096.

González-Illán, F., G. Ojeda-Torres, L. M. Díaz-Vázquez and O. Rosario (2011). "Detection of fatty acid ethyl esters in skin surface lipids as biomarkers of ethanol consumption in alcoholics, social drinkers, light drinkers, and teetotalers using a methodology based on microwave-assisted extraction followed by solid-phase microextraction and gas chromatography-mass spectrometry." J Anal Toxicol **35**(4): 232-237.

Habib, M. R. and M. R. Karim (2012). "Antitumour evaluation of di-(2-ethylhexyl) phthalate (DEHP) isolated from *Calotropis gigantea* L. flower." Acta Pharm **62**(4): 607-615.

Hafez, M. H., S. S. Elblehi and Y. S. El-Sayed (2020). "Date palm fruit extract ameliorated pancreatic apoptosis, endocrine dysfunction and regulatory inflammatory cytokines in Streptozotocin-induced diabetes in rats." Environmental Science and Pollution Research **27**(34): 43322-43339.

Harada, H., U. Yamashita, H. Kurihara, E. Fukushi, J. Kawabata and Y. Kamei (2002). "Antitumor activity of palmitic acid found as a selective cytotoxic substance in a marine red alga." Anticancer Res **22**(5): 2587-2590.

Haruenkit, R., S. Poovarodom, S. Veerasilp, J. Namiesnik, M. Sliwka-Kaszynska, Y.-S. Park, B.-G. Heo, J.-Y. Cho, H. G. Jang and S. Gorinstein (2010). "Comparison of bioactive compounds, antioxidant and antiproliferative activities of Mon Thong durian during ripening." Food Chemistry **118**(3): 540-547.

Heo, H. J., Y. J. Park, Y. M. Suh, S. J. Choi, M. J. Kim, H. Y. Cho, Y. J. Chang, B. Hong, H. K. Kim, E. Kim, C. J. Kim, B. G. Kim and D. H. Shin (2003). "Effects of oleamide on choline acetyltransferase and cognitive activities." Biosci Biotechnol Biochem **67**(6): 1284-1291.

Hidayathulla, S., A. A. Shahat, S. R. Ahamad, A. A. N. Al Moqbil, M. S. Alsaied and D. D. Divakar (2018). "GC/MS analysis and characterization of 2-Hexadecen-1-ol and beta sitosterol from *Schimpera arabica* extract for its bioactive potential as antioxidant and antimicrobial." Journal of Applied Microbiology **124**(5): 1082-1091.

Hoye, T. R. and Z. P. Zhuang (1988). "Validation of the proton NMR chemical shift method for determination of stereochemistry in the bistetrahydrofuran moiety of uvaricin-related acetogenins from Annonaceae: rolliniastatin 1 (and asimicin)." The Journal of Organic Chemistry **53**(23): 5578-5580.

Huang, Y., W.-j. Zheng, Y.-s. Ni, M.-s. Li, J.-k. Chen, X.-h. Liu, X.-h. Tan and J.-q. Li (2020). "Therapeutic mechanism of Toujie Quwen granules in COVID-19 based on network pharmacology." BioData Mining **13**(1): 15.

Islam, M. T. (2020). "Chemical profile and biological activities of *Sonneratia apetala* (Buch.-Ham.)." Advances in Traditional Medicine **20**(2): 123-132.

Jang, A., P. Srinivasan, N. Y. Lee, H. P. Song, J. W. Lee, M. Lee and C. Jo (2008). "Comparison of hypolipidemic activity of synthetic gallic acid-linoleic acid ester with mixture of gallic acid and linoleic acid, gallic acid, and linoleic acid on high-fat diet induced obesity in C57BL/6 Cr Slc mice." Chem Biol Interact **174**(2): 109-117.

Jeliaskova, E., D. Z. V, M. Kačániova, T. Astatkie and L. T. B (2018). "Sequential Elution of Essential Oil Constituents during Steam Distillation of Hops (*Humulus lupulus* L.) and Influence on Oil Yield and Antimicrobial Activity." J Oleo Sci **67**(7): 871-883.

Joshi-Barve, S., S. S. Barve, K. Amancherla, L. Gobejishvili, D. Hill, M. Cave, P. Hote and C. J. McClain (2007). "Palmitic acid induces production of proinflammatory cytokine interleukin-8 from hepatocytes." Hepatology **46**(3): 823-830.

Kar, P., N. R. Sharma, B. Singh, A. Sen and A. Roy (2020). "Natural compounds from *Clerodendrum* spp. as possible therapeutic candidates against SARS-CoV-2: An in silico investigation." Journal of Biomolecular Structure and Dynamics: 1-12.

Ketha, A., G. S. Vedula and A. V. S. Sastry (2020). "In vitro antioxidant, anti-inflammatory, and anticancer activities of methanolic extract and its metabolites of whole plant *Cardiospermum canescens* Wall." Future Journal of Pharmaceutical Sciences **6**(1): 11.

Kim, H. J., Y. W. Kim, S. H. Choi, B. M. Cho, R. Bandu, H. S. Ahn and K. P. Kim (2016). "Triolein Emulsion Infusion Into the Carotid Artery Increases Brain Permeability to Anticancer Agents." Neurosurgery **78**(5): 726-733.

Komba, S., E. Kotake-Nara and W. Tsuzuki (2019). "Simultaneous Synthesis of Vitamins D(2), D(4), D(5), D(6), and D(7) from Commercially Available Phytosterol, β -Sitosterol, and Identification of Each Vitamin D by HSQC NMR." Metabolites **9**(6).

Kothapalli, K. S. D., H. G. Park and J. T. Brenna (2020). "Polyunsaturated fatty acid biosynthesis pathway and genetics. implications for interindividual variability in prothrombotic, inflammatory conditions such as COVID-19." Prostaglandins, Leukotrienes and Essential Fatty Acids **162**.

Krim, S., R. Rihani, L. Marchal, A. Foucault, F. Bentahar and J. Legrand (2020). "Two-phase solvent extraction of phenolics from *Origanum vulgare* subsp. *glandulosum*." Journal of Applied Research on Medicinal and Aromatic Plants: 100273.

Krimat, S., H. Metidji, C. Tigrine, D. Dahmane, A. Nouasri and T. Dob (2017). "Chemical analysis, antioxidant, anti-inflammatory, and cytotoxic activities of hydromethanolic extract of *Origanum glandulosum* Desf." Phytothérapie.

Lee, J. H., D. Y. Song, S. H. Jun, S. H. Song, C. H. Shin, C. S. Ki, K. Lee and J. Song (2020). "High prevalence of increased sitosterol levels in hypercholesterolemic children suggest underestimation of sitosterolemia incidence." PLoS One **15**(8): e0238079.

Lee, S.-H. and O.-J. Park (2009). "Uses and production of chiral 3-hydroxy- γ -butyrolactones and structurally related chemicals." Applied Microbiology and Biotechnology **84**(5): 817-828.

Lenz, E. L., M. O. Krasnec and M. D. Breed (2013). "Identification of Undecane as an Alarm Pheromone of the Ant *Formica argentea*." Journal of Insect Behavior **26**(1): 101-108.

Li, M.-M., Z.-e. Jiang, L.-Y. Song, Z.-S. Quan and H.-L. Yu (2017). "Antidepressant and anxiolytic-like behavioral effects of erucamide, a bioactive fatty acid amide, involving the hypothalamus–pituitary–adrenal axis in mice." Neuroscience Letters **640**: 6-12.

Lingwood, D. and K. Simons (2010). "Lipid rafts as a membrane-organizing principle." Science **327**(5961): 46-50.

Liu, F., J. Chen, F. Shi, T. Wang, G. Watanabe and K. Taya (2012). "Phytosterol additive boosts adrenal response to ACTH in male Japanese quail (*Coturnix coturnix japonica*)." Endocrine **41**(2): 338-341.

Luo, L., J. Jiang, C. Wang, M. Fitzgerald, W. Hu, Y. Zhou, H. Zhang and S. Chen (2020). "Analysis on herbal medicines utilized for treatment of COVID-19." Acta Pharmaceutica Sinica B **10**(7): 1192-1204.

Ma, C., Q. Wang, Y. Shi, Y. Li, X. Wang, X. Li, Y. Chen and J. Chen (2017). "Three new antitumor annonaceous acetogenins from the seeds of *Annona squamosa*." Natural product research **31**(18): 2085-2090.

Malhotra, A., P. Kahlon, T. Donoho and I. C. Doyle (2014). "Pharmacogenomic considerations in the treatment of the pediatric cardiomyopathy called Barth syndrome." Recent Pat Biotechnol **8**(2): 136-143.

Mallampati, R., R. R. Patlolla, S. Agarwal, R. J. Babu, P. Hayden, M. Klausner and M. S. Singh (2010). "Evaluation of EpiDerm full thickness-300 (EFT-300) as an in vitro model for skin irritation: studies on aliphatic hydrocarbons." Toxicol In Vitro **24**(2): 669-676.

Manilal, A., S. Sujith, B. Sabarathnam, G. S. Kiran, J. Selvin, C. Shakir and A. P. Lipton (2010). "Bioactivity of the red algae *Asparagopsis taxiformis* collected from the southwestern coast of India." Brazilian Journal of Oceanography **58**(2): 93-100.

Manosroi, A., P. Jantrawut, M. Sainakham, W. Manosroi and J. Manosroi (2012). "Anticancer activities of the extract from Longkong (*Lansium domesticum*) young fruits." Pharm Biol **50**(11): 1397-1407.

Margret, A. A., T. N. Begum, S. Parthasarathy and S. Suvaithenamudhan (2015). "A Strategy to Employ *Clitoria ternatea* as a Prospective Brain Drug Confronting Monoamine Oxidase (MAO) Against Neurodegenerative Diseases and Depression." Natural Products and Bioprospecting **5**(6): 293-306.

Maruyama, H., T. Amanuma, M. Tsutsumi, T. Tsujiuchi, K. Horiguchi, A. Denda and Y. Konishi (1994). "Inhibition by catechol and di(2-ethylhexyl)phthalate of pancreatic carcinogenesis after initiation with N-nitrosobis(2-hydroxypropyl)amine in Syrian hamsters." Carcinogenesis **15**(6): 1193-1196.

Maurya, V. K., S. Kumar, M. L. B. Bhatt and S. K. Saxena (2020). "Antiviral activity of traditional medicinal plants from Ayurveda against SARS-CoV-2 infection." Journal of Biomolecular Structure and Dynamics: 1-17.

Monleón, D., J. M. Morales, A. Barrasa, J. A. López, C. Vázquez and B. Celda (2009). "Metabolite profiling of fecal water extracts from human colorectal cancer." NMR Biomed **22**(3): 342-348.

Morton, J. F. (1987). Fruits of warm climates, JF Morton.

Mozafari, A. A., Y. Vafaei and M. Shahyad (2018). "Phytochemical composition and in vitro antioxidant potential of *Cynodon dactylon* leaf and rhizome extracts as affected by drying methods and temperatures." Journal of Food Science and Technology **55**(6): 2220-2229.

Murugan, K., K. Sekar, S. Sangeetha, S. Ranjitha and S. A. Sohaibani (2013). "Antibiofilm and quorum sensing inhibitory activity of *Achyranthes aspera* on cariogenic *Streptococcus mutans*: An in vitro and in silico study." Pharmaceutical biology **51**(6): 728-736.

Narkhede, R. R., A. V. Pise, R. S. Cheke and S. D. Shinde (2020). "Recognition of Natural Products as Potential Inhibitors of COVID-19 Main Protease (Mpro): In-Silico Evidences." Natural Products and Bioprospecting **10**(5): 297-306.

Naseer, S., S. H. Lone, J. A. Lone, M. A. Khuroo and K. A. Bhat (2015). "LC-MS guided isolation, quantification and antioxidant evaluation of bioactive principles from *Epimedium elatum*." Journal of Chromatography B **989**: 62-70.

Neske, A., J. Ruiz Hidalgo, N. Cabedo and D. Cortes (2020). "Acetogenins from Annonaceae family. Their potential biological applications." Phytochemistry **174**: 112332.

Noda, A., T. Shibata, T. Hayakawa, T. Kondo, K. Nagai and H. Hamano (1984). "[Pancreatic stone dissolution with dimethadione (DMO). II. Roentgenological follow-up study in canine experimental pancreatic stones]." Nihon Shokakibyō Gakkai Zasshi **81**(2): 254-262.

Ogunlakin, A. D., M. A. Sonibare, A. Jabeen, F. Shaheen and S. F. Shah (2020). "Antiproliferative and ameliorative effects of *Tetracera potatoria* and its constituent." Advances in Traditional Medicine.

Okamoto, M., H. C. Rosenberg and N. R. Boisse (1977). "Evaluation of anticonvulsants in barbiturate withdrawal." J Pharmacol Exp Ther **202**(2): 479-489.

Oliveira-Tintino, C. D. M., R. T. Pessoa, M. N. M. Fernandes, I. S. Alcântara, B. A. F. da Silva, M. R. C. de Oliveira, A. Martins, M. D. S. da Silva, S. R. Tintino, F. F. G. Rodrigues, J. G. M. da Costa, S. G. de Lima, M. R. Kerntopf, T. G. da Silva and I. R. A. de Menezes (2018). "Anti-inflammatory and anti-edematogenic action of the *Croton campestris* A. St.-Hil (Euphorbiaceae) essential oil and the compound β -caryophyllene in in vivo models." Phytomedicine **41**: 82-95.

Petropoulos, S. A., Â. Fernandes, R. C. Calhelha, N. Danalatos, L. Barros and I. C. F. R. Ferreira (2018). "How extraction method affects yield, fatty acids composition and bioactive properties of cardoon seed oil?" Industrial Crops and Products **124**: 459-465.

Phua, L. C., X. P. Chue, P. K. Koh, P. Y. Cheah, H. K. Ho and E. C. Chan (2014). "Non-invasive fecal metabonomic detection of colorectal cancer." Cancer Biol Ther **15**(4): 389-397.

Piccolo, B. D., J. L. Graham, K. L. Stanhope, O. Fiehn, P. J. Havel and S. H. Adams (2016). "Plasma amino acid and metabolite signatures tracking diabetes progression in the UCD-T2DM rat model." Am J Physiol Endocrinol Metab **310**(11): E958-969.

Politi, L., F. Mari, S. Furlanetto, E. Del Bravo and E. Bertol (2011). "Determination of fatty acid ethyl esters in hair by GC-MS and application in a population of cocaine users." J Pharm Biomed Anal **54**(5): 1192-1195.

Poudel, A., P. Satyal and W. N. Setzer (2015). "Composition and bioactivities of the leaf essential oil of *Ficus religiosa* Linn." American Journal of Essential Oils and Natural Products **2**(3): 16-17.

Ritchie, S. A., P. W. Ahiahonu, D. Jayasinghe, D. Heath, J. Liu, Y. Lu, W. Jin, A. Kavianpour, Y. Yamazaki, A. M. Khan, M. Hossain, K. K. Su-Myat, P. L. Wood, K. Krenitsky, I. Takemasa, M. Miyake, M. Sekimoto, M. Monden, H. Matsubara, F. Nomura and D. B. Goodenowe (2010). "Reduced levels of hydroxylated, polyunsaturated ultra long-chain fatty acids in the serum of colorectal cancer patients: implications for early screening and detection." BMC Med **8**: 13.

Rupprecht, J. K., C. J. Chang, J. M. Cassady, J. L. McLaughlin, K. L. Mikolajczak and D. Weisleder (1986). "Asimicin, a new cytotoxic and pesticidal acetogenin from the pawpaw, *Asimina triloba* (Annonaceae)." Heterocycles **24**(5): 1197-1201.

Sales-Campos, H., P. R. Souza, B. C. Peghini, J. S. da Silva and C. R. Cardoso (2013). "An overview of the modulatory effects of oleic acid in health and disease." Mini Rev Med Chem **13**(2): 201-210.

Sharopov, F., P. Satyal and M. Wink (2020). "The Chemical Composition and Biological Activities of Essential Oil from the Leaves of *Philadelphus x purpureomaculatus* Lemoine." Pharmaceutical Chemistry Journal **54**(4): 386-388.

Sheng, Z., R. Jian, F. Xie, B. Chen, K. Zhang, D. Li, W. Chen, C. Huang, Y. Zhang, L. Hu, D. Zhao, X. Zheng, P. Wu and W. D. Hong (2020). "Screening of larvicidal activity of 53 essential oils and their synergistic effect for the improvement of deltamethrin efficacy against *Aedes albopictus*." Industrial Crops and Products **145**: 112131.

Sheu, M. Y., A. J. Fowler, J. Kao, M. Schmuth, K. Schoonjans, J. Auwerx, J. W. Fluhr, M. Q. Man, P. M. Elias and K. R. Feingold (2002). "Topical peroxisome proliferator activated receptor-alpha activators reduce inflammation in irritant and allergic contact dermatitis models." J Invest Dermatol **118**(1): 94-101.

Shobana, S., V. G. Vidhya and M. Ramya (2009). "Antibacterial activity of garlic varieties (*ophioscordon* and *sativum*) on enteric pathogens." Current Research Journal of Biological Sciences **1**(3): 123-126.

Sinha, R., J. Ahn, J. N. Sampson, J. Shi, G. Yu, X. Xiong, R. B. Hayes and J. J. Goedert (2016). "Fecal Microbiota, Fecal Metabolome, and Colorectal Cancer Interrelations." PLoS One **11**(3): e0152126.

Siqueira, C. A. T., A. F. Serain, A. C. R. F. Pascoal, N. L. Andreazza, C. C. de Lourenço, A. L. T. Góis Ruiz, J. E. de Carvalho, A. C. O. de Souza, J. Tonini Mesquita, A. G. Tempone and M. J. Salvador (2015). "Bioactivity and chemical composition of the essential oil from the leaves of *Guatteria australis* A.St.-Hil." Natural Product Research **29**(20): 1966-1969.

Spalding, J. W., J. E. French, S. Stasiewicz, M. Furedi-Machacek, F. Conner, R. R. Tice and R. W. Tennant (2000). "Responses of transgenic mouse lines p53(+/-) and Tg.AC to agents tested in conventional carcinogenicity bioassays." Toxicol Sci **53**(2): 213-223.

Stefani, T., E. Garza-González, V. M. Rivas-Galindo, M. Y. Rios, L. Alvarez and M. D. R. Camacho-Corona (2019). "Hechtia glomerata Zucc: Phytochemistry and Activity of Its Extracts and Major Constituents Against Resistant Bacteria." Molecules **24**(19).

Stopiglia, C. D., F. J. Vieira, A. G. Mondadori, T. P. Oppe and M. L. Scroferneker (2011). "In vitro antifungal activity of dihydroxyacetone against causative agents of dermatomycosis." Mycopathologia **171**(4): 267-271.

Suresh, A., R. Praveenkumar, R. Thangaraj, F. L. Oscar, E. Baldev, D. Dhanasekaran and N. Thajuddin (2014). "Microalgal fatty acid methyl ester a new source of bioactive compounds with antimicrobial activity." Asian Pacific Journal of Tropical Disease **4**: S979-S984.

Swantara, M. D., W. S. Rita, N. Suartha and K. K. Agustina (2019). "Anticancer activities of toxic isolate of *Xestospongia testudinaria* sponge." Vet World **12**(9): 1434-1440.

Taechowisan, T., C. Singtotong and W. S. Phutdhawong (2016). "Antibacterial and Antioxidant Activities of Acetogenins from *Streptomyces* sp. VE2; An Endophyte in *Vernonia cinerea* (L.) Less." Journal of Applied Pharmaceutical Science **6**(08): 067-072.

Tamfu, A. N., M. Tagatsing Fotsing, E. Talla, A. Jabeen, J. Mbafor Tanyi and F. Shaheen (2019). "Bioactive constituents from seeds of *Annona Senegalensis* Persoon (Annonaceae)." Natural Product Research: 1-6.

Tang, R., F. Zhang, N. G. Kone, J.-H. Chen, F. Zhu, R.-C. Han, C.-L. Lei, M. Kenis, L.-Q. Huang and C.-Z. Wang (2016). "Identification and testing of oviposition attractant chemical compounds for *Musca domestica*." Scientific Reports **6**(1): 33017.

Tang, W., A. G. Borel, T. Fujimiya and F. S. Abbott (1995). "Fluorinated analogues as mechanistic probes in valproic acid hepatotoxicity: hepatic microvesicular steatosis and glutathione status." Chem Res Toxicol **8**(5): 671-682.

Teal, P. E., R. R. Heath, J. H. Tumlinson and J. R. McLaughlin (1981). "Identification of a sex pheromone of *Heliothis subflexa* (GN.) (Lepidoptera: Noctuidae) and field trapping studies using different blends of components." J Chem Ecol **7**(6): 1011-1022.

Toelzer, C., K. Gupta, S. K. N. Yadav, U. Borucu, A. D. Davidson, M. Kavanagh Williamson, D. K. Shoemark, F. Garzoni, O. Staufer, R. Milligan, J. Capin, A. J. Mulholland, J. Spatz, D. Fitzgerald, I. Berger and C. Schaffitzel (2020). "Free fatty acid binding pocket in the locked structure of SARS-CoV-2 spike protein." Science: eabd3255.

Toriyama-Baba, H., M. Iigo, M. Asamoto, Y. Iwahori, C. B. Park, B. S. Han, N. Takasuka, T. Kakizoe, C. Ishikawa, K. Yazawa, E. Araki and H. Tsuda (2001). "Organotropic chemopreventive effects of n-3 unsaturated fatty acids in a rat multi-organ carcinogenesis model." Jpn J Cancer Res **92**(11): 1175-1183.

Ulbricht, C. E. (2016). "An Evidence-Based Systematic Review of Beta-Sitosterol, Sitosterol (22,23- dihydrostigmasterol, 24-ethylcholesterol) by the Natural Standard Research Collaboration." J Diet Suppl **13**(1): 35-92.

Walker, C. I. B., S. M. Oliveira, R. Tonello, M. F. Rossato, E. da Silva Brum, J. Ferreira and G. Trevisan (2017). "Anti-nociceptive effect of stigmasterol in mouse models of acute and chronic pain." Naunyn Schmiedebergs Arch Pharmacol **390**(11): 1163-1172.

Wang, J., X. Zhang, A. B. Omarini and B. Li (2020). "Virtual screening for functional foods against the main protease of SARS-CoV-2." Journal of Food Biochemistry **n/a**(n/a): e13481.

Weir, T. L., D. K. Manter, A. M. Sheflin, B. A. Barnett, A. L. Heuberger and E. P. Ryan (2013). "Stool microbiome and metabolome differences between colorectal cancer patients and healthy adults." PLoS One **8**(8): e70803.

Woyke, S., S. Rauch, M. Ströhle and H. Gatterer "Modulation of Hb-O₂ affinity to improve hypoxemia in COVID-19 patients." Clinical Nutrition.

Wu, C. F., C. L. Li, H. R. Song, H. F. Zhang, J. Y. Yang and Y. L. Wang (2003). "Selective effect of oleamide, an endogenous sleep-inducing lipid amide, on pentylenetetrazole-induced seizures in mice." J Pharm Pharmacol **55**(8): 1159-1162.

Xu, F. J., S. J. Yuan, S. O. Pehkonen, E. T. Kang and K. G. Neoh (2006). "Antimicrobial surfaces of viologen-quaternized poly((2-dimethyl amino)ethyl methacrylate)-Si(100) hybrids from surface-initiated atom transfer radical polymerization." NanoBiotechnology **2**(3): 123-134.

Yamagata, N., N. Fujiwara-Tsujii, R. Yamaoka and M. Mizunami (2005). "Pheromone communication and the mushroom body of the ant, *Camponotus obscuripes* (Hymenoptera: Formicidae)." Naturwissenschaften **92**(11): 532-536.

Yano, M., M. Ikeda, K. Abe, H. Dansako, S. Ohkoshi, Y. Aoyagi and N. Kato (2007). "Comprehensive analysis of the effects of ordinary nutrients on hepatitis C virus RNA replication in cell culture." Antimicrob Agents Chemother **51**(6): 2016-2027.

Zafra-Polo, M. C., B. Figadère, T. Gallardo, J. Tormo and D. Cortes (1998). "Natural acetogenins from Annonaceae, synthesis and mechanisms of action." Phytochemistry **48**(7): 1087-1117.

Zhao, L., J. Chen, J. Su, L. Li, S. Hu, B. Li, X. Zhang, Z. Xu and T. Chen (2013). "In vitro antioxidant and antiproliferative activities of 5-hydroxymethylfurfural." J Agric Food Chem **61**(44): 10604-10611.

Zhao, Y., B. Wang, G. Wang, L. Huang, T. Yin, X. Li, X. Liu, Q. Wang, J. Jing, J. Yang and Y. Zhang (2020). "Functional interaction between plasma phospholipid fatty acids and insulin resistance in leucocyte telomere length maintenance." Lipids in Health and Disease **19**(1): 11.

Zhenjie, Z., Z. Xiaoying, Z. Huanhuan, C. Huiqi, H. Boxiang and W. Dongqun Lin and Junmao (2020). "Exploring the Potential Mechanism of Shufeng Jiedu Capsule for Treating COVID-19 by Comprehensive Network Pharmacological Approaches and Molecular Docking Validation." Combinatorial Chemistry & High Throughput Screening **23**: 1-20.